



5-1999

**Early-transition-metal alkylidene chemistry. Synthesis of tantalum silyl alkylidene complexes and reactions of tantalum alkylidene complexes with silanes**

Jonathan Bruce Diminnie

Follow this and additional works at: [https://trace.tennessee.edu/utk\\_graddiss](https://trace.tennessee.edu/utk_graddiss)

---

**Recommended Citation**

Diminnie, Jonathan Bruce, "Early-transition-metal alkylidene chemistry. Synthesis of tantalum silyl alkylidene complexes and reactions of tantalum alkylidene complexes with silanes. " PhD diss., University of Tennessee, 1999.

[https://trace.tennessee.edu/utk\\_graddiss/8800](https://trace.tennessee.edu/utk_graddiss/8800)

This Dissertation is brought to you for free and open access by the Graduate School at TRACE: Tennessee Research and Creative Exchange. It has been accepted for inclusion in Doctoral Dissertations by an authorized administrator of TRACE: Tennessee Research and Creative Exchange. For more information, please contact [trace@utk.edu](mailto:trace@utk.edu).

To the Graduate Council:

I am submitting herewith a dissertation written by Jonathan Bruce Diminnie entitled "Early-transition-metal alkylidene chemistry. Synthesis of tantalum silyl alkylidene complexes and reactions of tantalum alkylidene complexes with silanes." I have examined the final electronic copy of this dissertation for form and content and recommend that it be accepted in partial fulfillment of the requirements for the degree of Doctor of Philosophy, with a major in Chemistry.

Ziling Xue, Major Professor

We have read this dissertation and recommend its acceptance:

Clifton Woods, James Q. Chambers, David C. Joy

Accepted for the Council:

Carolyn R. Hodges

Vice Provost and Dean of the Graduate School

(Original signatures are on file with official student records.)

To the Graduate Council:

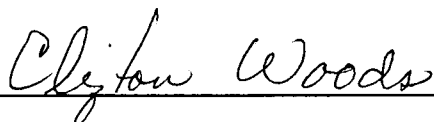
I am submitting herewith a dissertation written by Jonathan Diminnie entitled "Early-Transition-Metal Alkylidene Chemistry. Synthesis of Tantalum Silyl Alkylidene Complexes and Reactions of Tantalum Alkylidene Complexes with Silanes." I have examined the final copy of this dissertation for form and content and recommend that it be accepted in partial fulfillment of the requirements for the degree of Doctor of Philosophy, with a major in Chemistry.



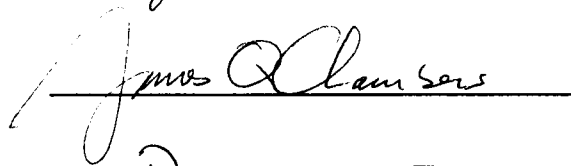
---

Ziling Xue, Major Professor

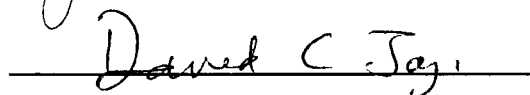
We have read this dissertation  
and recommend its acceptance:



---



---



---

Accepted for the Council:



---

Associate Vice Chancellor and  
Dean of The Graduate School

**Early-Transition-Metal Alkylidene Chemistry. Synthesis of  
Tantalum Silyl Alkylidene Complexes and Reactions of Tantalum  
Alkylidene Complexes with Silanes.**

A Dissertation

Presented for the

Doctor of Philosophy

Degree

The University of Tennessee, Knoxville

Jonathan Bruce Diminnie

May 1999

## ACKNOWLEDGMENTS

There are many people who I would like to thank for their support and friendship during my five years at the University of Tennessee. I would first like to thank God, without Whom nothing is possible, and Who has blessed me in so many ways, both personally and professionally. I would also like to thank my parents, Drs. Charles and Carol Diminnie, and my brothers, Dan and Dave, for their constant and steadfast support, particularly during the difficult times of finishing my research and writing this dissertation. I also would like to acknowledge my research advisor, Prof. Ziling (Ben) Xue, who has been a mentor to me while at the University of Tennessee, and who has taught me the value of hard work and dedication to a project, and not to accept mediocrity, even though I sometimes resisted having to run "just one more experiment".

I extend thanks as well to the support staff in the Chemistry Department: Bobby and Darrell Lay, Marilyn Ownby, Art Pratt, Gene French, Bill Gurley, Johnny Jones, Sharon Marshall, Susan Hartzog, Jan McGuire, Maria Motoyama, Rachelle Allen, Theresa Turner, and Carol Moulton -- you were always willing to assist me, and you are the best at what you do.

I would also like to thank my committee members, Prof. James Chambers, Prof. Clifton Woods III, and Prof. David Joy for their consideration of my dissertation and constructive comments. Special thanks go out to Dr. Woods for his assistance and support of me as the student operator of the

departmental X-ray diffractometer.

The following individuals extended technical support for various aspects of my research at the University of Tennessee, for which I am grateful: Dr. Holger Foesterling, Neil Whittemore, and Dr. Hongjun Pan for their assistance with NMR, Dr. Al Tuinman for assistance with mass spectrometry, and Dr. Jeffrey C. Bryan of Oak Ridge National Laboratory for assistance with problematic X-ray crystal structures. I would also like to acknowledge the following for financial support during my tenure at the University of Tennessee: the NSF Young Investigator Award, the DuPont Young Professor Award, the Petroleum Research Fund, the Camille Dreyfus Teacher-Scholar Award, Science Alliance, and the University of Tennessee.

Finally I would like to thank all my co-workers and colleagues, both past and present, for putting up with me, even on days when I was not the most pleasant to be around, for many, many helpful discussions about my research, and for making the lab a productive and pleasant environment. Special thanks goes out to Mark Burleigh, Sven Eklund, and John Chaney for helping me to maintain my sanity during the last six months, to Jaime Blanton, who will be carrying on my research projects, and to Tianniu Chen, who will be succeeding me as student operator of the departmental X-ray diffractometer--best of luck to you both! I also wish all the best to the rest of my co-workers and colleagues, both past and present: Dr. Liting Li, Dr. Lenore McAlexander, Vivian Liu, Dr. Zhongzhi Wu, Leonardo Allain, Hee-Jung Im, Bryan Fagan, Terry Yost, Cheri

Whitehead, Jon Morrell, Andy Canada, Karn Sorasaene, Heather Hall, Keith  
Quisenberry, Meiling Hung, Kris Scaboo, Neil Whittemore, Matt Ogle, Ken  
Smith, Dr. Yvette Yang, and Rebecca Mack.

## ABSTRACT

This dissertation describes research conducted on the chemistry of tantalum silyl complexes, reactions of alkylidene complexes with phenylsilanes, kinetic and mechanistic studies of the reaction of a tantalum alkylidene complex with phenylsilanes, and related organometallic chemistry. An overview and summary of the Ph.D. research project is given in Chapter 1. Chapter 2 describes the synthesis and characterization of the thermally unstable tantalum silyl alkylidene complexes  $(\text{Me}_3\text{ECH}_2)_2\text{Ta}[\text{=CHMe}_3]\text{SiPh}_2\text{Bu}^t$  ( $\text{E} = \text{C}$ , **1**;  $\text{Si}$ , **2**). Complexes **1** and **2** were found to decompose by elimination of  $\text{HSiPh}_2\text{Bu}^t$  to unidentified products and  $(\text{Me}_3\text{SiCH}_2)_4\text{Ta}_2(\mu\text{-CSiMe}_3)_2$ , respectively. Reaction of **1** or **2** with  $\text{PMe}_3$  leads to elimination of  $\text{HSiPh}_2\text{Bu}^t$  and the formation of bis(phosphine)bis(alkylidene) complexes  $(\text{Me}_3\text{ECH}_2)\text{Ta}(\text{PMe}_3)_2[\text{=CHMe}_3]_2$  ( $\text{E} = \text{C}$ , **3**;  $\text{Si}$ , **4**). Chapter 3 presents the reactions of the tantalum alkylidene complexes  $(\text{Me}_3\text{SiCH}_2)_3\text{Ta}(\text{PMe}_3)=\text{CHSiMe}_3$  (**7**), **4**, and  $(\text{Me}_3\text{SiCH}_2)_2\text{Ta}(\text{PMe}_3)_2[\text{=CHCMe}_3]_2$  (**8**) with phenylsilanes  $\text{PhRSiH}_2$  ( $\text{R} = \text{Ph}, \text{Me}$ ) and  $(\text{PhSiH}_2)_2\text{CH}_2$  to yield novel bis(silyl)-substituted alkylidene complexes as well as the first reported 1,1'-metalla-3-silacyclobutadiene and 1,1'-metalla-3,5-disilacyclohexadiene complexes through the preferential reaction of the silanes with the alkylidene ligands of **4**, **7**, and **8**. Chapter 4 describes the mechanistic investigation of the formation of the bis(silyl)-substituted alkylidene complex



$(\text{Me}_3\text{SiCH}_2)_3\text{Ta}=\text{C}(\text{SiMe}_3)\text{SiPhMeH}$  (**9a**) from the reaction of **7** with  $\text{PhMeSiH}_2$ . Kinetic studies were found to be consistent with a dissociative mechanism in which a  $\text{PMe}_3$  molecule dissociated from the tantalum center in **7**, forming an open coordination site on the metal for the reaction with  $\text{PhMeSiH}_2$ . Deuterium labeling studies were consistent with a mechanism involving hydride and silyl intermediates. The final chapter discusses attempted syntheses of dianionic bis(silyl)lithium and -potassium compounds as potential ligands for the synthesis of poly- or persilyl early-transition-metal complexes. Two previously unreported bis(silyl)methane and -ethane complexes  $[(\text{Me}_3\text{Si})_3\text{Si}]_2\text{CH}_2$  (**18**) and  $(\text{Me}_3\text{Si})_3\text{SiCH}_2\text{CH}_2\text{Si}(\text{SiMe}_3)_3$  (**19**) were synthesized as possible ligand precursors.

## TABLE OF CONTENTS

Chapter	Page
1. Introduction .....	1
2. Synthesis of Thermally Unstable Tantalum Silyl Alkylidene Complexes and Reactivity of These Complexes with $\text{PMe}_3$	
2.1. Introduction .....	9
2.2. Results and Discussion .....	12
2.2.1. Synthesis and Characterization of $(\text{Me}_3\text{ECH}_2)_2\text{Ta}[\text{CHEMe}_3]\text{SiPh}_2\text{Bu}^t$ (E = C, Si) .....	12
2.2.2. Reactions of <b>1</b> and <b>2</b> with Trimethylphosphine .....	15
2.2.3. X-ray Crystal Structure of <b>4</b> .....	24
2.3. Experimental Section .....	31
3. Reactions of Tantalum Alkylidene Complexes with Silanes	
3.1. Introduction .....	38
3.2. Results and Discussion .....	39
3.2.1. Synthesis of Bis(silyl)-Substituted Alkylidene Complexes .....	39
3.2.2. Synthesis of Novel Metallasilacyclobutadiene Complexes .....	41

3.2.3. Synthesis of the Metalladisilacyclohexdiene Complex	
<b>12</b> .....	45
3.2.4. X-ray Crystal Structures of <b>10a</b> , <b>10b</b> , <b>11</b> , and <b>12</b> .....	53
3.3. Experimental Section .....	77
4. Kinetic and Mechanistic Studies of Reactions of Tantalum Alkyldiene Complexes with Silanes	
4.1. Introduction .....	87
4.2. Results and Discussion .....	90
4.2.1. Deuterium Labeling Studies of the Conversion of <b>7</b> to <b>9a</b> .....	90
4.2.2. Kinetic Studies of the Conversion of <b>7</b> to <b>9a</b> .....	94
4.2.3. Mechanism of the Conversion of <b>7</b> to <b>9a</b> .....	107
4.3. Experimental Section .....	114
5. Synthesis of Bis[tris(trimethylsilyl)silyl]methane and 1,2- Bis[tris(trimethylsilyl)silyl]ethane and Attempted Synthesis of Dianionic Bis(silyl) Compounds	
5.1. Introduction .....	117
5.2. Results and Discussion .....	124
5.2.1. Synthesis of Bis[tris(trimethylsilyl)silyl]methane ( <b>18</b> ) and 1,2-Bis[tris(trimethylsilyl)silyl]ethane ( <b>19</b> ) .....	124

5.2.2. Attempted Metalation of <b>18</b> and <b>19</b> .....	127
5.3. Experimental Section .....	135
References .....	141
Vita .....	151

## LIST OF TABLES

### Table

- 2.1 Crystal Data for **4**
- 2.2 Interatomic Distances in **4**
- 2.3 Intramolecular Bond Angles in **4**
- 3.1 Crystal Data for **10a**
- 3.2 Interatomic Distances in **10a**
- 3.3 Intramolecular Bond Angles in **10a**
- 3.4 Crystal Data for **10b**
- 3.5 Interatomic Distances in **10b**
- 3.6 Intramolecular Bond Angles in **10b**
- 3.7 Crystal Data for **11**
- 3.8 Interatomic Distances in **11**
- 3.9 Intramolecular Bond Angles in **11**
- 3.10 Crystal Data for **12**
- 3.11 Interatomic Distances in **12**
- 3.12 Intramolecular Bond Angles in **12**
- 4.1 Observed Rate Constants for the Conversion **7-9a**
- 4.2 Observed Rate Constants for the Conversion **7-9a-d<sub>1</sub>**

## LIST OF FIGURES

- 1.1 Proposed Intermediates in the Formation of Silicide Materials and Model Complexes for These Intermediates.
- 2.1 Variable Temperature NMR Spectra of **4**.
- 2.2 ORTEP Diagram of **4**, Showing 30% Ellipsoids.
- 3.1 <sup>1</sup>H NMR Spectrum of *meso*-**12**.
- 3.2 <sup>1</sup>H NMR Spectrum of *meso*-**12** and *rac*-**12**.
- 3.3 TOCSY Spectrum of *meso*-**12** and *rac*-**12**.
- 3.4 HMQC Spectrum of *meso*-**12** and *rac*-**12**.
- 3.5 ORTEP Diagram of **10a**, Showing 50% Ellipsoids.
- 3.6 ORTEP Diagram of **10b**, Showing 50% Ellipsoids.
- 3.7 ORTEP Diagram of **11**, Showing 50% Ellipsoids.
- 3.8 ORTEP Diagram of **12**, Showing 30% Ellipsoids.
- 4.1 <sup>2</sup>H NMR Spectrum of a Reaction Solution of **7** with 10.4 Equiv of PhMeSiD<sub>2</sub>.
- 4.2 Mass Spectrum of the Gaseous Products from the Reaction of **7** with 4.7 Equiv of PhMeSiD<sub>2</sub>.
- 4.3 Kinetic Plots of the Reaction of **7** with PhMeSiH<sub>2</sub> ( $[\text{PhMeSiH}_2]_{\text{av}}/[\text{PMe}_3]_{\text{av}} = 9.68 - 35.2$ ).
- 4.4 Kinetic Plots of the Reaction of **7** with PhMeSiH<sub>2</sub> ( $[\text{PhMeSiH}_2]_{\text{av}}/[\text{PMe}_3]_{\text{av}} = 38.6 - 68.6$ ).

- 4.5 Kinetic Plots of the Reaction of **7** with  $\text{PhMeSiD}_2$  ( $[\text{PhMeSiD}_2]_{\text{av}}/[\text{PMe}_3]_{\text{av}}$   
= 9.00 - 69.2).
- 4.6 Plot of  $k_{\text{obs}}$  vs.  $[\text{PhMeSiH}_2]_{\text{av}}/[\text{PMe}_3]_{\text{av}}$ .
- 4.7 Plot of  $k_{\text{obs}}^{-1}$  vs.  $[\text{PMe}_3]_{\text{av}}/[\text{Silane}]_{\text{av}}$ .
- 5.1 GC/MS Peak for **24** from the Reaction of **19** with  $\text{KOBU}^t$ .
- 5.2 GC/MS Peak for **25** from the Reaction of **19** with  $\text{KOBU}^t$ .

## NUMBERING SCHEME FOR COMPOUNDS IN THE TEXT

1.  $(\text{Me}_3\text{CCH}_2)_2\text{Ta}[\text{=CHCMe}_3]\text{SiPh}_2\text{Bu}^t$
2.  $(\text{Me}_3\text{SiCH}_2)_2\text{Ta}[\text{=CHSiMe}_3]\text{SiPh}_2\text{Bu}^t$
3.  $(\text{Me}_3\text{CCH}_2)\text{Ta}(\text{PMe}_3)_2[\text{=CHCMe}_3]_2$
4.  $(\text{Me}_3\text{SiCH}_2)\text{Ta}(\text{PMe}_3)_2[\text{=CHSiMe}_3]_2$
5.  $(\text{Me}_3\text{SiCH}_2)_2\text{Ta}(\text{PMe}_3)[\text{=CHSiMe}_3]\text{SiPh}_2\text{Bu}^t$
6.  $(\text{Me}_3\text{P})_2\text{ClTa}(\mu\text{-CSiMe}_3)_2\text{TaCl}(\text{CH}_2\text{SiMe}_3)_2$
7.  $(\text{Me}_3\text{SiCH}_2)_3\text{Ta}(\text{PMe}_3)[\text{=CHSiMe}_3]$
8.  $(\text{Me}_3\text{SiCH}_2)\text{Ta}(\text{PMe}_3)_2[\text{=CHCMe}_3]_2$
- 9a.  $(\text{Me}_3\text{SiCH}_2)_3\text{Ta}=\text{C}(\text{SiMe}_3)\text{SiPhMeH}$
- 9a-d<sub>1</sub>.  $(\text{Me}_3\text{SiCH}_2)_3\text{Ta}=\text{C}(\text{SiMe}_3)\text{SiPhMeD}$
- 9b.  $(\text{Me}_3\text{SiCH}_2)_3\text{Ta}=\text{C}(\text{SiMe}_3)\text{SiPh}_2\text{H}$
- 10a.  $(\text{Me}_3\text{SiCH}_2)\text{Ta}(\text{PMe}_3)_2[\text{=C}(\text{SiMe}_3)\text{SiPhMeC}(\text{SiMe}_3)]$
- 10b.  $(\text{Me}_3\text{SiCH}_2)\text{Ta}(\text{PMe}_3)_2[\text{=C}(\text{SiMe}_3)\text{SiPh}_2\text{C}(\text{SiMe}_3)]$
11.  $(\text{Me}_3\text{SiCH}_2)\text{Ta}(\text{PMe}_3)_2[\text{=C}(\text{CMe}_3)\text{SiPhMeC}(\text{CMe}_3)]$
12.  $(\text{MeSiCH}_2)\text{Ta}(\text{PMe}_3)_2[\text{=C}(\text{SiMe}_3)\text{Si}\{\text{Ph}\}\text{HCH}_2\text{Si}\{\text{Ph}\}\text{HC}(\text{SiMe}_3)]$



13.  $(\text{Me}_3\text{SiCH}_2)\text{Ta}(\text{PMe}_3)[\text{=C}(\text{CMe}_3)\text{SiPhMeC}(\text{CMe}_3)]$
14.  $(\text{Me}_3\text{CCH}_2)\text{Ta}(\text{PMe}_3)[\text{=C}(\text{CMe}_3)\text{SiPhMeC}(\text{CMe}_3)]$
15.  $(\text{Me}_3\text{SiCH}_2)_3\text{Ta}(\text{H})[\text{CH}(\text{SiMe}_3)\text{SiPhMeH}]$
16.  $(\text{Me}_3\text{SiCH}_2)_3\text{Ta}(\text{SiPhMeH})[\text{CH}(\text{SiMe}_3)\text{SiPhMeH}]$
17.  $[(\text{Me}_3\text{Si})_3\text{Si}]_2\text{CHOH}$
18.  $[(\text{Me}_3\text{Si})_3\text{Si}]_2\text{CH}_2$
19.  $(\text{Me}_3\text{Si})_3\text{SiCH}_2\text{CH}_2\text{Si}(\text{SiMe}_3)_3$
20.  $[(\text{Me}_3\text{Si})_3\text{Si}]_2\text{CHI}$
21.  $[\text{LiSi}(\text{SiMe}_3)_2]_2\text{CH}_2$
22.  $\text{LiSi}(\text{SiMe}_3)_2\text{CH}_2\text{CH}_2(\text{SiMe}_3)_2\text{SiLi}$
23.  $\text{LiSi}(\text{SiMe}_3)_2\text{CH}_2\text{CH}_2\text{Si}(\text{SiMe}_3)_3$
24.  $\text{H}(\text{SiMe}_3)_2\text{SiCH}_2\text{CH}_2\text{Si}(\text{SiMe}_3)_2\text{H}$
25.  $\text{H}(\text{SiMe}_3)\text{SiCH}_2\text{CH}_2\text{Si}(\text{SiMe}_3)_2$

# CHAPTER 1

## Introduction

Transition-metal silyl chemistry dates back over four decades,<sup>1,2</sup> beginning with the first reported silyl complex,  $\text{Cp}(\text{CO})_2\text{FeSiMe}_3$ , in 1956.<sup>1</sup> Over the past decade, the field has seen rapid growth, as applications of metal silyl complexes as catalysts in areas such as hydrosilation and dehydrogenative polymerization of silanes have either been developed or expanded.<sup>2h,3,14</sup> Despite the increase in interest in metal silyl complexes, the chemistry of early-transition-metal silyl complexes has mainly been focused on complexes containing anionic  $\pi$ -ligands, such as  $\eta^5$ -cyclopentadienyl (Cp), or stabilizing ligands such as carbonyls,<sup>4</sup> alkoxides,<sup>5</sup> amides,<sup>6</sup> or phosphines.<sup>7</sup> Cp-free early-transition-metal silyl chemistry remains a largely unexplored area.

Our initial interest in early-transition-metal silyl complexes free of anionic  $\pi$ -ligands was inspired by our studies of the structures and reactivities of such complexes as models for possible reactive intermediates in molecular approaches to metal silicides, a class of solid-state materials widely used in the electronic, aerospace and machine-tool industries.<sup>8-10</sup> Such molecular approaches to silicides involve the reactions of early-transition-metal alkyl,

alkylidene, or alkylidyne complexes  $M(\text{CH}_2\text{R})_4$  ( $M = \text{Ti triad}$ ),  $(\text{RCH}_2)_3\text{M}=\text{CHR}$  ( $M = \text{Nb, Ta}$ ) and  $(\text{RCH}_2)_3\text{W}\equiv\text{CR}$  with silane gas ( $\text{SiH}_4$ ) to potentially produce silicide materials. A recent Japanese patent described the reaction of a tetraalkyl titanium complex  $\text{Ti}(\text{CH}_2\text{SiMe}_3)_4$  with  $\text{SiH}_4$  and  $\text{H}_2$  to produce titanium silicide materials;<sup>10</sup> however, no studies of the chemistry involved in this reaction have been reported. If such reactions of alkyl complexes with silane proceed via a  $\sigma$ -bond metathesis pathway, it is possible that metal-silyl intermediates may be formed at some stage in the process. By synthesizing metal silyl complexes containing less reactive  $-\text{SiR}_3$  ligands ( $\text{R} = \text{alkyl, silyl}$ ), we hoped to isolate and study the structures and reactivities of these complexes as models for metal silyl intermediates in the reactions with  $\text{SiH}_4$  (Figure 1.1)

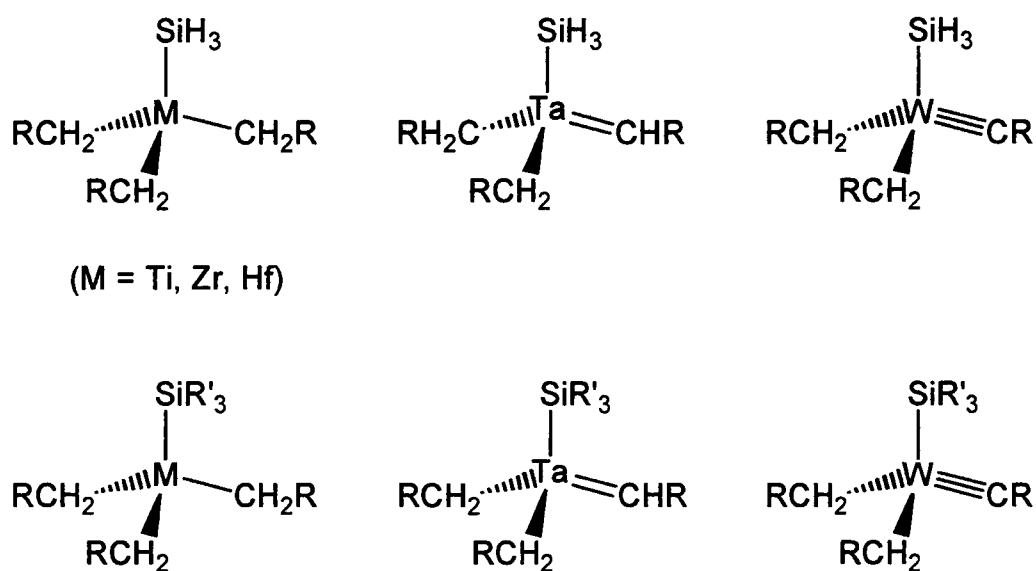


Figure 1.1 Proposed Intermediates in the Formation of Silicide Materials and Model Complexes for These Intermediates

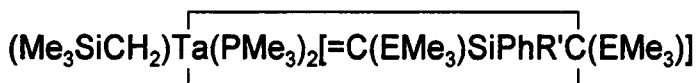
We are particularly interested in studying the reactions of alkyl complexes with silanes in order to understand the fundamental chemistry involved in these reactions. By learning more about the chemistry involved in the transition of a metal alkyl, alkylidene, or alkylidyne complex to a metal silicide material through reaction with silanes, it may be possible to develop novel routes to silicide materials using molecular precursors.

In previous research in our group, a series of early-transition-metal alkyl, alkylidene, and alkylidyne silyl complexes  $(\text{Me}_3\text{ECH}_2)_3\text{MSi}(\text{SiMe}_3)_3$  ( $\text{E} = \text{C}, \text{Si}; \text{M} = \text{Ti}, \text{Zr}$ ),  $(\text{Me}_3\text{ECH}_2)_2\text{Ta}[\text{=CHMe}_3]\text{Si}(\text{SiMe}_3)_3$  ( $\text{E} = \text{C}, \text{Si}$ ), and  $(\text{tBuCH}_2)_2\text{W}[\text{=CBu}^t]\text{Si}(\text{SiMe}_3)_3$  were synthesized and characterized.<sup>11a,b</sup> However, attempts to obtain detailed structural information on the alkyl and alkylidene ligands in  $(\text{Me}_3\text{ECH}_2)_2\text{Ta}[\text{=CHMe}_3]\text{Si}(\text{SiMe}_3)_3$  by X-ray crystallography was prevented by crystallographically imposed 3-fold axes containing the Ta-Si bond in the structures, resulting in a disordering of the alkyl and alkylidene ligands and the refinement of an averaged structure. In an effort to avoid such disorder and also extend the number of Cp-free tantalum alkylidene silyl complexes, we decided to employ the less symmetric  $-\text{SiPh}_2\text{Bu}^t$  ligand. Chapter 2 describes the synthesis and characterization of the thermally unstable tantalum alkylidene silyl complexes  $(\text{Me}_3\text{ECH}_2)_2\text{Ta}[\text{=CHMe}_3]\text{SiPh}_2\text{Bu}^t$  ( $\text{E} = \text{C}, \mathbf{1}; \text{Si}, \mathbf{2}$ ) resulting from this study. Complex **1** was found to decompose over the course of several hours at room temperature by elimination of  $\text{HSiPh}_2\text{Bu}^t$  to give unidentified products, while **2** decomposed within minutes of

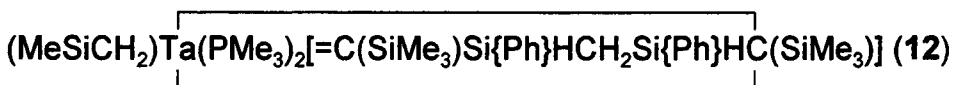
its formation at room temperature also by elimination of  $\text{HSiPh}_2\text{Bu}^t$  to yield a dimeric alkylidyne complex  $(\text{Me}_3\text{SiCH}_2)_4\text{Ta}_2(\mu\text{-CSiMe}_3)_2$ . When **1** or **2** was treated with  $\text{PMe}_3$ , elimination of  $\text{HSiPh}_2\text{Bu}^t$  along with coordination of  $\text{PMe}_3$  occurred to yield bis(phosphine)bis(alkylidene) complexes  $(\text{Me}_3\text{ECH}_2)\text{Ta}(\text{PMe}_3)_2[=\text{CHEMe}_3]_2$  ( $\text{E} = \text{C}$ , **3**;  $\text{Si}$ , **4**). Monitoring of the conversion of **2** to **4** by low temperature NMR showed the reaction to proceed by the formation of a  $\text{PMe}_3$  adduct of **2**,  $(\text{Me}_3\text{SiCH}_2)_2\text{Ta}(\text{PMe}_3)[=\text{CHSiMe}_3]\text{SiPh}_2\text{Bu}^t$  (**5**), followed by the elimination of  $\text{HSiPh}_2\text{Bu}^t$  and the coordination of a second  $\text{PMe}_3$  molecule to give **4**. The previously unreported complex **4** was also characterized by X-ray crystallography.

In the reaction of a tantalum alkyl alkylidene complex with silane, there exist two possible functional groups on tantalum which may react with the silane. To explore this chemistry and understand the factors which may influence the reactivity and mechanisms by which reactions of alkyl and alkylidene ligands occur with silanes, studies of the reactions of phosphine-containing alkylidene complexes  $(\text{Me}_3\text{SiCH}_2)_3\text{Ta}(\text{PMe}_3)[=\text{CHSiMe}_3]$  (**7**) and  $(\text{RCH}_2)\text{Ta}(\text{PMe}_3)_2[=\text{CHR}]_2$  ( $\text{R} = \text{SiMe}_3, \text{Bu}^t$ ) with silanes  $\text{PhR}'\text{SiH}_2$  ( $\text{R}' = \text{Ph}, \text{Me}, \text{H}$ ) were conducted and are discussed in Chapter 3. **7** was found to react with  $\text{PhMeSiH}_2$  or  $\text{Ph}_2\text{SiH}_2$  to give  $\text{H}_2$ ,  $\text{PMe}_3$ , and a disilyl substituted alkylidene complex  $(\text{Me}_3\text{SiCH}_2)_3\text{Ta}=\text{C}(\text{SiMe}_3)\text{SiPhRH}$  ( $\text{R} = \text{Ph}, \text{Me}$ ) (**9**), while  $(\text{Me}_3\text{SiCH}_2)\text{Ta}(\text{PMe}_3)_2[=\text{CHSiMe}_3]_2$  (**4**) and  $(\text{Me}_3\text{SiCH}_2)\text{Ta}(\text{PMe}_3)_2[=\text{CHBu}^t]_2$  (**8**)

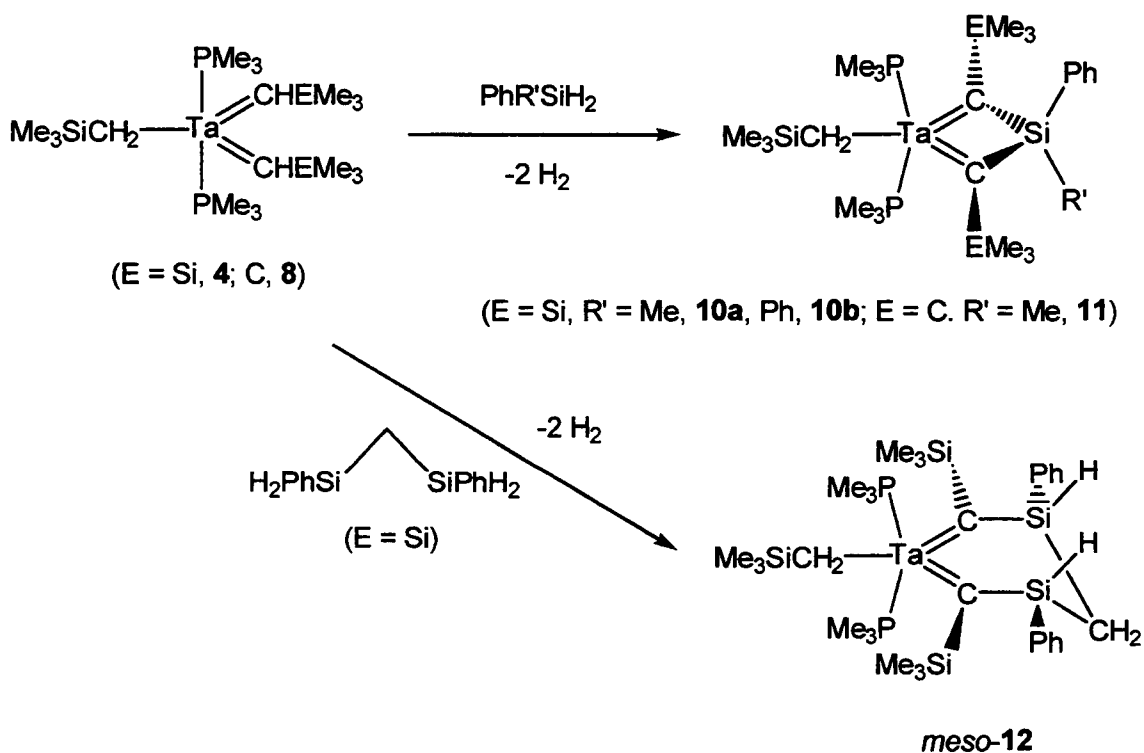
reacted with  $\text{PhR}'\text{SiH}_2$  ( $\text{R}' = \text{Ph}, \text{Me}$ ) and  $\text{PhMeSiH}_2$ , respectively, to produce novel metallasilacyclobutadiene complexes



[ $\text{E} = \text{Si}, \text{R}' = \text{Me}$  (**10a**),  $\text{Ph}$  (**10b**);  $\text{E} = \text{C}, \text{R}' = \text{Me}$ , (**11**)] (Scheme 1.1). In addition, reaction of **4** with the disilylmethane derivative  $(\text{PhSiH}_2)_2\text{CH}_2$  produced a metalladisilacyclohexadiene complex



(Scheme 1.1). Reaction of the neopentylidene complex **3** with  $\text{PhMeSiH}_2$



Scheme 1.1

yielded only  $\text{PMe}_3$ ,  $\text{H}_2$ ,  $\text{CMe}_4$ , and unidentified species, and the neopentylidene complex **11** was found to be unstable in solution, decomposing to  $\text{SiMe}_4$ ,  $\text{PMe}_3$ , and unidentified products. In contrast, the trimethylsilylmethylidene complexes **10a-b** were found to be stable indefinitely both in the solid state and in solution. Complexes **10a**, **10b**, **11**, and **12** were characterized by X-ray crystallography.

The selectivity of the reactions of only the alkylidene ligands of **4**, **7**, and **8** with phenyl-containing silanes was unexpected and prompted us to study the mechanism of these novel reactions, the results of which are presented in Chapter 4. Kinetic studies of the reaction of **7** with  $\text{PhMeSiH}_2$  and  $\text{PhMeSiD}_2$  were found to be consistent with a dissociative mechanism involving loss of the phosphine ligand before rate controlling reaction of the alkylidene ligand with the silane. In addition, deuterium labeling studies revealed that the hydrogen produced in this reaction was predominantly  $\text{D}_2$ , and H incorporation into unreacted  $\text{PhMeSiD}_2$  was observed when excess silane was employed in the reaction. This led us to propose a mechanism which is consistent with these findings involving hydride and silyl intermediates.

In addition to the reactions of alkyl, alkylidene, or alkylidyne complexes with  $\text{SiH}_4$  in a CVD process as a possible molecular route to metal silicide materials, the use of a early-transition-metal poly- or persilyl complex as a single source precursor to silicides may offer additional benefits over the above route, including the elimination of the need to utilize a pyrophoric reactant

(SiH<sub>4</sub>), and the possibility of tailoring the precursor to produce silicide materials of specific metal to silicon stoichiometries. Metal silyl complexes have seen limited use as single source precursors in the production of middle- and late-transition-metal silicides;<sup>9</sup> however, preparation of early-transition-metal poly- and persilyl complexes is a considerable synthetic challenge, owing primarily to the tendency of multiple silyl groups on an early-transition-metal center to reductively eliminate from the metal as disilanes. Until recently, the only isolated polysilyl complexes of the early-transition-metals employed Cp ligands as stabilizing groups. We have recently prepared the first isolated Cp-free early-transition-metal disilyl complexes Li(THF)<sub>4</sub>(Me<sub>2</sub>N)<sub>3</sub>Zr(SiPh<sub>2</sub>Bu<sup>t</sup>)<sub>2</sub> and (Me<sub>2</sub>N)<sub>3</sub>Ta[Si(SiMe<sub>3</sub>)<sub>3</sub>]<sub>2</sub> as part of studies of amido complexes as possible precursors to silicides.<sup>6c</sup> There have been two previous reports of *d*<sup>0</sup> early-transition-metal persilyl complexes: the first, Ti(SiPh<sub>3</sub>)<sub>4</sub>, was later found to be Ti(OSiPh<sub>3</sub>)<sub>4</sub>,<sup>12</sup> and Ti(SiMe<sub>3</sub>)<sub>4</sub> was reported to exist at -78 °C, but no characterization data were given for this complex.<sup>13</sup>

To overcome the problem of reductive elimination of silyl groups from the metal center, we decided to use chelating ligands with two silyl functionalities such as MSi(SiMe<sub>3</sub>)<sub>2</sub>[CH<sub>2</sub>]<sub>n</sub>(SiMe<sub>3</sub>)<sub>2</sub>SiM (M = Li, K) with *n* chosen such that reductive elimination would result in the formation of a strained ring, such as a disilacyclopropane or -butane. We anticipated that this would increase the activation barrier for reductive elimination and lower the likelihood of such a reaction. In addition, it was hoped that the entropic advantages of a



chelating ligand would further help stabilize metal complexes containing these ligands. The results of this study are presented in Chapter 5. Previously unreported compounds  $[(\text{Me}_3\text{Si})_3\text{Si}]_2\text{CH}_2$  (**18**) and  $(\text{Me}_3\text{Si})_3\text{SiCH}_2\text{CH}_2\text{Si}(\text{SiMe}_3)_3$  (**19**) were prepared as ligand precursors.

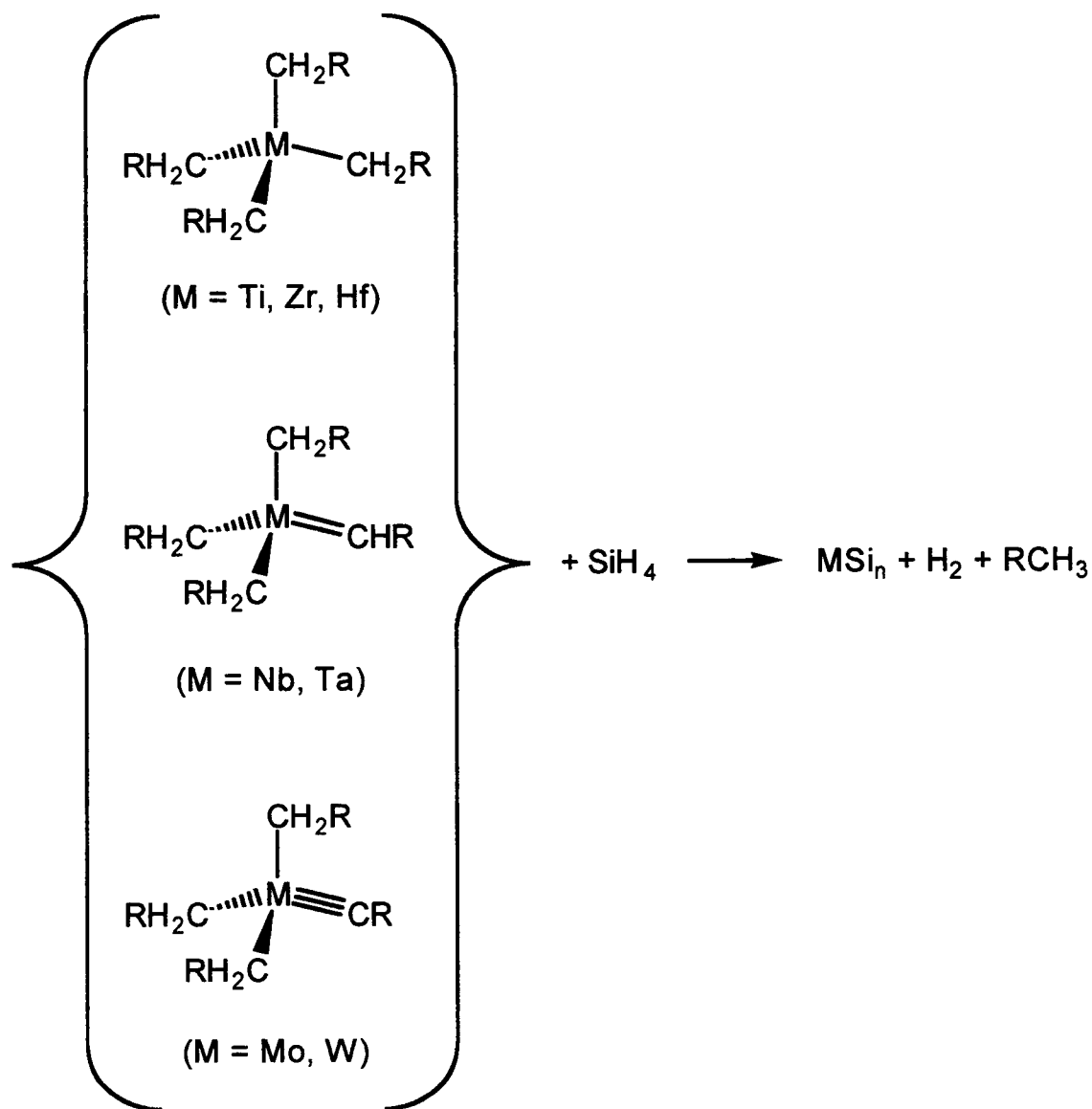
## CHAPTER 2

# Synthesis of Thermally Unstable Tantalum Silyl Alkylidene Complexes and Reactivity of These Complexes with $\text{PMe}_3$

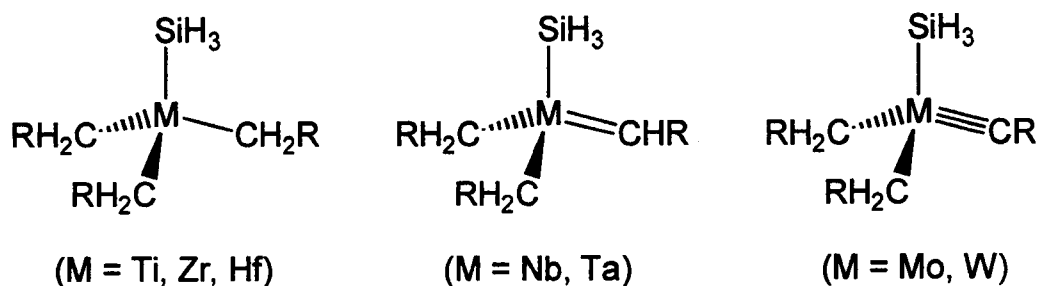
### 2.1 Introduction

Early-transition-metal silyl chemistry, while still less studied than early-transition-metal alkyl, alkylidene, and alkylidyne chemistry, has seen an ever increasing interest over the past two decades.<sup>2</sup> Studies in this area have focused on syntheses of metal-silyl complexes, as well as catalytic properties of silyl complexes in areas such as polysilane synthesis and hydrosilation of alkenes and alkynes.<sup>2d-e,14</sup>

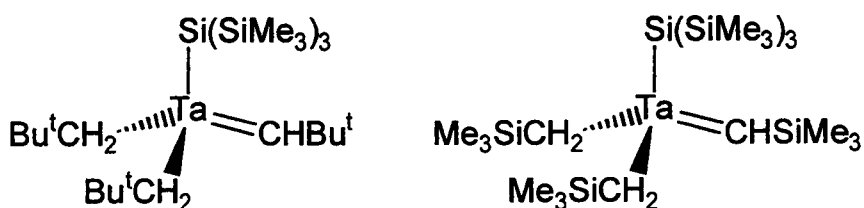
The majority of early-transition-metal silyl complexes contain  $\pi$ -anionic ancillary ligands, such as  $\eta^5$ -cyclopentadienyl (Cp);<sup>2,14</sup> only a handful of complexes free of such ligands have been reported.<sup>4-7,11</sup> Our interest in Cp-free silyl complexes initially arose from our investigations of molecular routes to metal silicide materials through the reactions of early-transition-metal alkyl, alkylidene, and alkylidyne complexes with silane ( $\text{SiH}_4$ ) (Scheme 2.1).<sup>10</sup> In such reactions, possible intermediates may include metal-silyl complexes shown in Scheme 2.2. Such intermediates would be expected to be highly reactive and thus difficult to observe. By synthesizing models for these



Scheme 2.1



Scheme 2.2



Scheme 2.3

intermediates, we hoped to be able to study the structure, bonding and reactivity of these model complexes with an aim towards gaining a better understanding of possible mechanistic pathways in the formation of silicide materials.

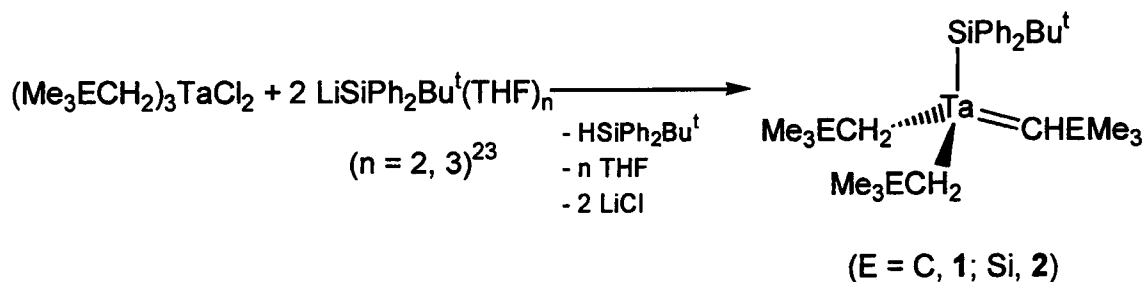
In work previously done in our group, two new Cp-free tantalum silyl alkylidene complexes were synthesized and characterized (Scheme 2.3).<sup>11a,b</sup> These complexes represented the first known stable alkylidene silyl complexes of the early transition metals. However, attempts to structurally characterize these complexes by X-ray crystallography were hindered by the presence of a crystallographically imposed 3-fold axis through the tantalum-silicon bond, which led to disordering of the alkyl and alkylidene ligands and the refinement

of an averaged structure. Thus we endeavored to synthesize other silyl alkylidene complexes with a twofold interest: (1) to expand this family of Cp-free silyl alkylidene complexes, and (2) to utilize a silyl ligand of lower symmetry to minimize the possibility of disorder in structural studies of these complexes. The tert-butyl-diphenylsilyl ligand  $-\text{SiPh}_2\text{Bu}^t$  was chosen for use in this study due to its ease of synthesis from readily available starting materials.<sup>23</sup> While the thermal instability of the tantalum silyl alkylidene complexes formed with this ligand precluded any structural studies, reaction of these complexes with trimethylphosphine led to some interesting and novel chemistry which is discussed below.

## 2.2 Results and Discussion

### 2.2.1 Synthesis and Characterization of $(\text{Me}_3\text{ECH}_2)_2\text{Ta}[\text{=CHMe}_3]\text{SiPh}_2\text{Bu}^t$ (E = C, Si)

The reaction of 2 equivalents of the lithium silylating reagent  $\text{LiSiPh}_2\text{Bu}^t(\text{THF})_3$ <sup>23</sup> with trialkyl tantalum dichloride  $(\text{Me}_3\text{ECH}_2)_3\text{TaCl}_2$ <sup>11b,22</sup> gave the silyl alkylidene complexes  $(\text{Me}_3\text{ECH}_2)_2\text{Ta}[\text{=CHMe}_3]\text{SiPh}_2\text{Bu}^t$  [E = C, **1**; Si, **2**] (Scheme 2.4). Complexes **1** and **2** were found to be thermally unstable. **1** decomposed slowly over the course of several hours in solution at room temperature by loss of  $\text{HSiPh}_2\text{Bu}^t$  (as monitored by <sup>1</sup>H NMR) to give unidentified products. **2** decomposed within minutes of its formation in solution at room temperature to form  $\text{HSiPh}_2\text{Bu}^t$  and  $(\text{Me}_3\text{SiCH}_2)_4\text{Ta}_2(\mu\text{-CSiMe}_3)_2$

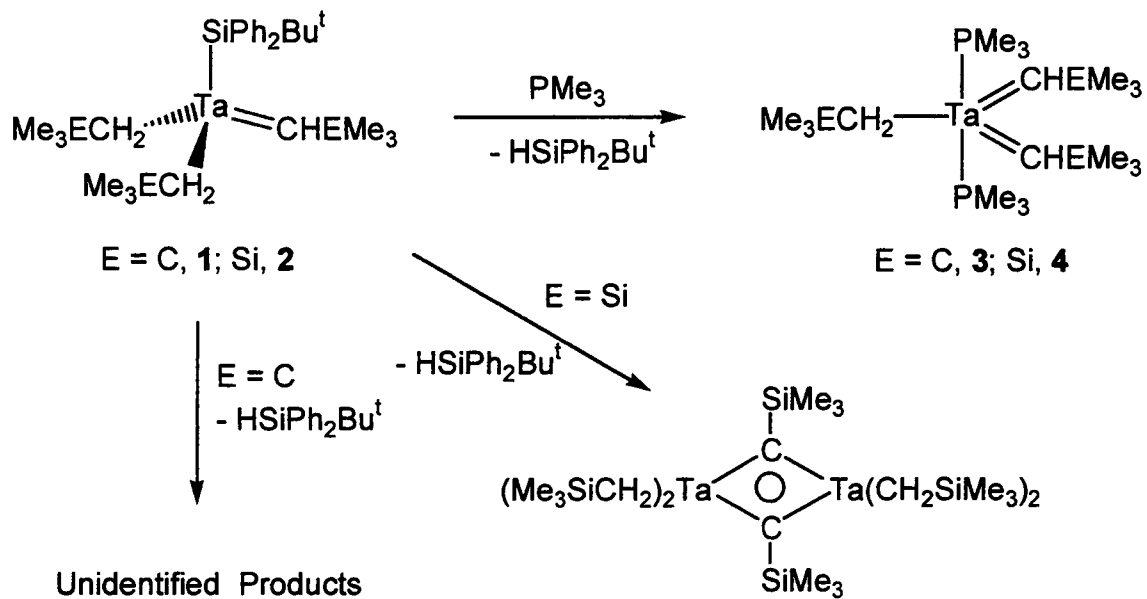


Scheme 2.4

(Scheme 2.5).<sup>15</sup> In both cases decomposition was observed to occur via a preferential silane elimination over alkane elimination. In comparison, the analogous complexes  $(\text{Me}_3\text{ECH}_2)_2\text{Ta}[\text{=CHEMe}_3]\text{Si}(\text{SiMe}_3)_3$  (E = C, Si) were found to be stable at room temperature.<sup>11a,b</sup>

Complexes **1** and **2** may be synthesized *in situ* at low temperatures in aromatic, aliphatic and ether solvents. Although **1** is stable for hours at room temperature, all attempts to isolate **1** at low temperature by crystallization from toluene, aliphatic solvents, or Et<sub>2</sub>O were unsuccessful. No attempts were made to isolate **2** due to its low stability at room temperature. Both complexes **1** and **2** are red-orange in solution.

Complexes **1** and **2** are stable for much longer periods of time in solution at -50 °C and have been characterized at this temperature by <sup>1</sup>H, <sup>13</sup>C{<sup>1</sup>H}, and <sup>13</sup>C-<sup>1</sup>H HETCOR NMR. The spectroscopic properties of the complexes are consistent with the structure assignments. The Ta=CHEMe<sub>3</sub> resonances for **1** and **2** appear at δ 2.84 (**1**) and 7.41 (**2**) ppm in the <sup>1</sup>H NMR spectrum as well as at δ 269.0 (**1**) and 271.1 (**2**) in the <sup>13</sup>C spectrum, respectively; the <sup>13</sup>C

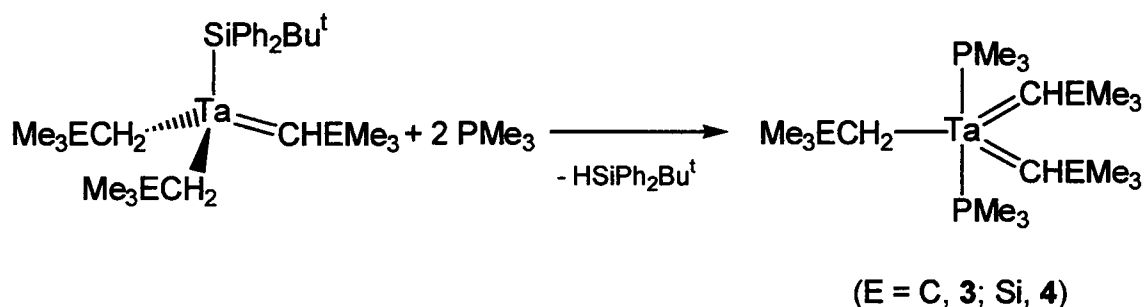


Scheme 2.5

resonances appear as doublets in the gated-decoupled  $^{13}\text{C}$  NMR spectra with C-H coupling constants of 87.0 and 90.8 Hz. In addition, the  $\alpha$ -protons of the alkyl groups are diastereotopic and appear as two doublets separated by 0.86 ppm (1) and 1.18 ppm (2) in the  $^1\text{H}$  NMR spectra. Similar large chemical shift differences were observed in the alkyl resonances of the analogous complexes  $(\text{Me}_3\text{ECH}_2)_2\text{Ta}[\text{=CHMe}_3]\text{Si}(\text{SiMe}_3)_3$  ( $\text{E} = \text{C}, \text{Si}$ ),  $^{11\text{b}}$  and may be attributed to the diamagnetic anisotropy of the metal-carbon multiple bonds.

### 2.2.2 Reactions of 1 and 2 with Trimethylphosphine

In an attempt to stabilize 1 and 2, the reactions of these complexes with  $\text{PMe}_3$  were studied. Treatment of a solution of either 1 or 2 (generated *in situ* at  $-70\text{ }^\circ\text{C}$ ) with excess  $\text{PMe}_3$  resulted in the reaction of 2 equivalents of  $\text{PMe}_3$  with 1 or 2 to give bis(phosphine)bis(alkylidene) complexes  $(\text{Me}_3\text{ECH}_2)_2\text{Ta}(\text{PMe}_3)_2[\text{=CHMe}_3]_2$  [ $\text{E} = \text{C}$ , 3; $^{16}$  Si, 4], along with one equivalent



Scheme 2.6



of  $\text{HSiPh}_2\text{Bu}^t$  (Scheme 2.6). Again, preferential silane elimination from **1** and **2** was observed. It is interesting to note that silane elimination from **2** in the absence of  $\text{PMe}_3$  yielded a product having *two* alkyl and *one* alkylidyne ligands per metal atom, while silane elimination from **2** in the presence of  $\text{PMe}_3$  yielded a product with *one* alkyl and *two* alkylidene ligands (Scheme 2.5). To our knowledge, this is the first case in which the formation of an alkyl alkylidyne complex, through the thermal decomposition of **2**, and phosphine-promoted formation of a bis(alkylidene) complex from the same complex are observed. No reaction was observed between **1** and the bulkier phosphine  $\text{PPh}_3$ . Schrock and coworkers have reported that the reaction of the alkyl alkylidene complex  $(\text{Me}_3\text{CCH}_2)_3\text{Ta}=\text{CHCMe}_3$  with  $\text{PMe}_3$  gives **3**.<sup>16</sup>

In the NMR spectra of **4**, the alkylidene resonances were found to be fluxional and chemically inequivalent at room temperature, appearing as two broad singlets at  $\delta$  7.92 and 7.06 ppm for the  $=\text{CHSiMe}_3$  resonances, and two broad singlets at 0.34 and 0.16 ppm for the  $=\text{CHSiMe}_3$  resonances. Variable temperature  $^1\text{H}$  NMR spectra of **4** are shown in Figure 2.1. Cooling a solution of **4** resulted in a sharpening of the  $=\text{CHSiMe}_3$  resonances, and the signal at 7.92 ppm resolved into a virtual triplet due to coupling of the alkylidene proton to the phosphine ligands. Increasing the temperature resulted in a coalescence of the alkylidene resonances at 60 °C, which sharpened into a single peak at 90 °C. The fact that the signals from the  $\alpha$ -protons of the alkyl and alkylidene ligands did not coalesce into a single signal indicates that the

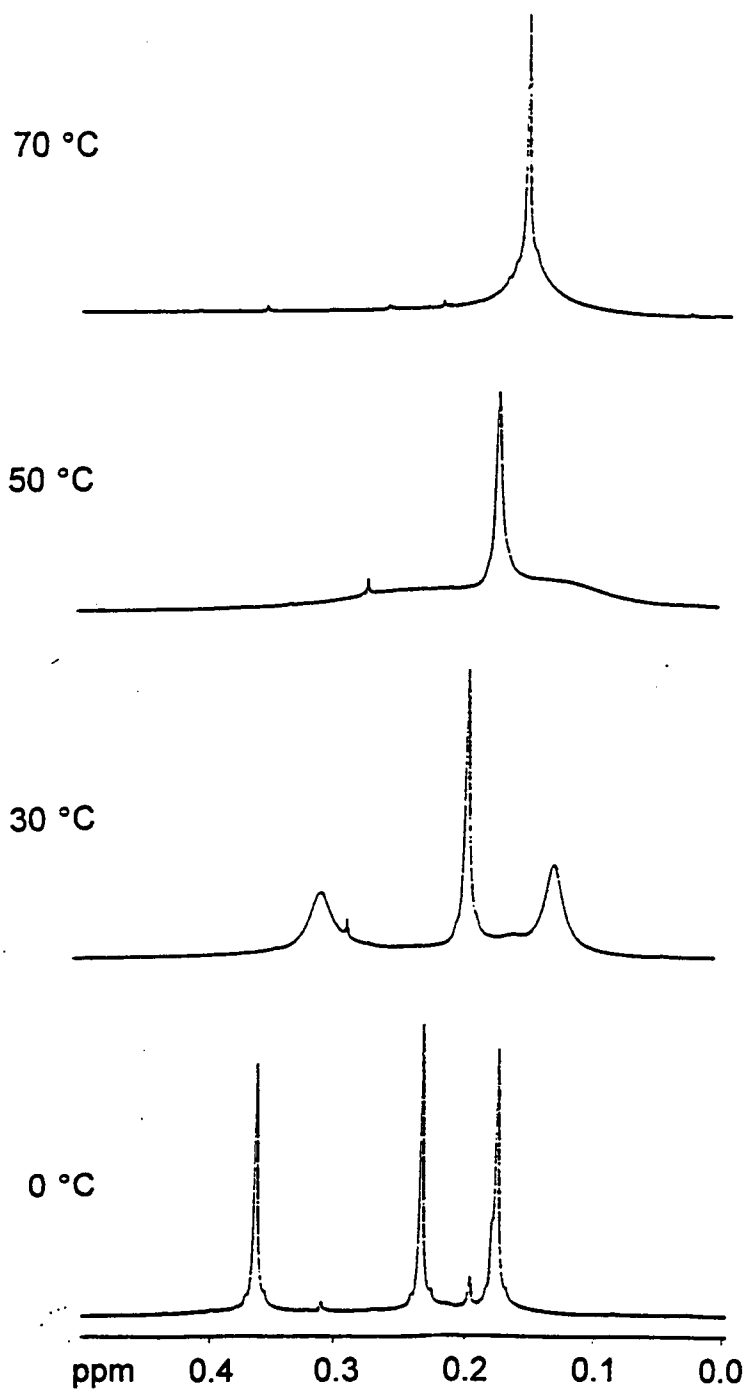
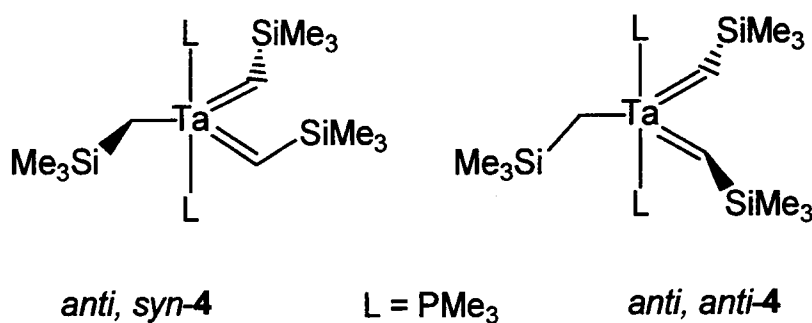


Figure 2.1 Variable temperature NMR spectra of 4

fluxional process involves the alkylidene ligands only. In addition, at temperatures below room temperature, a set of resonances due to a second isomer of **4** appeared in which both alkylidene ligands were chemically equivalent. It thus appears that the fluxional process observed in the NMR spectra of **4** is due to restricted rotation of the M=C bonds: the isomer observed at room temperature and above being one with the tantalum atom in a trigonal pyramidal geometry with axial phosphine ligands and the alkyl/alkylidene ligands arranged in a "pinwheel" conformation (Scheme 2.7). At low temperatures, the bond rotation is essentially frozen, resulting in the observation of a second isomer in which the alkylidene ligands are in an *anti,anti*-conformation. Such an *anti,anti*-conformation has been observed in an osmium bis(alkylidene) complex  $(\text{Me}_3\text{CCH}_2)_2\text{Os}[\text{=CHCMe}_3]_2$ <sup>17</sup> as well as a tungsten silyl bis(alkylidene) complex  $(\text{Me}_3\text{CCH}_2)\text{W}[\text{=CHCMe}_3]_2\text{SiPh}_2\text{Bu}^\dagger$ <sup>11h</sup>

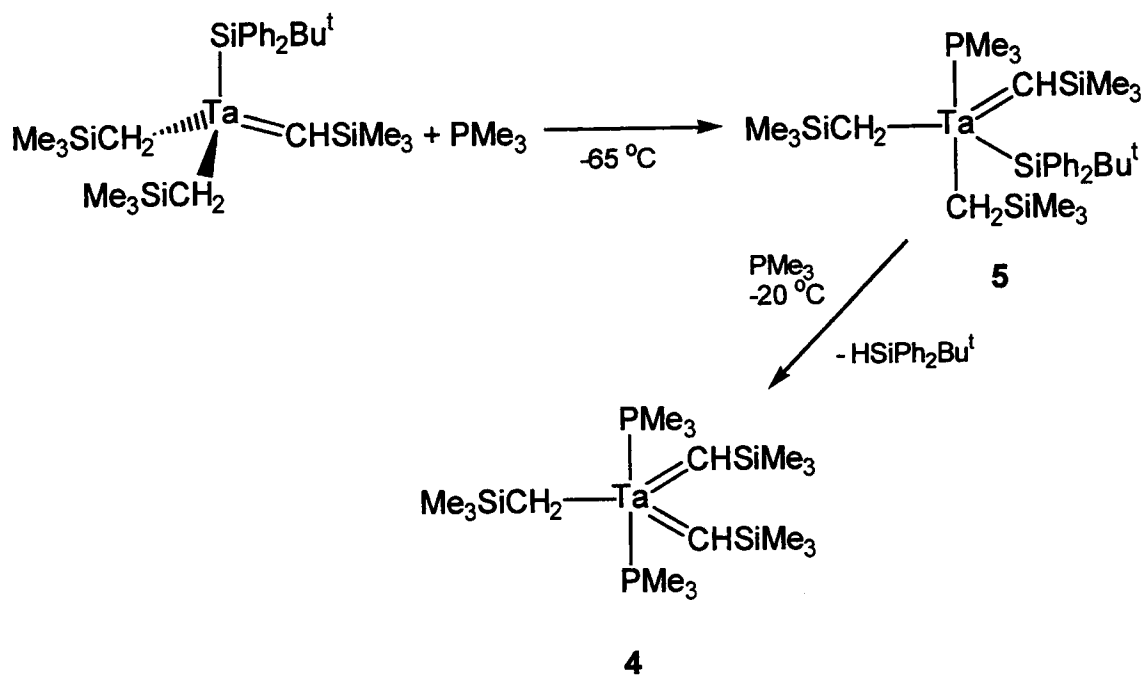


Scheme 2.7

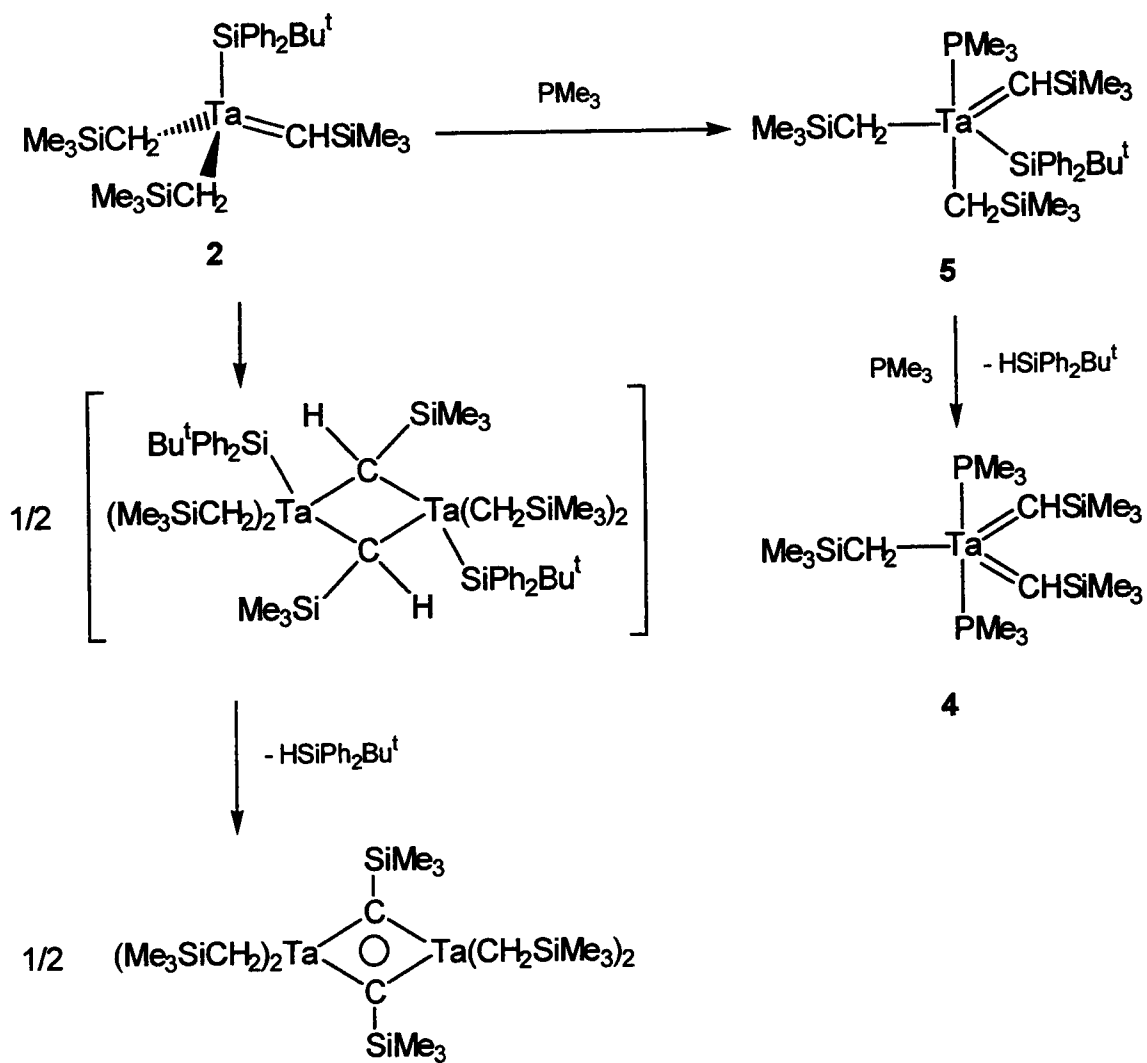
The pinwheel conformation of the alkyl and alkylidene ligands in **4** is confirmed by an X-ray crystal structure, which is discussed in Section 2.2.3.

When the reaction of **2** with  $\text{PMe}_3$  was conducted in an NMR tube at  $-65$  °C and monitored by NMR, a phosphine adduct of **2** ( $(\text{Me}_3\text{SiCH}_2)_2\text{Ta}(\text{PMe}_3)[=\text{CHSiMe}_3]\text{SiPh}_2\text{Bu}^t$  (**5**) was observed to form rapidly after the addition of  $\text{PMe}_3$  to **2** (Scheme 2.8). Warming the solution to  $-20$  °C resulted in the conversion of **5** to **4**; no further intermediates were observed.

Possible mechanisms for the decomposition of **2** are shown in Scheme 2.9. In the absence of  $\text{PMe}_3$ , the thermal decomposition of **2** may take a path that involves the initial dimerization of **2** through the coordination of the alkylidene ligands, followed by an  $\alpha$ -hydrogen abstraction between the silyl ligands and the bridging alkylidene ligands to give an alkylidyne bridged complex. However, the initial coordination of  $\text{PMe}_3$  to **2** to form **5** may make the tantalum atom less electron deficient and more sterically crowded, making dimerization unfavorable. Subsequent  $\alpha$ -hydrogen abstraction between the silyl ligand and an alkyl ligand, followed by rapid coordination of a second  $\text{PMe}_3$  molecule, gives **4**. An alternative mechanism involving an  $\alpha$ -hydrogen abstraction between the silyl ligand and the alkylidene ligand to give an alkylidyne bis(alkyl) intermediate  $(\text{Me}_3\text{SiCH}_2)_2\text{Ta}[\equiv\text{CSiMe}_3](\text{PMe}_3)_2$ , followed by an  $\alpha$ -hydrogen exchange between an alkyl and the alkylidyne ligands, is less likely. No such  $\alpha$ -hydrogen exchange was observed in  $(\text{Me}_3\text{CCD}_2)\text{Ta}(\text{PMe}_3)_2[=\text{CHCMe}_3]_2$ .<sup>16a</sup>

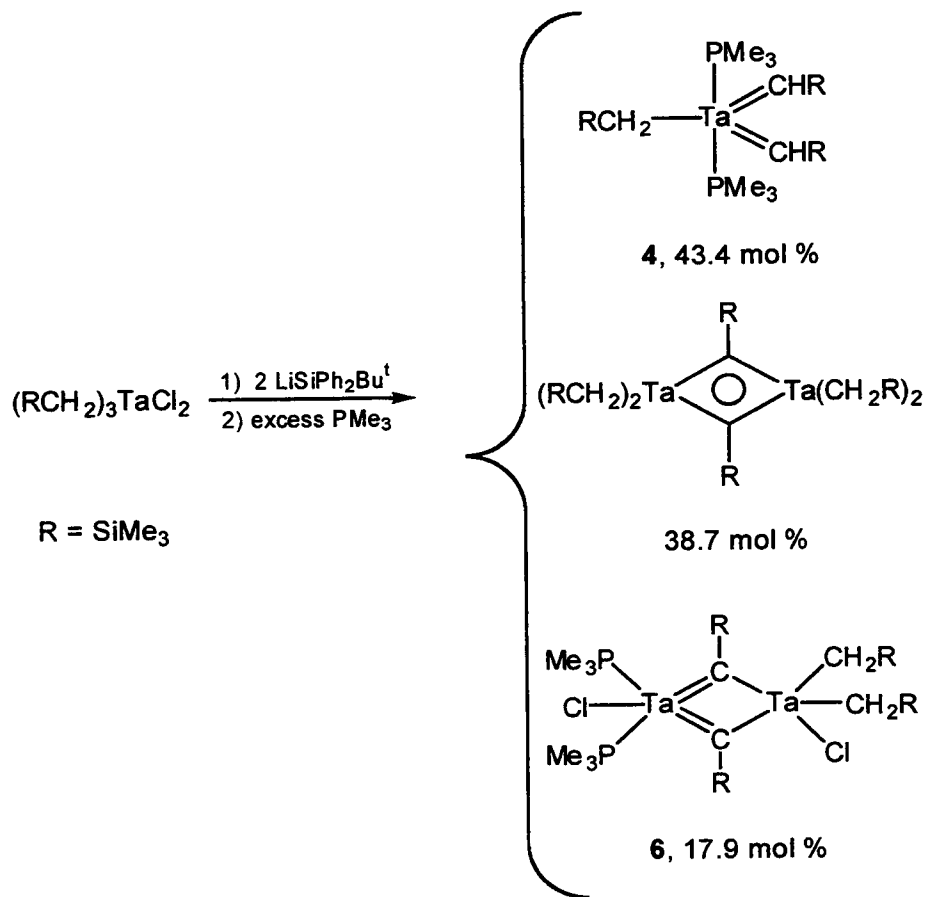


Scheme 2.8



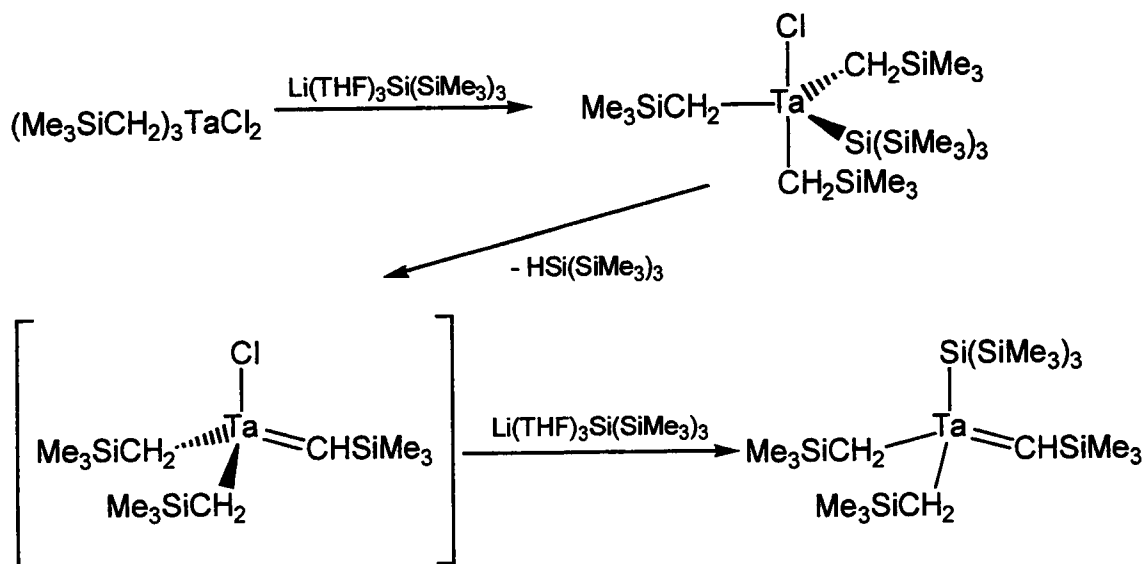
Scheme 2.9

When the reaction of  $(\text{Me}_3\text{SiCH}_2)_3\text{TaCl}_2$  with 2 equivalents of  $\text{LiSiPh}_2\text{Bu}^t(\text{THF})_3$  was followed immediately by the addition of excess  $\text{PMe}_3$ , a mixture of **4**,  $(\text{Me}_3\text{SiCH}_2)_4\text{Ta}_2(\mu\text{-CSiMe}_3)_2$ , and  $(\text{Me}_3\text{P})_2\text{ClTa}(\mu\text{-CSiMe}_3)_2\text{TaCl}(\text{CH}_2\text{SiMe}_3)_2$  (**6**)<sup>18</sup> was obtained (Scheme 2.10). The formation of complex **6** is particularly noteworthy. Mechanistic studies of the formation of the silyl alkylidene complex  $(\text{Me}_3\text{SiCH}_2)_2\text{Ta}[\text{=CHSiMe}_3]\text{Si}(\text{SiMe}_3)_3$  conducted previously in our group showed that the first step in this reaction was replacement of one of the chlorides in  $(\text{Me}_3\text{SiCH}_2)_3\text{TaCl}_2$  to give a chlorotrialkyl tantalum silyl intermediate  $(\text{Me}_3\text{SiCH}_2)_3\text{Ta}[\text{Cl}]\text{Si}(\text{SiMe}_3)_3$ , which then eliminated  $\text{HSi}(\text{SiMe}_3)_3$  to give a chlorodialkyl tantalum alkylidene intermediate “ $(\text{Me}_3\text{SiCH}_2)_2\text{Ta}[\text{=CHSiMe}_3]\text{Cl}$ ” (Scheme 2.11).<sup>11b</sup> Replacement of the chloride ligand by a second equivalent of  $\text{Li}(\text{THF})_3\text{Si}(\text{SiMe}_3)_3$  gave the silyl alkylidene complex. In a related study, it was found that the addition of 2 equivalents of anhydrous  $\text{HCl}$  to the bis(alkylidyne) complex  $(\text{Me}_3\text{SiCH}_2)_4\text{Ta}_2(\mu\text{-CSiMe}_3)_2$  yielded a dimeric bis(alkylidene) complex  $(\text{Me}_3\text{SiCH}_2)_4\text{Ta}_2\text{Cl}_2[\text{=CHSiMe}_3]_2$ , which is the dimer of the yet unobserved “ $(\text{Me}_3\text{SiCH}_2)_2\text{Ta}[\text{=CHSiMe}_3]\text{Cl}$ ”.<sup>18</sup> Reaction of this dimeric bis(alkylidene) complex with  $\text{LiSiR}_3$  [ $\text{SiR}_3 = \text{Si}(\text{SiMe}_3)_3, \text{SiPh}_2\text{Bu}^t$ ] or  $\text{PMe}_3$  led to the formation of  $(\text{Me}_3\text{SiCH}_2)_4\text{Ta}_2(\mu\text{-CSiMe}_3)_2$  or **6**, respectively. In the current study, the isolation of  $(\text{Me}_3\text{SiCH}_2)_4\text{Ta}_2(\mu\text{-CSiMe}_3)_2$  and **6** from the reaction of  $(\text{Me}_3\text{SiCH}_2)_3\text{TaCl}_2$  and 2 equivalents of  $\text{Li}(\text{THF})_n\text{SiPh}_2\text{Bu}^t$ <sup>23</sup> in the presence of  $\text{PMe}_3$  is consistent with the presence of  $(\text{Me}_3\text{SiCH}_2)_4\text{Ta}_2\text{Cl}_2[\text{=CHSiMe}_3]_2$ , and



Scheme 2.10



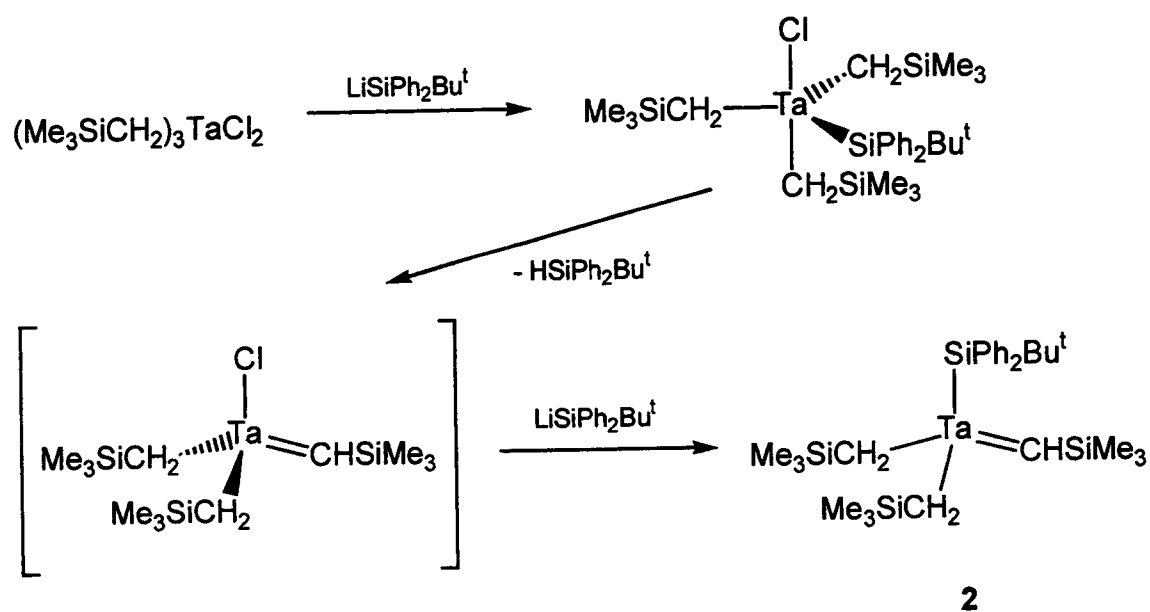


Scheme 2.11

thus “ $(\text{Me}_3\text{SiCH}_2)_2\text{Ta}[\text{=CHSiMe}_3]\text{Cl}$ ”, in the reaction solution. This result indicates that the mechanism for the formation of **2** may follow a pathway similar to that found in the formation of  $(\text{Me}_3\text{SiCH}_2)_2\text{Ta}[\text{=CHSiMe}_3]\text{Si}(\text{SiMe}_3)_3$ : replacement of a chloride ligand in  $(\text{Me}_3\text{SiCH}_2)_3\text{TaCl}_2$  followed by the loss of  $\text{HSiPh}_2\text{Bu}^t$  to give  $(\text{Me}_3\text{SiCH}_2)_2\text{Ta}[\text{=CHSiMe}_3]\text{Cl}$ . Replacement of the remaining chloride by  $-\text{SiPh}_2\text{Bu}^t$  gives **2**. These reactions are summarized in Scheme 2.12.

### 2.2.3 X-ray Crystal Structure of **4**

Slow cooling of a hexanes solution of **4** resulted in single crystals suitable for an X-ray diffraction study. The molecular structure of **4** is shown in Figure 2.2. During refinement of the structure of **4**, a two site positional



Scheme 2.12

disorder involving two of the  $\alpha$ -carbons of the alkyl/alkylidene ligands [C(2) and C(3) in Figure 2.2] was found, and was resolved by refining two positions at each site with site occupancy factors of 0.5. Crystal data, results of analyses, and selected bond distances and angles are given in Tables 2.1-2.3.

Complex 4 adopts a distorted trigonal-bipyramidal geometry in the solid state, with  $\text{PMe}_3$  ligands occupying axial positions. The angle between the phosphorus atoms is nearly  $180^\circ$  [ $175.73(7)^\circ$ ]. The P-Ta-C angles range from  $86.0(6)^\circ$  to  $91.9(2)^\circ$ , and the C-Ta-C angles range from  $114.0(6)^\circ$  to  $129.3(8)^\circ$ . The alkylidene M=C bonds range from  $1.95(2) \text{ \AA}$  to  $1.998(8) \text{ \AA}$ , and are consistent with other alkylidene complexes of tantalum which have been structurally characterized [ $1.932(7)$  and  $1.955(7) \text{ \AA}$  in  $\text{Ta}(\text{=CHBu}^t)_2(\text{mesityl})(\text{PMe}_3)_2$ ,<sup>19</sup>  $1.89(3)$  in

**Table 2.1. Crystal Data for 4**

---

formula	$C_{18}H_{49}P_2Si_3Ta$	
formula weight	592.73	
crystal size (mm)	0.80 x 0.60 x 0.40	
temperature (K)	173(2)	
crystal system	Monoclinic	
space group	$P2_1/c$	
lattice parameters	$a = 10.504(4) \text{ \AA}$	$\alpha = 90^\circ$
	$b = 16.699(6) \text{ \AA}$	$\beta = 91.84(3)^\circ$
	$c = 16.848(7) \text{ \AA}$	$\gamma = 90^\circ$
volume, $\text{\AA}^3$	2954(2)	
Z	4	
density (calc) ( $\text{g/cm}^3$ )	1.333	
$\mu$ ( $\text{mm}^{-1}$ )	3.952	
$F(000)$	1196	
scan type	$\omega$ -2 $\theta$	
$\theta$ range (deg)	1.72-22.54	
index ranges	$h, k, \pm l$	
unique reflections	3886 ( $R_{\text{int}} = 0.0840$ )	
parameters varied	216	
R indices	0.0333 ( $R_w F^2 = 0.1123$ )	
goodness-of-fit on $F^2$	1.026	

---

**Table 2.2. Interatomic Distances (Å) in 4**

---

Ta-P(1)	2.583(2)	Ta-P(2)	2.581(2)
Ta-C(1)	1.998(8)	Ta-C(2)	2.21(2)
Ta-C(3)	1.95(2)	Ta-C(2A)	1.95(2)
Ta-C(3A)	2.30(2)	P(1)-C(4)	1.813(9)
P(1)-C(5)	1.808(8)	P(1)-C(6)	1.804(9)
P(2)-C(7)	1.819(11)	P(2)-C(8)	1.811(10)
P(2)-C(9)	1.810(11)	Si(1)-C(10)	1.852(10)
Si(1)-C(11)	1.856(9)	Si(1)-C(12)	1.874(10)
Si(2)-C(2)	1.86(2)	Si(2)-C(2A)	1.85(2)
Si(3)-C(3)	1.87(2)	Si(3)-C(3A)	1.82(2)
Si(2)-C(13)	1.891(8)	Si(2)-C(14)	1.850(9)
Si(2)-C(15)	1.846(10)	Si(3)-C(16)	1.849(9)
Si(3)-C(17)	1.868(9)	Si(3)-C(18)	1.844(9)

---

**Table 2.3. Intramolecular Bond Angles (°) in 4**

---

C(2A)-Ta-C(3)	121.6(9)	C(2A)-Ta-C(1)	121.5(7)
C(3)-Ta-C(1)	116.8(6)	C(3)-Ta-C(2)	129.3(8)
C(1)-Ta-C(2)	114.0(6)	C(2A)-Ta-C(3A)	115.6(9)
C(1)-Ta-C(3A)	112.9(6)	C(2)-Ta-C(3A)	123.0(8)
C(2A)-Ta-P(2)	88.6(6)	C(3)-Ta-P(2)	86.0(6)
C(1)-Ta-P(2)	91.8(2)	C(2)-Ta-P(2)	91.6(6)
C(3A)-Ta-P(2)	90.5(5)	C(2A)-Ta-P(1)	91.9(2)
C(3)-Ta-P(1)	90.4(6)	C(1)-Ta-P(1)	91.9(2)
C(2)-Ta-P(1)	88.8(6)	C(3A)-Ta-P(1)	85.7(5)
P(2)-Ta-P(1)	175.73(7)	C(4)-P(1)-C(6)	101.4(4)
C(4)-P(1)-C(5)	103.5(5)	C(6)-P(1)-C(5)	102.0(5)
C(4)-P(1)-Ta	117.1(3)	C(5)-P(1)-Ta	114.8(3)
C(6)-P(1)-Ta	115.9(3)	C(8)-P(2)-C(7)	101.4(5)
C(8)-P(2)-C(9)	102.8(6)	C(7)-P(2)-C(9)	102.5(6)
C(7)-P(2)-Ta	115.8(4)	C(8)-P(2)-Ta	115.8(4)
C(9)-P(2)-Ta	116.3(4)	C(10)-Si(1)-C(1)	111.2(4)
C(10)-Si(1)-C(11)	107.6(6)	C(1)-Si(1)-C(11)	112.1(4)
C(10)-Si(1)-C(12)	107.0(5)	C(1)-Si(1)-C(12)	111.1(4)
C(11)-Si(1)-C(12)	107.5(4)	C(3A)-Si(3)-C(18)	105.9(8)
C(3)-Si(3)-C(16)	107.6(7)	C(3A)-Si(3)-C(16)	119.9(7)
C(3)-Si(3)-C(18)	117.9(7)	C(18)-Si(3)-C(16)	107.4(5)

**Table 2.3 (continued)**

---

C(3A)-Si(3)-C(17)	109.3(7)	C(3)-Si(3)-C(17)	110.4(7)
C(18)-Si(3)-C(17)	104.7(5)	C(16)-Si(3)-C(17)	108.6(5)
C(15)-Si(2)-C(2)	106.0(8)	C(15)-Si(2)-C(14)	106.9(6)
C(2)-Si(2)-C(14)	111.1(8)	C(15)-Si(2)-C(2A)	115.6(8)
C(14)-Si(2)-C(2A)	112.9(8)	C(15)-Si(2)-C(13)	107.2(5)
C(2)-Si(2)-C(13)	118.9(8)	C(14)-Si(2)-C(13)	106.2(5)
C(2A)-Si(2)-C(13)	107.5(8)	Si(1)-C(1)-Ta	133.7(5)
Si(2)-C(2A)-Ta	144.2(13)	Si(2)-C(2)-Ta	124.6(12)
Si(3)-C(3)-Ta	142.0(13)	Si(3)-C(3A)-Ta	122.2(11)

---

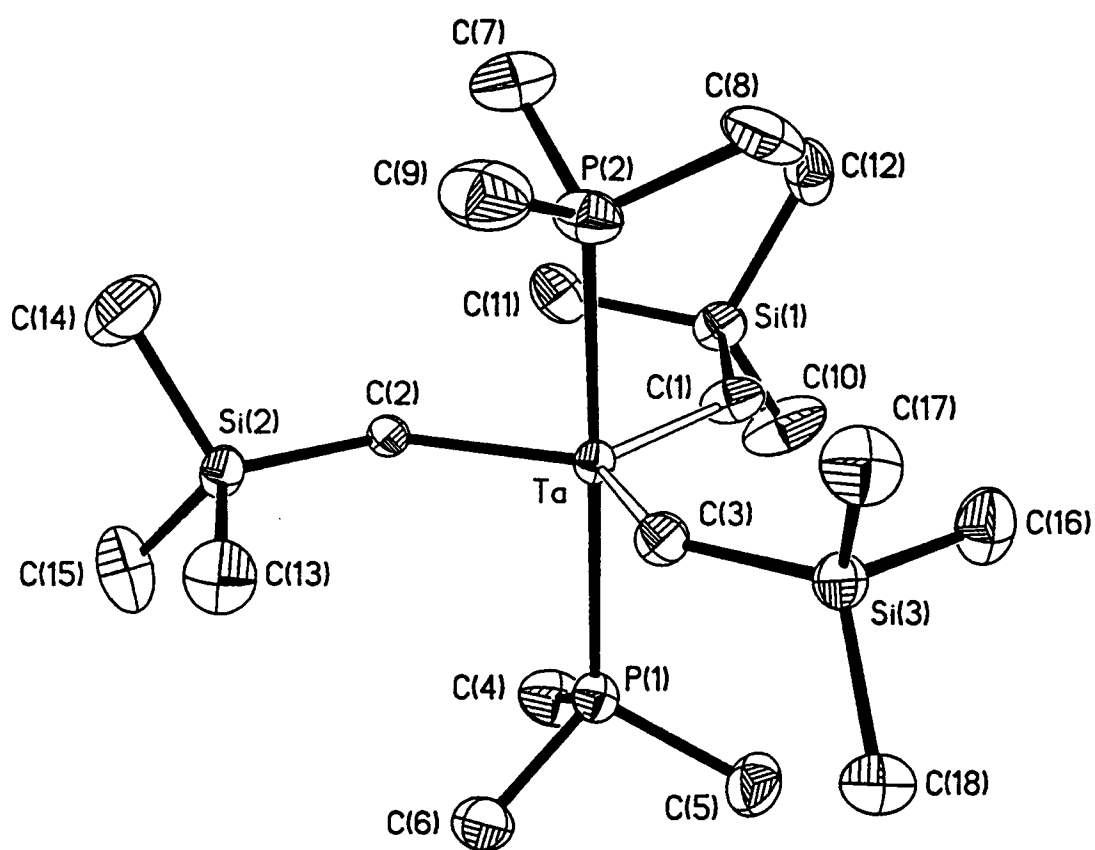


Figure 2.2 ORTEP diagram of 4, showing 30% ellipsoids

Ta(=CHSiMe<sub>3</sub>)(CH<sub>2</sub>SiMe<sub>3</sub>)(OC<sub>6</sub>H<sub>3</sub>Bu<sup>t</sup><sub>2</sub>)<sub>2</sub>,<sup>20</sup> and 1.932(9) Å in [Ta(=CHBu<sup>t</sup>)(CH<sub>2</sub>Bu<sup>t</sup>)(PMe<sub>3</sub>)<sub>2</sub>]<sub>2</sub>(μ-N<sub>2</sub>)<sup>21</sup>]. In addition, the Si-C-Ta angles of the two alkylidene ligands differ from each other significantly [133.7(5)° for Si(1)-C(1)-Ta vs. 142.0(12)° and 144.2(13)° for Si(3)-C(3)-Ta and Si(2A)-C(2A)-Ta, respectively]. A similar distortion is observed in a bis(neopentylidene) complex Ta(=CHBu<sup>t</sup>)<sub>2</sub>(mesityl)(PMe<sub>3</sub>)<sub>2</sub><sup>19</sup> and may be attributed to an α-agostic interaction between the distorted alkylidene hydrogen atom and the metal center. The alkyl and alkylidene ligands arrange themselves in a "pinwheel" geometry around the metal center. This geometry is consistent with the NMR spectrum of **4** at room temperature, in which the two alkylidene ligands are chemically inequivalent.

### 2.3 Experimental Section

All manipulations were performed under a dry nitrogen atmosphere with the use of either a drybox or standard Schlenk techniques. Solvents were purified by distillation from potassium/benzophenone ketyl. Benzene-*d*<sub>6</sub> and toluene-*d*<sub>8</sub> were dried over activated molecular sieves and stored under N<sub>2</sub>. NMR spectra, unless noted, were recorded at 23 °C on a Bruker AC-250, AMX-400 or JEOL FQ-90 Fourier transform spectrometer. <sup>1</sup>H and <sup>13</sup>C NMR chemical shifts were referenced to solvents (residual protons in the <sup>1</sup>H spectra). <sup>29</sup>Si{<sup>1</sup>H} and <sup>31</sup>P{<sup>1</sup>H} chemical shifts were referenced to SiMe<sub>4</sub> and external 85% H<sub>3</sub>PO<sub>4</sub>, respectively. PMe<sub>3</sub> (Aldrich) was used as received. (Me<sub>3</sub>ECH<sub>2</sub>)<sub>3</sub>TaCl<sub>2</sub><sup>11b,22</sup> and



$\text{Li}(\text{THF})_n\text{SiPh}_2\text{Bu}^t$ <sup>23</sup> were prepared by the literature procedures. Elemental analyses were performed by Desert Analytical, Tucson, AZ.

**Preparation of  $(\text{Me}_3\text{ECH}_2)_2\text{Ta}[\text{=CHEMe}_3]\text{SiPh}_2\text{Bu}^t$  (E = C, 1; Si, 2).** The thermally unstable complexes 1 and 2 were prepared by the addition of a solution of 0.049 g (0.11 mmol) or 0.060 g (0.11 mmol) of  $(^t\text{BuCH}_2)_3\text{TaCl}_2$  or  $(\text{Me}_3\text{SiCH}_2)_3\text{TaCl}_2$ , respectively, in 0.5 mL of toluene-*d*<sub>8</sub> to a solution of 0.102 g (0.22 mmol) of  $\text{Li}(\text{THF})_3\text{SiPh}_2\text{Bu}^t$  in 0.5 mL of toluene-*d*<sub>8</sub> in a glovebox. The resulting red-orange mixtures were then immediately filtered through Celite (to remove LiCl) into NMR tubes and cooled to -78 °C. Complexes 1 and 2 were then characterized at -50 °C by <sup>1</sup>H, <sup>13</sup>C{<sup>1</sup>H}, and <sup>13</sup>C-<sup>1</sup>H HETCOR NMR. The resonances were assigned based on those for

$(\text{Me}_3\text{ECH}_2)_2\text{Ta}[\text{=CHEMe}_3]\text{Si}(\text{SiMe}_3)_3$  (E = C, Si).<sup>11b</sup> Data for 1: <sup>1</sup>H NMR (toluene-*d*<sub>8</sub>, 400.1 MHz, -50 °C)  $\delta$  7.89-7.23 (m, 10H, *SiPh}\_2\text{Bu}^t*), 2.84 (s, 1H, =*CHBu}^t*), 1.39 (s, 9H, *SiPh}\_2\text{CMe}\_3*), 1.35 (s, 9H, =*CHCMe}\_3*), 1.05 (s, 18H, *CH}\_2\text{CMe}\_3*), 1.02 (d, 2H, <sup>2</sup>J<sub>H-H} = 12.8 Hz, *CH}\_a\text{H}\_b\text{Bu}^t*), 0.16 (d, 2H, *CH}\_a\text{H}\_b\text{Bu}^t*). <sup>13</sup>C{<sup>1</sup>H} NMR (toluene-*d*<sub>8</sub>, 100.6 MHz, -50 °C)  $\delta$  268.0 (=CH*Bu}^t*, <sup>1</sup>J<sub>C-H} = 87.0 Hz), 145.4 (*CH}\_2\text{Bu}^t*, <sup>1</sup>J<sub>C-H} = 106.6 Hz), 144.6, 137.6, 137.3, 136.7 (*SiPh}\_2\text{Bu}^t*), 47.7 (=CH*CMe}\_3*), 37.7 (*CH}\_2\text{CMe}\_3*), 34.5 (*CH}\_2\text{CMe}\_3*, <sup>1</sup>J<sub>C-H} = 123.7 Hz), 33.7 (*SiPhCMe}\_3*), 30.4 (=CH*CMe}\_3*, <sup>1</sup>J<sub>C-H} = 125.7 Hz), 21.8 (*SiPh}\_2\text{CMe}\_3*). Data for 2: <sup>1</sup>H NMR (toluene-*d*<sub>8</sub>, 400.1 MHz, -50 °C)  $\delta$  7.41 (s, 1H, =*CHSiMe}\_3*), 7.80-7.24 (m, 10H, *SiPh}\_2\text{Bu}^t*), 1.32 (s, 9H, *SiPh}\_2\text{CMe}\_3*), 0.86 (d, 2H, <sup>2</sup>J<sub>H-H} = 11.6 Hz, *CH}\_a\text{H}\_b\text{SiMe}\_3*), 0.35 (s, 9H, =*CHSiMe}\_3*), 0.11 (s, 18H, *CH}\_2\text{SiMe}\_3*), -0.32 (d, 2H,</sub></sub></sub></sub></sub></sub>

$\text{CH}_a\text{H}_b\text{SiMe}_3$ ).  $^{13}\text{C}\{^1\text{H}\}$  NMR (toluene- $d_6$ , 100.6 MHz,  $-50\text{ }^\circ\text{C}$ )  $\delta$  271.1  
( $=\text{CHSiMe}_3$ ,  $^1J_{\text{C-H}} = 90.8\text{ Hz}$ ), 145.6, 138.6, 137.9, 126.7 ( $\text{SiPh}_2\text{Bu}^t$ ), 106.2  
( $\text{CH}_2\text{SiMe}_3$ ,  $^1J_{\text{C-H}} = 96.8\text{ Hz}$ ), 30.5 ( $\text{SiPh}_2\text{CMe}_3$ ,  $^1J_{\text{C-H}} = 125.8\text{ Hz}$ ), 22.5  
( $\text{SiPh}_2\text{CMe}_3$ ), 4.9 ( $=\text{CHSiMe}_3$ ,  $^1J_{\text{C-H}} = 118.6\text{ Hz}$ ), 3.1 ( $\text{CH}_2\text{SiMe}_3$ ,  $^1J_{\text{C-H}} = 115.6$   
Hz).

**Preparation of  $(\text{Me}_3\text{ECH}_2)\text{Ta}(\text{PMe}_3)_2[=\text{CHEMe}_3]_2$  (E = C, 3; Si, 4).** The silyl alkylidene complex **1** was prepared by the addition of 0.050 g (0.107 mmol) of  $(^t\text{BuCH}_2)_3\text{TaCl}_2$  in 1.0 mL of  $\text{Et}_2\text{O}$  to a solution of 0.085 g (0.214 mmol) of  $\text{Li}(\text{THF})_2\text{SiPh}_2\text{Bu}^t$  in 2.0 mL of  $\text{Et}_2\text{O}$  in a glovebox. The resulting red-orange mixture was immediately filtered through Celite into a Schlenk tube and cooled to  $0\text{ }^\circ\text{C}$ . Excess  $\text{PMe}_3$  was then added to the tube via syringe and the solution allowed to stir for 2 hr, at which time the volatiles were removed by vacuum. The oily orange residue was dissolved in benzene- $d_6$ , and NMR spectra of the residue showed it to be a 2:1 mixture of  $\text{HSiPh}_2\text{Bu}^t$  and **3**.<sup>16</sup>

1.001 g (1.91 mmol) of  $(\text{Me}_3\text{SiCH}_2)_3\text{TaCl}_2$  in 20 mL of  $\text{Et}_2\text{O}$  was added slowly to 1.567 g (4.01 mmol) of  $\text{Li}(\text{THF})_2\text{SiPh}_2\text{Bu}^t$  in 20 mL of  $\text{Et}_2\text{O}$  at  $-70\text{ }^\circ\text{C}$ . The resulting dark red solution was stirred for 30 min at this temperature, and 0.60 mL (5.7 mmol, excess) of  $\text{PMe}_3$  was added via syringe. The solution was then allowed to warm to room temperature, during which time the color gradually changed from red to bright orange. The solution was filtered, concentrated, and cooled to  $-60\text{ }^\circ\text{C}$ , yielding 0.626 g of microcrystalline **4** [55.5% based on  $(\text{Me}_3\text{SiCH}_2)_3\text{TaCl}_2$ ]. Data for **4**:  $^1\text{H}$  NMR (benzene- $d_6$ , 250.1

MHz, 23 °C)  $\delta$  7.92 (s, 1H, =CHSiMe<sub>3</sub>), 7.06 (s, 1H, =CHSiMe<sub>3</sub>), 1.18 (t, 18H, <sup>2</sup>J<sub>H-P</sub> = 2.95 Hz, PMe<sub>3</sub>), 0.34 (br s, 9H, =CHSiMe<sub>3</sub>), 0.22 (s, 9H, CH<sub>2</sub>SiMe<sub>3</sub>), 0.16 (br s, 9H, =CHSiMe<sub>3</sub>), -0.33 (t, 2H, <sup>3</sup>J<sub>H-P</sub> = 19.8 Hz, CH<sub>2</sub>SiMe<sub>3</sub>). <sup>13</sup>C{<sup>1</sup>H} NMR (benzene-*d*<sub>6</sub>, 62.9 MHz, 23 °C)  $\delta$  258.0 (=CHSiMe<sub>3</sub>, <sup>1</sup>J<sub>C-H</sub> = 97.7 Hz), 252.1 (=CHSiMe<sub>3</sub>, <sup>1</sup>J<sub>C-H</sub> = 99.6 Hz), 50.3 (CH<sub>2</sub>SiMe<sub>3</sub>, <sup>1</sup>J<sub>C-H</sub> = 106.9 Hz), 18.4 (t, PMe<sub>3</sub>, <sup>1</sup>J<sub>C-P</sub> = 12.0 Hz), 5.2 (CH<sub>2</sub>SiMe<sub>3</sub>), 4.1 (=CHSiMe<sub>3</sub>), 3.7 (=CHSiMe<sub>3</sub>). <sup>31</sup>P{<sup>1</sup>H} NMR (benzene-*d*<sub>6</sub>, 36.2 MHz, 23 °C)  $\delta$  -2.31. <sup>29</sup>Si{<sup>1</sup>H} NMR (toluene-*d*<sub>8</sub>, 79.5 MHz, 23 °C)  $\delta$  -3.10 (CH<sub>2</sub>SiMe<sub>3</sub>), -15.65 (=CHSiMe<sub>3</sub>). Anal. Calcd for C<sub>18</sub>H<sub>49</sub>P<sub>2</sub>Si<sub>3</sub>Ta: C, 36.47; H, 8.33. Found: C, 36.73; H, 8.18. Data for *anti,anti*-4: <sup>1</sup>H NMR (toluene-*d*<sub>8</sub>, 400.1 MHz, -10 °C)  $\delta$  8.64 (s, 2H, =CHSiMe<sub>3</sub>), 1.22 (t, 18H, <sup>2</sup>J<sub>H-P</sub> = 3.2 Hz, PMe<sub>3</sub>), 0.24 (s, 2H, CH<sub>2</sub>SiMe<sub>3</sub>), 0.20 (s, 9H, CH<sub>2</sub>SiMe<sub>3</sub>), 0.18 (s, 18H, =CHSiMe<sub>3</sub>). <sup>13</sup>C{<sup>1</sup>H} NMR (toluene-*d*<sub>8</sub>, 100.6 MHz, -10 °C)  $\delta$  247.0 (=CHSiMe<sub>3</sub>), 56.5 (CH<sub>2</sub>SiMe<sub>3</sub>), 18.3 (t, <sup>1</sup>J<sub>C-P</sub> = 12.1 Hz, PMe<sub>3</sub>), 4.1 (=CHSiMe<sub>3</sub>), 3.6 (CH<sub>2</sub>SiMe<sub>3</sub>).

**Trapping of “(Me<sub>3</sub>SiCH<sub>2</sub>)<sub>2</sub>Ta[=CHSiMe<sub>3</sub>]Cl” as (PMe<sub>3</sub>)<sub>2</sub>(Cl)Ta(μ-CSiMe<sub>3</sub>)<sub>2</sub>Ta(Cl)(CH<sub>2</sub>SiMe<sub>3</sub>)<sub>2</sub> (6) in the Reaction of (Me<sub>3</sub>SiCH<sub>2</sub>)<sub>3</sub>TaCl<sub>2</sub> with Li(THF)<sub>2</sub>SiPh<sub>2</sub>Bu<sup>t</sup>. 1.00 g (1.90 mmol) of (Me<sub>3</sub>SiCH<sub>2</sub>)<sub>3</sub>TaCl<sub>2</sub> in 15 mL of Et<sub>2</sub>O was added slowly at -70 °C to a solution of 1.51 g (3.87 mmol) of Li(THF)<sub>2</sub>SiPh<sub>2</sub>Bu<sup>t</sup> in 15 mL of Et<sub>2</sub>O. The resulting dark red solution was immediately treated with 0.60 mL (5.8 mmol) of PMe<sub>3</sub>, and the reaction mixture was slowly allowed to warm to room temperature with stirring. The orange-red solution was then filtered, concentrated, and cooled to -70 °C, producing 0.377**

g (0.636 mmol) of **4**. Further concentration and cooling of the supernatant solution produced 0.090 g (0.103 mmol) of **6**. Removal of solvent from the supernatant solution yielded a red oil which NMR showed to contain  $\text{HSiPh}_2\text{Bu}^t$  and a 3:1:1 ratio of  $(\text{Me}_3\text{SiCH}_2)_4\text{Ta}_2(\mu\text{-CSiMe}_3)_2$ ,<sup>15</sup> **6**,<sup>18</sup> and **4**.

**Observation of  $(\text{Me}_3\text{SiCH}_2)_2\text{Ta}(\text{PMe}_3)[=\text{CHSiMe}_3]\text{SiPh}_2\text{Bu}^t$  (**5**) as an Intermediate in the Formation of **4** from **2** and  $\text{PMe}_3$ .** **2** was prepared *in situ* by the addition of 0.030 g (0.057 mmol) of  $(\text{Me}_3\text{SiCH}_2)_3\text{TaCl}_2$  in 0.5 mL of toluene- $d_8$  to a solution of 0.050 g (0.13 mmol) of  $\text{Li}(\text{THF})_2\text{SiPh}_2\text{Bu}^t$  in 0.5 mL of toluene- $d_8$  in a glovebox. The resulting orange-red solution was immediately filtered through Celite into an NMR tube and cooled to  $-78\text{ }^\circ\text{C}$ . NMR spectra were then taken at  $-65(1)\text{ }^\circ\text{C}$  to confirm the complete formation of **2**. The NMR tube was then placed in a Schlenk tube cooled to  $-78\text{ }^\circ\text{C}$ , and 1 drop of  $\text{PMe}_3$  delivered to the solution through a 22-gauge needle. The tube was shaken to ensure complete mixing, and NMR spectra at  $-65(1)\text{ }^\circ\text{C}$  were immediately taken. **5** was observed to immediately form upon addition of  $\text{PMe}_3$  (as was confirmed by repeating the experiment but placing 1 drop of  $\text{PMe}_3$  on the inside wall of the NMR tube and dissolving it into the solution immediately before placing the tube in the NMR spectrometer), and was characterized by  $^1\text{H}$ ,  $^{13}\text{C}\{^1\text{H}\}$ , and HMQC NMR. Upon warming the NMR probe to  $-20\text{ }^\circ\text{C}$ , **5** was observed to convert to **4** with formation of  $\text{HSiPh}_2\text{Bu}^t$ ; no further intermediates were observed by NMR. Data for **5**:  $^1\text{H}$  NMR (toluene- $d_8$ , 400.1 MHz,  $-65\text{ }^\circ\text{C}$ )  $\delta$  8.41 (s, 1H,  $=\text{CHSiMe}_3$ ), 7.20-7.75 (m, 10H,  $\text{SiPh}_2\text{Bu}^t$ ), 1.51 (s, 9H,

SiPh<sub>2</sub>CMe<sub>3</sub>), 0.89 (d, 9H, <sup>2</sup>J<sub>H-P</sub> = 4.0 Hz, PMe<sub>3</sub>), 0.32 (br s, 18H, CH<sub>2</sub>SiMe<sub>3</sub>), 0.01 (br s, 9H, =CHSiMe<sub>3</sub>), -0.28 (br s, 4H, CH<sub>2</sub>SiMe<sub>3</sub>). <sup>13</sup>C{<sup>1</sup>H} NMR (toluene-*d*<sub>8</sub>, 100.6 MHz, -65 °C) δ 269.8 (=CHSiMe<sub>3</sub>), 151.4, 131.0, 130.5, 128.4 (SiPh<sub>2</sub>Bu<sup>t</sup>), 86.1 (CH<sub>2</sub>SiMe<sub>3</sub>), 31.0 (SiPh<sub>2</sub>CMe<sub>3</sub>), 22.8 (SiPh<sub>2</sub>CMe<sub>3</sub>), 15.2 (d, <sup>1</sup>J<sub>C-P</sub> = 16.1 Hz, PMe<sub>3</sub>), 4.49 (=CHSiMe<sub>3</sub>), 3.11 (CH<sub>2</sub>SiMe<sub>3</sub>).

**X-ray Crystal Structure Determination of 4.** The crystal structure of **4** was determined on a Siemens R3m/V diffractometer fitted with a Nicolet LT-2 low temperature device. A suitable crystal was coated in Paratone oil (Exxon) and mounted under a stream of nitrogen at -100 °C. The unit cell parameters and orientation matrix were determined from a least-squares fit of 30 reflections obtained from a rotation photograph and automatic peak search routine. The refined lattice parameters and other pertinent crystallographic information are given in Table 2.1.

Intensity data were measured with graphite-monochromated Mo K $\alpha$  radiation ( $\lambda = 0.71073$  Å). Background counts were measured at the beginning and end of each scan with the crystal and counter kept stationary. The intensities of three standard reflections were measured after every 97 reflections. The intensity data were corrected for Lorentz and polarization effects and for absorption based upon  $\psi$  scans.

The structure was solved by direct methods using the Siemens SHELXTL 93 (version 5.0) software package. All non-hydrogen atoms were refined anisotropically except for the disordered  $\alpha$ -carbon atoms C(2) and C(3).

Hydrogen atoms of the methyl groups were placed in calculated positions and introduced into the refinement as fixed contributors with an isotropic  $U$  value of  $0.08 \text{ \AA}^2$ .

## CHAPTER 3

### Reactions of Tantalum Alkylidene Complexes with Silanes

#### 3.1 Introduction

Early-transition-metal alkylidene complexes have been the subject of enthusiastic study since the first alkylidene complex,  $(t\text{BuCH}_2)_3\text{Ta}=\text{CHBu}^t$ , was prepared by Schrock in 1973.<sup>16</sup> Alkylidene complexes have been widely studied for their roles in effecting reactions such as alkene, alkyne, and carbonyl metathesis reactions, as well as olefin polymerization.<sup>24</sup> However, the reactivity of alkylidene complexes towards silanes is a relatively unexplored area. The complex  $\text{Cp}_2\text{Ta}(=\text{CH}_2)\text{CH}_3$  was found to react with  $t\text{Bu}_2\text{SiH}_2$  to give  $\text{Cp}_2\text{Ta}(\text{H})=\text{CHSiH}t\text{Bu}_2$  through a mechanism involving oxidative addition of the silane to a  $d^2$  Ta(III) center, followed by  $\text{CH}_4$  elimination and alkylidene transfer and insertion steps.<sup>25</sup> The formation of  $d^0$   $\text{Cp}^*_2\text{Ta}(\text{H})(\text{CH}_3)\text{SiH}_3$  ( $\text{Cp}^*$  = pentamethylcyclopentadienyl) from the reaction of  $\text{Cp}^*_2\text{Ta}(\text{H})=\text{CH}_2$  with  $\text{SiH}_4$  was found to occur via oxidative addition of  $\text{SiH}_4$  to  $d^2$   $\text{Cp}^*_2\text{Ta}-\text{CH}_3$ , which is in equilibrium with  $\text{Cp}^*_2\text{Ta}(\text{H})=\text{CH}_2$ .<sup>26</sup>

Our interest in studying the reactions of alkylidene complexes with silanes is a result of our studies of the reactions of  $\text{SiH}_4$  with tantalum alkylidene complexes as a possible molecular route to silicide materials. Our aims in these studies are two fold: (1) to understand how the different ligands

(alkyl and alkylidene) react with silanes, and (2) to establish the factors which may influence such reactions and determine at what stage M-Si bonds are formed. In work previously done in our group, the alkylidene complex  $({}^t\text{BuCH}_2)_3\text{Ta}=\text{CHBu}^t$  was found to react with  $\text{SiH}_4$  to produce amorphous solids which contained both tantalum and silicon. Trapping of the volatiles from the reaction and analysis by NMR showed neopentane ( $\text{CMe}_4$ ) to be among the reaction products.<sup>27</sup> Reactions of  $({}^t\text{BuCH}_2)_3\text{Ta}=\text{CHBu}^t$  with substituted silanes  $\text{PhSiH}_3$  and  $\text{Ph}_2\text{SiH}_2$  in benzene- $d_6$  were also investigated, but the reactions were found to be very slow and only unidentified products were formed. Addition of  $({}^t\text{BuCH}_2)_3\text{Ta}=\text{CHBu}^t$  to neat  $\text{PhSiH}_3$  resulted in an immediate vigorous reaction with gas evolution and the formation of an intractable black tar.

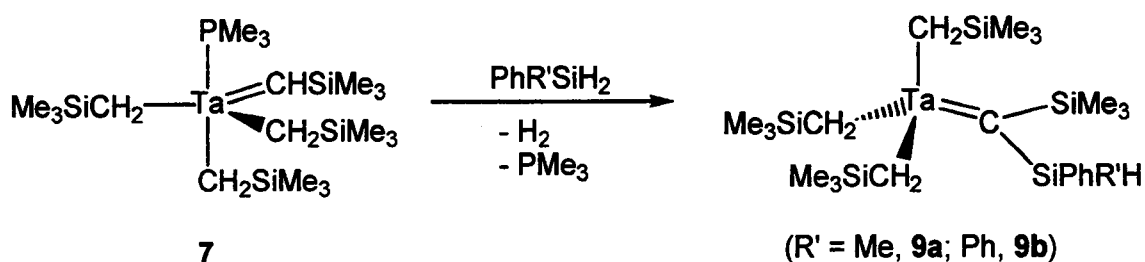
In order to further study the reaction of alkylidene complexes with silanes, we turned to alkylidene complexes containing phosphine ligands, in the hope that such ligands would help to stabilize the resulting reaction products. These studies, which resulted in unexpected chemistry and the isolation of complexes possessing novel structural features, are discussed below.

## **3.2 Results and Discussion**

### **3.2.1 Synthesis of Disilyl-Substituted Alkylidene Complexes**

The addition of a solution of  $\text{PhR}'\text{SiH}_2$  ( $\text{R}' = \text{Me}, \text{Ph}$ ) to a solution of the



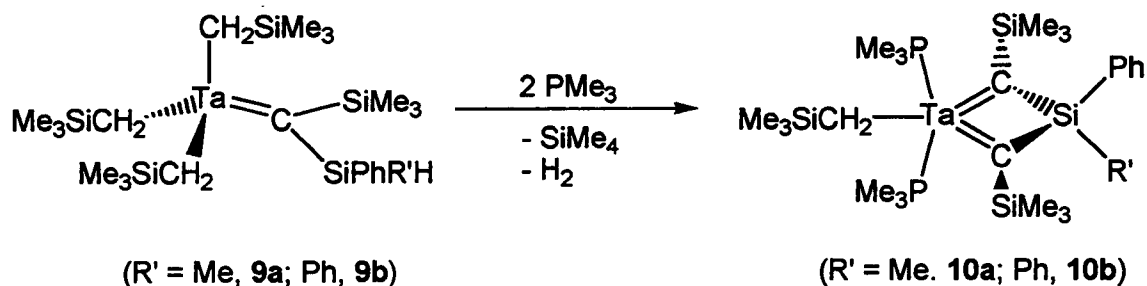


Scheme 3.1

phosphine alkylidene complex  $(\text{Me}_3\text{SiCH}_2)_3\text{Ta}(\text{PMe}_3)=\text{CHSiMe}_3$  (**7**)<sup>28</sup> resulted in the evolution of  $\text{H}_2$  and the nearly quantitative conversion (by NMR) of **7** to the disilyl-substituted alkylidene complex  $(\text{Me}_3\text{SiCH}_2)_3\text{Ta}[\text{C}(\text{SiMe}_3)\text{SiPhR}'\text{H}]$  ( $\text{R}' = \text{Me}$ , **9a**;  $\text{Ph}$ , **9b**) (Scheme 3.1). The reaction of the silane occurred exclusively with the alkylidene ( $=\text{CHSiMe}_3$ ) ligand, and the resulting complexes **9a-b** were found to be unreactive towards excess silane. No reaction was observed between **7** and  $\text{Ph}_3\text{SiH}$  at room temperature.

Spectroscopic properties of **9** are consistent with the structure assignments. The alkylidene resonances of **9a** and **9b** occur at 240.6 and 238.2 ppm, respectively, in the  $^{13}\text{C}\{^1\text{H}\}$  NMR spectra, and appear as singlets in the gated-decoupled  $^{13}\text{C}$  spectra. The  $\alpha$ -H resonances of the methylene groups of the  $(\text{Me}_3\text{SiCH}_2-)$  groups in **9a** are diastereotopic and appear as two doublets in the  $^1\text{H}$  spectrum due to the stereogenic Si center in the  $=\text{C}(\text{SiMe}_3)\text{Si}^*\text{PhMeH}$  moiety.

Workup of the reaction mixture to produce **9** yielded a red oil of reasonably pure ( $> 95\%$  by  $^1\text{H}$  NMR) **9**. However, all attempts to isolate

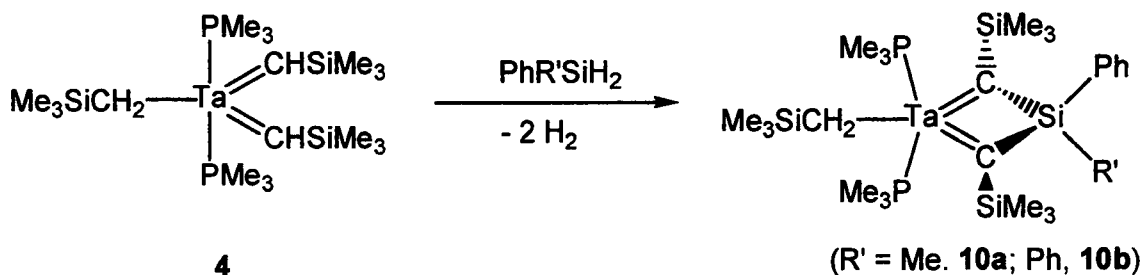


Scheme 3.2

analytically pure samples of this compound were unsuccessful, as **9** was found to slowly decompose in solution. When monitored by NMR in benzene- $d_6$ , **9** slowly decomposed through  $\text{SiMe}_4$  elimination; however a solution of **9** in benzene could be frozen and stored at  $-20\text{ }^\circ\text{C}$  for several weeks without significant decomposition. When the reaction to form **9** was monitored by NMR, a partial conversion of **9** to a metallasilacyclobutadiene complex **10** was observed after several days (ca. 3-5% by NMR, Scheme 3.2), but no **10** was observed during the formation of **9**.

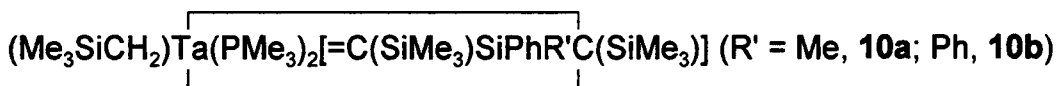
### 3.2.2 Synthesis of Novel Metallasilacyclobutadiene Complexes

Addition of  $\text{PhR}'\text{SiH}_2$  (R' = Me, Ph, H) to



Scheme 3.3

$(\text{Me}_3\text{SiCH}_2)\text{Ta}(\text{PMe}_3)_2[=\text{CHSiMe}_3]_2$  (**4**) led to the evolution of  $\text{H}_2$  and the formation of novel 1,1'-metalla-3-silacyclobutadiene complexes



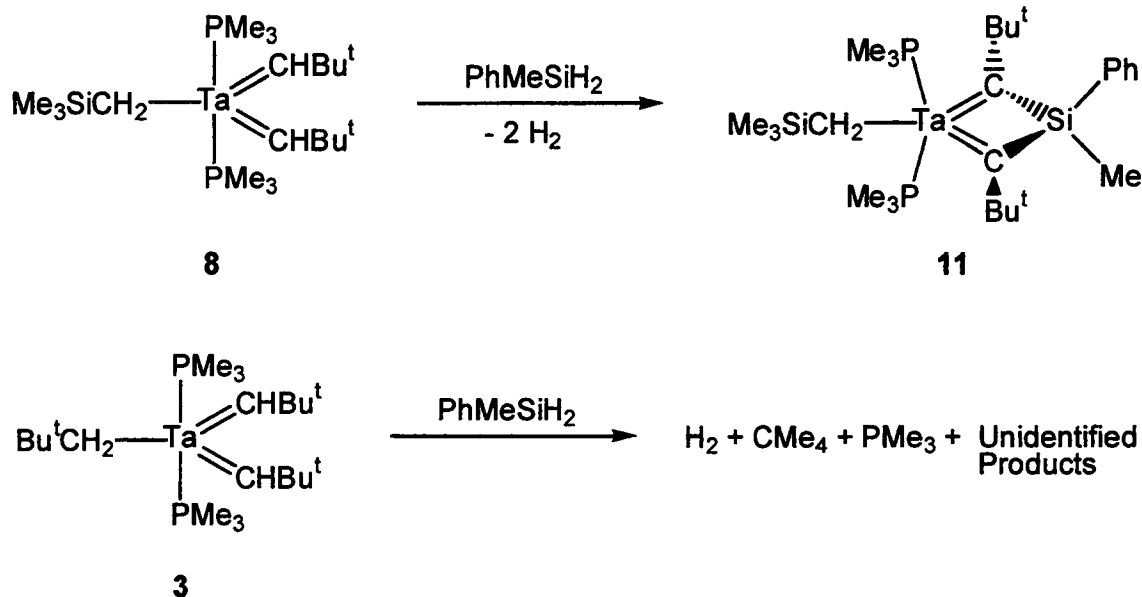
(Scheme 3.3). Again, preferential reactions with the alkylidene ligands were observed, and the products were inert to excess silane. In contrast to **9**, complexes **10a-b** are stable indefinitely in both solution and the solid state, and are soluble in a variety of aromatic, aliphatic, and ethereal solvents. No reaction was observed between **4** and  $\text{Ph}_3\text{SiH}$ ,  $\text{Ph}_2^t\text{BuSiH}$ , or  $^t\text{Bu}_2\text{SiH}_2$ .

The spectroscopic properties of **10** support the structure assignments. The  $^{13}\text{C}\{^1\text{H}\}$  NMR resonances of the alkylidene ligands range from 250.3 to 255.4 ppm, and appear as singlets in the gated-decoupled  $^{13}\text{C}$  spectra. The phosphine ligands in **10a** are chemically inequivalent, resulting in the appearance of two doublets in the  $^1\text{H}$ ,  $^{13}\text{C}\{^1\text{H}\}$ , and  $^{31}\text{P}\{^1\text{H}\}$  NMR spectra. This is consistent with a trigonal bipyramidal structure with axial phosphine ligands and a planar metallasilacyclobutadiene ring with the Ph and Me ligands above

and below the ring, thus making the phosphine ligands chemically inequivalent. The two phosphine ligands in **10b** are equivalent, leading to virtual triplets in the  $^1\text{H}$  and  $^{13}\text{C}\{^1\text{H}\}$  spectra, and a singlet in the  $^{31}\text{P}\{^1\text{H}\}$  spectrum. The methylene resonances of the  $\text{Me}_3\text{SiCH}_2$ - ligands in **10a-b** appear as virtual triplets in the  $^1\text{H}$  NMR spectra. The structural assignments of **10a** and **10b** were confirmed by X-ray crystallography, which is discussed in Section 3.2.4.

The preferential reactions of the alkylidene ligands, rather than the alkyl ligands, of **4** with  $\text{PhR}'\text{SiH}_2$  were unexpected. In order to probe whether such a preference was general, the reactions of the neopentyl analog of **4**,  $(^t\text{BuCH}_2)\text{Ta}(\text{PMe}_3)_2[=\text{CHBu}^t]_2$  (**3**),<sup>16a</sup> and a mixed-ligand complex  $(\text{Me}_3\text{SiCH}_2)\text{Ta}(\text{PMe}_3)_2[=\text{CHBu}^t]_2$  (**8**) with  $\text{PhMeSiH}_2$  were studied. The reaction of **8** with  $\text{PhMeSiH}_2$  also generated  $\text{H}_2$  and a metallasilacyclobutadiene complex **11** (Scheme 3.4). However, the reaction of **3** with  $\text{PhMeSiH}_2$  gave as products  $\text{H}_2$ ,  $\text{CMe}_4$ ,  $\text{PMe}_3$ , and a mixture of unidentified complexes.

Spectroscopic properties of **11** are similar to those of **10a**. The alkylidene carbon resonance occurs at 271.9 ppm in the  $^{13}\text{C}\{^1\text{H}\}$  NMR spectrum, and appears as a singlet in the gated decoupled  $^{13}\text{C}$  spectrum. The phosphine ligands are chemically inequivalent, and appear as two doublets in both the  $^1\text{H}$  and  $^{13}\text{C}\{^1\text{H}\}$  spectra. However, one of the two phosphine signals in the  $^1\text{H}$  spectrum is broad, indicating some kind of fluxional process involving one of the two phosphine ligands. The structure of **11** was confirmed by X-ray crystallography, which is discussed in Section 3.2.4.



Scheme 3.4

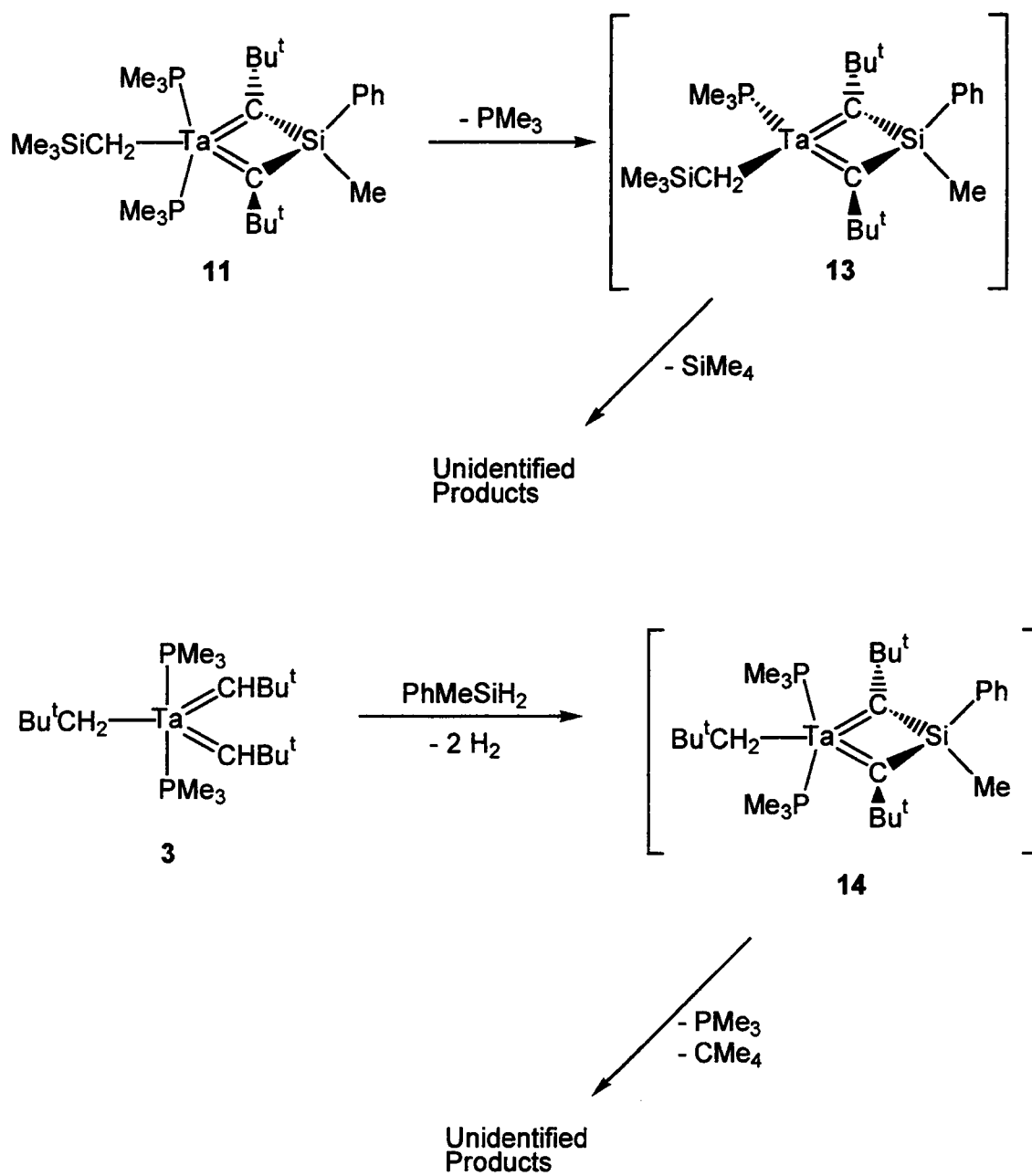
In contrast to complexes **10a-b**, which are stable in solution, **11** was found to be unstable in solution, decomposing by loss of  $\text{PMe}_3$  followed by loss of  $\text{SiMe}_4$  to give a mixture of decomposition products whose NMR spectra are similar to those from the reaction of **3** with  $\text{PhMeSiH}_2$ . One possibility for the lower stability of **11** in solution may be due to increased steric crowding around the Ta center caused by the  $-\text{Bu}^t$  groups on the alkylidene ligands; a C-C bond (ca. 1.54 Å) is shorter than a C-Si bond (ca. 1.85 Å), resulting in the two groups *exo*- to the metallasilacyclobutadiene ring being closer to the metal center. This may lead to the dissociation of a phosphine ligand (as is supported by the broadened signal for one of the  $\text{PMe}_3$  ligands in the  $^1\text{H}$  NMR spectrum of **11**) resulting in a pseudo-tetrahedral complex **13**, which further decomposes by

loss of  $\text{SiMe}_4$  (possibly via  $\gamma$ -H abstraction from a  $^t\text{Bu}$  group) to give unidentified products (Scheme 3.5). It is therefore likely that the reaction of **3** with  $\text{PhMeSiH}_2$  may also form a metallasilacyclobutadiene complex **14**, which then rapidly loses  $\text{PMe}_3$  followed by  $\text{CMe}_4$  to give a product mixture similar to that from the decomposition of **11** (Scheme 3.5).

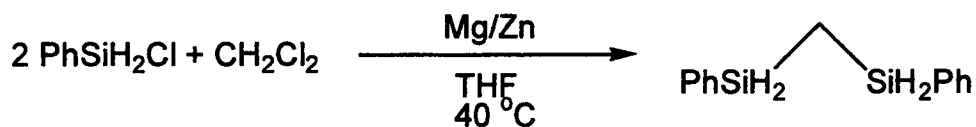
### 3.2.3 Synthesis of the Metalladisilacyclohexadiene Complex **12**

The unexpected formation of metallasilacyclobutadiene complexes **10a-b** from the reactions of **4** with  $\text{PhR}'\text{SiH}_2$  led us to study whether such chemistry could be extended to include reactions of alkylidene complexes with compounds containing more than one silyl functionality. The reactions of such compounds, such as a disilylmethane  $(\text{H}_2\text{PhSi})_2\text{CH}_2$ , which contain two reactive groups, could possibly lead to the formation of oligomeric, cyclic, or polymeric complexes in which the disilylmethane moiety could bridge two metal centers, as well as to the formation of a metalladisilacyclohexadiene complex. We therefore synthesized the disilylmethane complex bis(phenylsilyl)methane  $(\text{PhH}_2\text{Si})_2\text{CH}_2$ , and studied its reactivity towards **4**.

The previously unreported compound bis(phenylsilyl)methane was prepared by the Grignard-Wurtz coupling of  $\text{PhSiH}_2\text{Cl}$  with  $\text{CH}_2\text{Cl}_2$  using  $\text{Mg/Zn}$  in THF (Scheme 3.6).<sup>29</sup> The reaction of this compound with **4**, when conducted in an NMR tube in benzene- $d_6$  and monitored by  $^1\text{H}$  NMR, was found to immediately produce  $\text{H}_2$  and other products. Increasing the scale of the

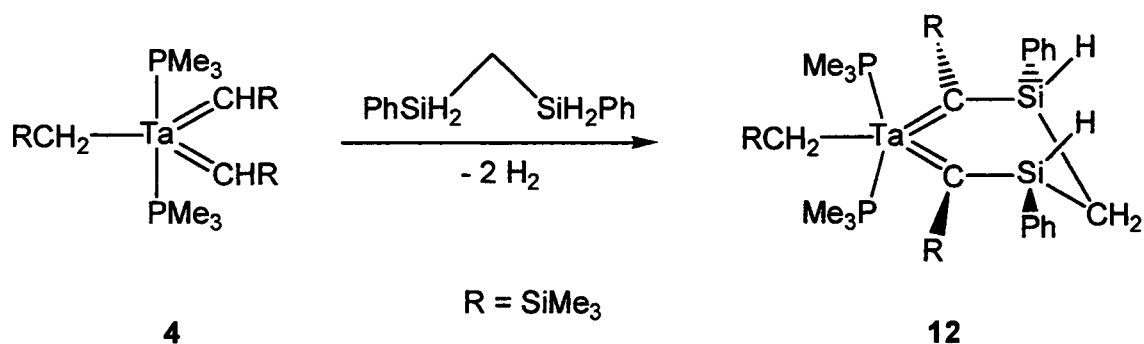


Scheme 3.5



Scheme 3.6

reaction in pentane and cooling the reaction mixture to  $-20^\circ\text{C}$  led to the isolation of a 1,1'-metalla-3,5-disilacyclohexadiene complex **12** in low yield (Scheme 3.7). No further products could be isolated from the reaction mixture.

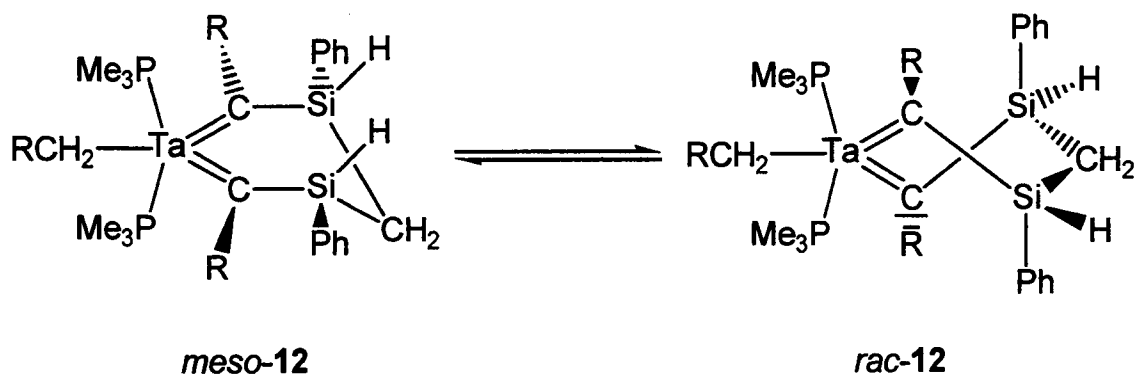


Scheme 3.7

There exist two possible sets of isomers of **12**, as there are two stereogenic Si centers in the metalladisilacyclohexadiene ring. Crystals of **12** were found by X-ray crystallography to be those of a *meso*-isomer (Section 3.2.4), in which both phenyl rings on the Si atoms are occupying pseudo-equatorial positions on the metalladisilacyclohexadiene ring. The spectroscopic properties of *meso*-**12** are in agreement with the structure assignment. The alkylidene carbons appear at 262.7 ppm in the  $^{13}\text{C}\{^1\text{H}\}$



spectrum, and this signal appears as a singlet in the gated decoupled  $^{13}\text{C}$  spectrum. The phosphine ligands are chemically inequivalent and lead to two doublets in the  $^1\text{H}$ ,  $^{13}\text{C}\{^1\text{H}\}$ , and  $^{31}\text{P}\{^1\text{H}\}$  spectra. The Si-H and Si-CH<sub>2</sub>-Si protons give rise to an ABXX' system, as is shown in the  $^1\text{H}$  NMR spectra in Figures 3.1 and 3.2, as well as the TOCSY and HMQC spectra in Figures 3.3 and 3.4. The silane protons appear as a multiplet at 5.82 ppm and the methylene protons as two doublets of doublets at 0.88 and 1.41 ppm. **12** has an extremely low solubility in benzene, but surprisingly is soluble in toluene.



Scheme 3.8

When monitored by NMR in a toluene-*d*<sub>6</sub> solution, *meso*-**12** was observed to slowly isomerize over the course of several weeks at 23 °C to yield a mixture of *meso*-**12** and racemic isomers of **12** (*rac*-**12**) (Scheme 3.8).  $^1\text{H}$  NMR spectra of a solution of **12** before and after isomerization are shown in Figures 3.1 and 3.2. Such an isomerization involves the inversion of configuration of one of the ring Si atoms in *meso*-**12**. How this inversion of configuration occurs is unclear; however, a closer analysis of the  $^1\text{H}$  and

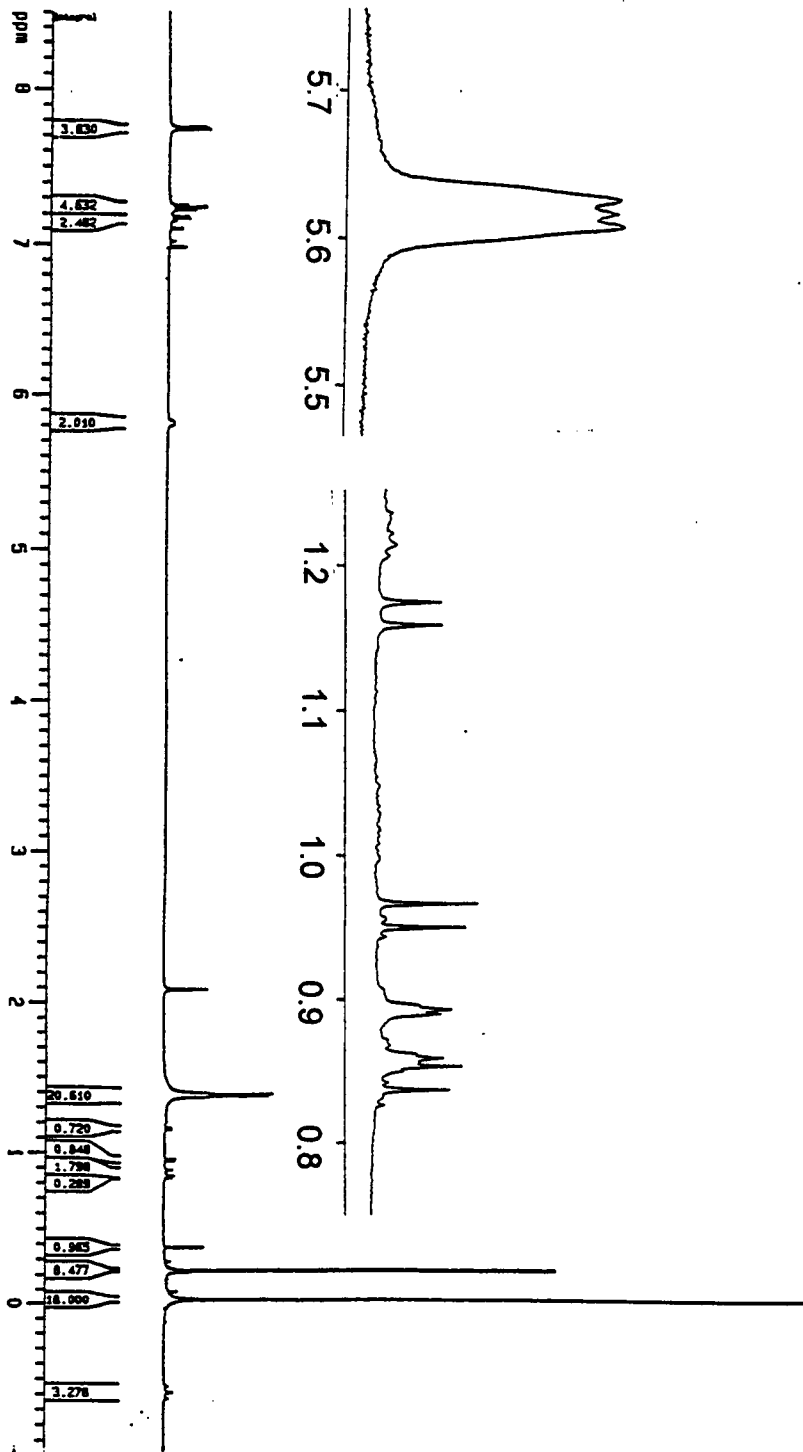


Figure 3.1  $^1\text{H}$  NMR spectrum of *meso*-12.

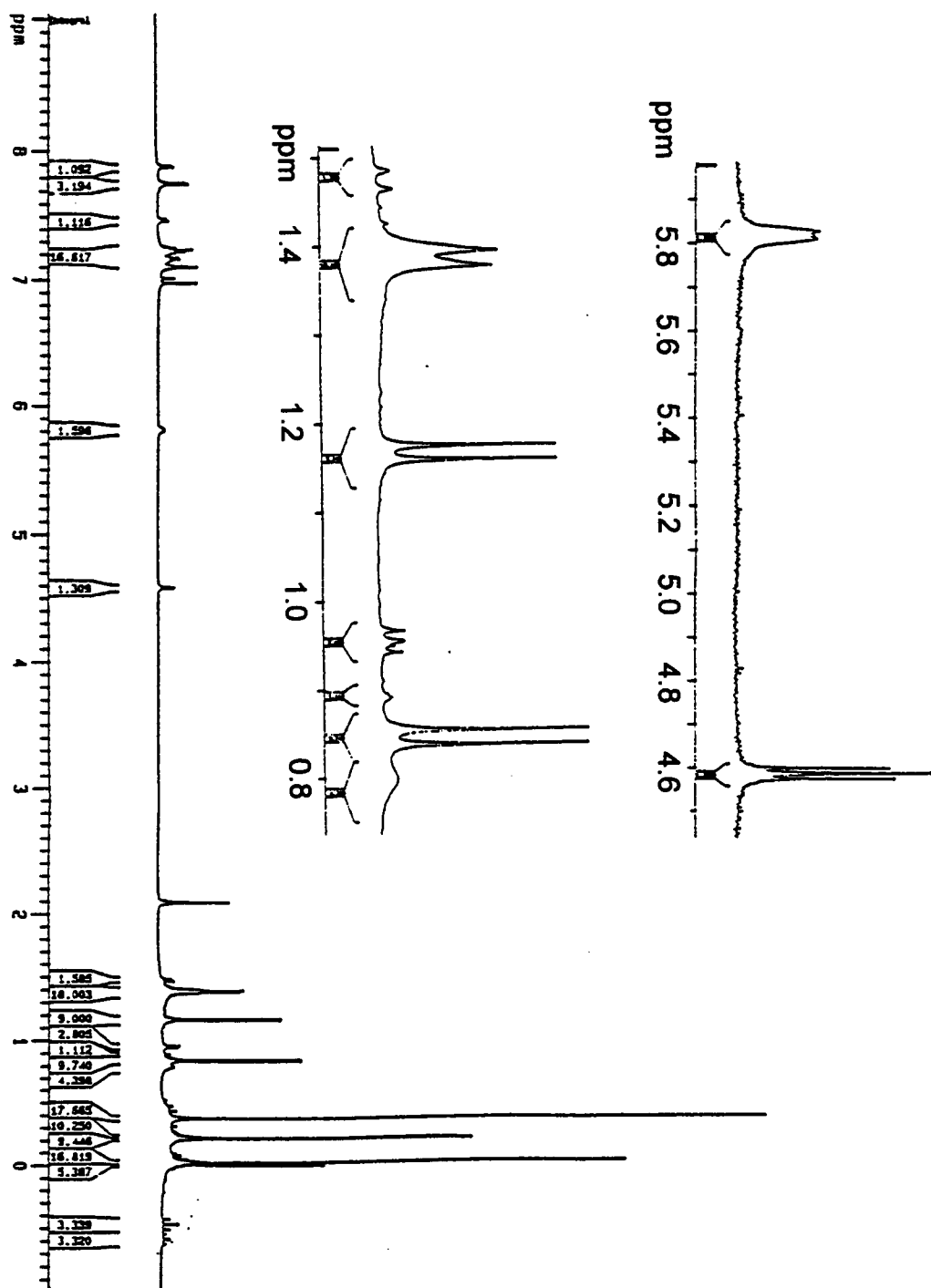


Figure 3.2  $^1\text{H}$  NMR spectrum of *meso*-12 and *rac*-12.

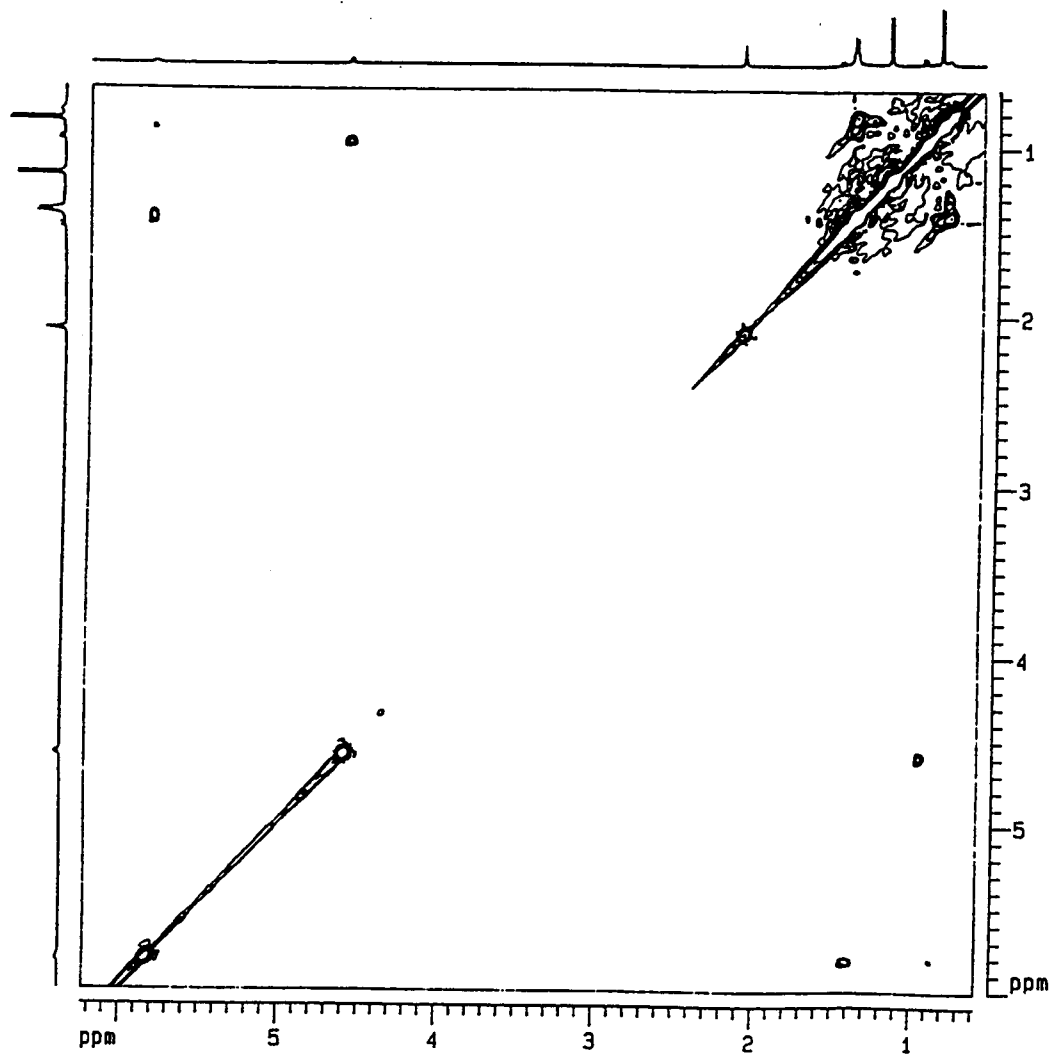


Figure 3.3 TOCSY spectrum of *meso*-12 and *rac*-12.

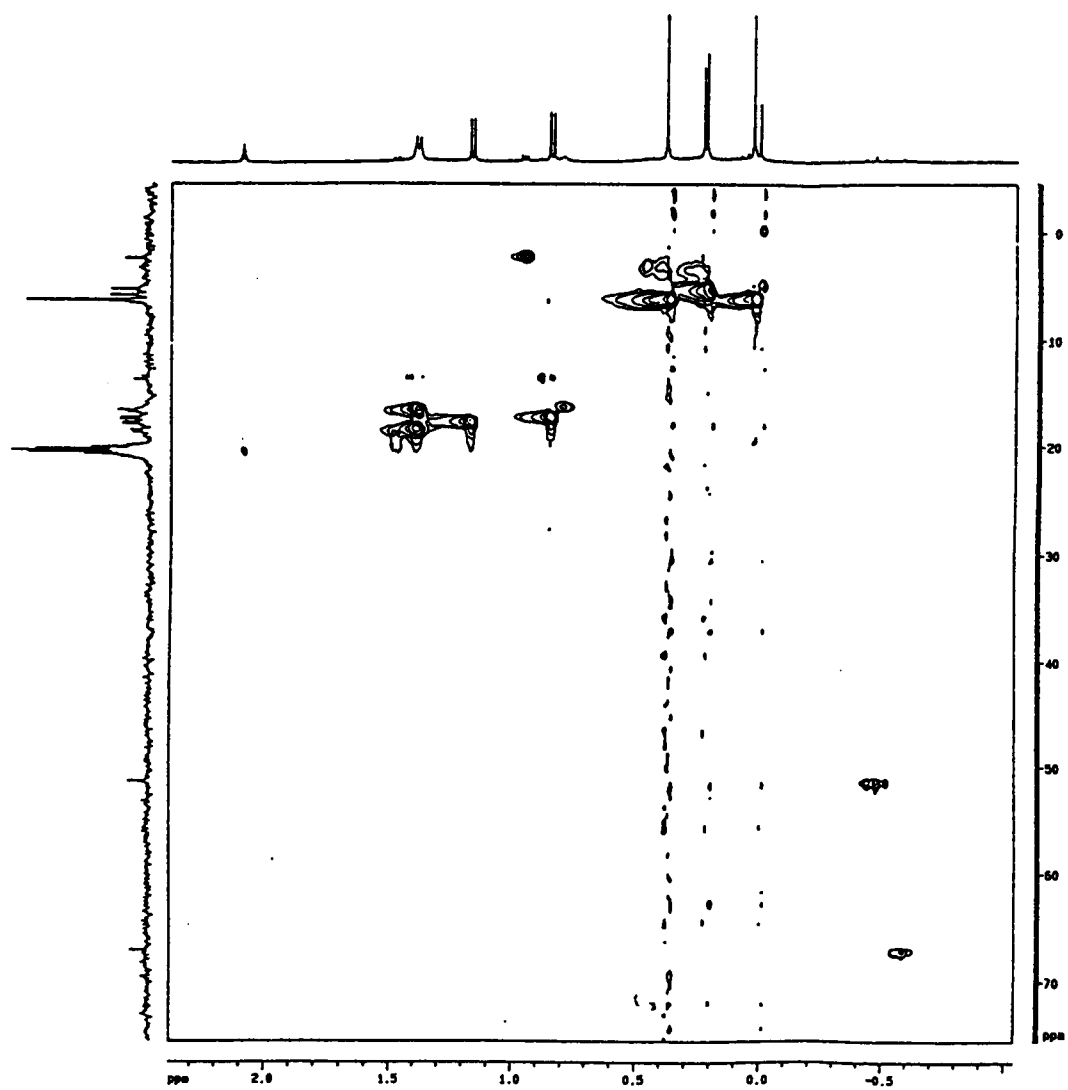
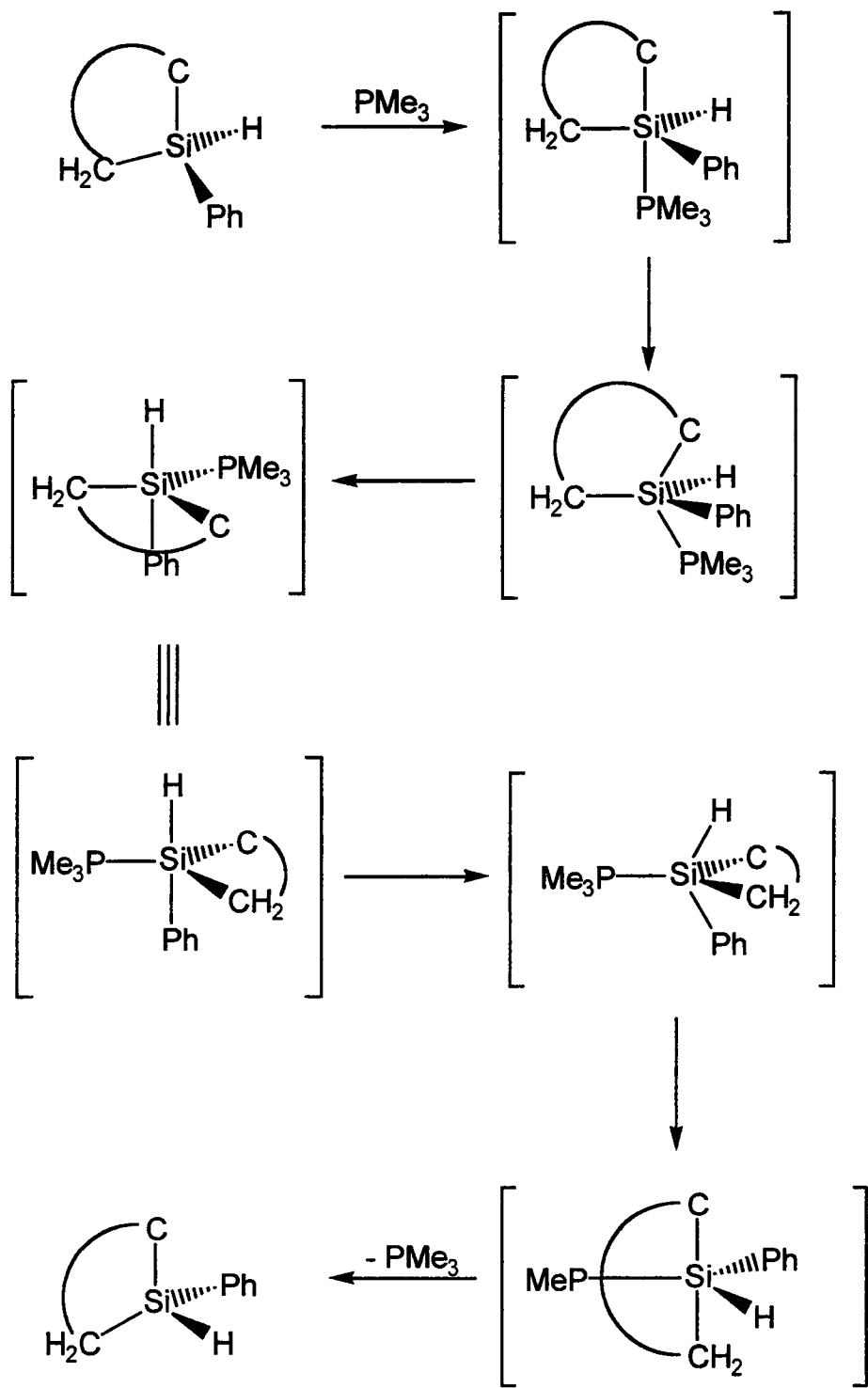


Figure 3.4 HMQC spectrum of *meso*-12 and *rac*-12.

$^{13}\text{C}\{^1\text{H}\}$  NMR spectra of *meso*-12 reveals that one of the two  $\text{PMe}_3$  resonances is broadened, indicating that this phosphine ligand is involved in a fluxional process. It is possible that one of the two phosphine ligands in *meso*-12 may dissociate from the metal and coordinate to one of the ring silicon atoms, forming a pentacoordinate silicon center. A fluxional exchange mechanism, such as a Berry pseudorotation or trigonal twist at the resulting pentacoordinate silicon center, followed by dissociation of the  $\text{PMe}_3$  from the silicon may lead to inversion of configuration of the silicon, resulting in the formation of *rac*-12 (Scheme 3.9). A similar mechanism has been proposed to explain the racemization of optically active silanes in polar coordinating solvents.<sup>33</sup> The NMR spectra of *rac*-12 show some significant differences from those of *meso*-12. The  $\text{PMe}_3$  resonances appear in the  $^1\text{H}$  NMR spectrum as two sharp doublets at 1.17 and 0.85 ppm. The Si-H and Si- $\text{CH}_2$ -Si resonances give rise to an AA'XX' system, appearing as two doublets of doublets at 4.59 and 0.96 ppm (Figures 3.2, 3.3 and 3.4). This is consistent with a twist conformation with the phenyl groups occupying pseudo-axial positions so as to minimize steric interactions with the adjacent  $\text{SiMe}_3$  groups on the alkylidene carbons.

#### 3.2.4 X-ray Crystal Structures of 10a, 10b, 11, and 12

Slow cooling of solutions of 10a-b in hexanes and 11 and 12 in pentane, respectively, produced crystals suitable for analysis by X-ray crystallography.



Scheme 3.9

Crystal data, results of analyses, and bond distances and angles are given in Tables 3.1-3.12. The molecular structures of **10a**, **10b**, **11**, and **12** are shown in Figures 3.5-3.8.

Complex **10a** exhibits distorted trigonal bipyramidal geometry around the tantalum center, with the  $\text{PMe}_3$  ligands occupying axial positions (Figure 3.5). The Ta=C bond distances of 1.947(12) and 1.962(12) Å are consistent with those observed for other alkylidene complexes of tantalum [1.998(8) and 1.95(2) Å in **4**, 1.932(7) and 1.955(7) Å in  $\text{Ta}(=\text{CHBu}^t)_2(\text{mesityl})(\text{PMe}_3)_2$ ,<sup>19</sup> and 1.932(9) Å in  $[\text{Ta}(=\text{CHBu}^t)(\text{CH}_2\text{Bu}^t)(\text{PMe}_3)_2]_2(\mu\text{-N}_2)^{21}$ ]. The metallasilacyclobutadiene ring is planar (average deviation from the least squares plane = 0.007 Å), which brings the silicon atom in close proximity to the tantalum center [Ta-Si distance of 2.607(3) Å]; however, the fact that the metal center is formally  $d^0$  makes any metal-silicon bonding interaction unlikely. The silicon atom of the metallasilacyclobutadiene ring exhibits distorted tetrahedral geometry, with bond angles ranging from 96.7(5)° to 115.9(6)°.

The structure of **10b** is similar to **10a** (Figure 3.6). As in **10a**, the tantalum atom exhibits distorted trigonal bipyramidal geometry with the  $\text{PMe}_3$  ligands occupying axial positions. The Ta=C bond distances of 1.951(12) and 1.977(12) Å are similar to those listed above. The metallasilacyclobutadiene ring is also planar, and the silicon atom of the ring exhibits distorted tetrahedral geometry, with bond angles ranging from 97.7(6)° to 115.7(6)°. Again, the planar nature of the ring brings the Si atom in close contact to the Ta center



**Table 3.1. Crystal Data for 10a**

---

formula	$C_{25}H_{55}P_2Si_4Ta$
formula weight	710.94
crystal size (mm)	0.30 x 0.20 x 0.20
temperature (K)	173(2)
crystal system	Monoclinic
space group	$P2_1/n$
lattice parameters	$a = 10.647(3) \text{ \AA}$ $\alpha = 90^\circ$ $b = 17.757(6) \text{ \AA}$ $\beta = 96.91(3)^\circ$ $c = 18.686(5) \text{ \AA}$ $\gamma = 90^\circ$
volume, $\text{\AA}^3$	3507(2)
Z	4
density (calc) ( $\text{g/cm}^3$ )	1.346
$\mu$ ( $\text{mm}^{-1}$ )	3.374
$F(000)$	1456
scan type	$\omega$ -2 $\theta$
$\theta$ range (deg)	2.10-22.55
index ranges	$h, k, \pm l$
unique reflections	4617 ( $R_{\text{int}} = 0.0386$ )
parameters varied	289
R indices	0.0610 ( $R_w F^2 = 1440$ )
goodness-of-fit on $F^2$	1.150

---

**Table 3.2. Interatomic Distances (Å) in 10a**

---

Ta-P(1)	2.605(3)	Ta-P(2)	2.664(3)
Ta-C(1)	1.955(13)	Ta-C(2)	1.969(12)
Ta-C(3)	2.289(12)	Ta--Si(4)	2.607(3)
P(1)-C(4)	1.830(14)	P(1)-C(5)	1.829(14)
P(1)-C(6)	1.813(13)	P(2)-C(7)	1.810(14)
P(2)-C(8)	1.821(14)	P(2)-C(9)	1.825(13)
Si(1)-C(1)	1.824(13)	Si(1)-C(10)	1.89(2)
Si(1)-C(11)	1.892(14)	Si(1)-C(12)	1.86(2)
Si(2)-C(2)	1.811(12)	Si(2)-C(13)	1.88(2)
Si(2)-C(14)	1.84(2)	Si(2)-C(15)	1.855(14)
Si(3)-C(3)	1.879(12)	Si(3)-C(16)	1.86(2)
Si(3)-C(17)	1.882(14)	Si(3)-C(18)	1.888(14)
Si(4)-C(1)	1.904(12)	Si(4)-C(2)	1.905(12)
Si(4)-C(19)	1.899(13)	Si(4)-C(20)	1.889(13)
C(20)-C(21)	1.43(2)	C(21)-C(22)	1.36(2)
C(22)-C(23)	1.37(2)	C(23)-C(24)	1.40(2)
C(24)-C(25)	1.37(2)	C(20)-C(25)	1.39(2)

---

**Table 3.3. Intramolecular Bond Angles (°) in 10a**

---

C(1)-Ta-C(2)	93.3(5)	C(1)-Ta-C(3)	134.2(5)
C(2)-Ta-C(3)	132.4(5)	C(1)-Ta-P(1)	90.1(4)
C(2)-Ta-P(1)	101.0(4)	C(3)-Ta-P(1)	80.7(3)
C(1)-Ta-P(2)	91.0(4)	C(2)-Ta-P(2)	96.9(4)
C(3)-Ta-P(2)	85.6(3)	P(1)-Ta-P(2)	161.96(11)
C(6)-P(1)-C(5)	102.0(7)	C(6)-P(1)-C(4)	102.0(7)
C(5)-P(1)-C(4)	101.7(7)	C(6)-P(1)-Ta	118.2(5)
C(5)-P(1)-Ta	119.0(5)	C(4)-P(1)-Ta	111.5(5)
C(7)-P(2)-C(8)	100.9(7)	C(7)-P(2)-C(9)	100.9(7)
C(8)-P(2)-C(9)	101.8(7)	C(7)-P(2)-Ta	112.0(4)
C(8)-P(2)-Ta	117.3(5)	C(9)-P(2)-Ta	120.9(5)
C(1)-Si(1)-C(12)	115.0(6)	C(1)-Si(1)-C(11)	108.3(6)
C(1)-Si(1)-C(10)	112.1(6)	C(12)-Si(1)-C(11)	105.9(8)
C(12)-Si(1)-C(10)	106.9(7)	C(11)-Si(1)-C(10)	108.2(7)
C(2)-Si(2)-C(13)	113.0(6)	C(2)-Si(2)-C(14)	112.5(7)
C(2)-Si(2)-C(15)	110.5(6)	C(14)-Si(2)-C(15)	107.3(8)
C(14)-Si(2)-C(13)	107.5(9)	C(15)-Si(2)-C(13)	105.5(7)
C(3)-Si(3)-C(16)	114.4(6)	C(3)-Si(3)-C(17)	111.3(6)
C(3)-Si(3)-C(18)	112.0(6)	C(16)-Si(3)-C(17)	106.8(7)
C(16)-Si(3)-C(18)	105.1(7)	C(17)-Si(3)-C(18)	106.8(7)
C(1)-Si(4)-C(2)	97.1(6)	C(1)-Si(4)-C(19)	115.0(6)

**Table 3.3 (continued)**

---

C(1)-Si(4)-C(20)	114.0(6)	C(2)-Si(4)-C(19)	116.2(6)
C(2)-Si(4)-C(20)	111.9(6)	Si(1)-C(1)-Si(4)	130.4(7)
Si(1)-C(1)-Ta	144.6(7)	Si(4)-C(1)-Ta	85.0(5)
Si(2)-C(2)-Si(4)	127.9(7)	Si(2)-C(2)-Ta	146.8(7)
Si(4)-C(2)-Ta	84.6(5)	Si(3)-C(3)-Ta	121.2(6)
C(21)-C(20)-Si(4)	119.8(10)	C(25)-C(20)-Si(4)	123.8(10)
C(25)-C(20)-C(21)	116.4(12)	C(22)-C(21)-C(20)	120.4(13)
C(23)-C(22)-C(21)	121.6(13)	C(22)-C(23)-C(24)	119.3(12)
C(25)-C(24)-C(23)	119.4(13)	C(24)-C(25)-C(20)	122.8(13)

---

**Table 3.4. Crystal Data for 10b**

---

formula	$C_{30}H_{57}P_2Si_4Ta$
formula weight	773.01
crystal size (mm)	0.36 x 0.20 x 0.05
temperature (K)	173(2)
crystal system	Monoclinic
space group	$P2_1/n$
lattice parameters	$a = 12.199(5) \text{ \AA}$ $\alpha = 90^\circ$ $b = 16.428(5) \text{ \AA}$ $\beta = 93.96(3)^\circ$ $c = 19.526(6) \text{ \AA}$ $\gamma = 90^\circ$
volume, $\text{\AA}^3$	3904(2)
Z	4
density (calc) ( $\text{g/cm}^3$ )	1.315
$\mu$ ( $\text{mm}^{-1}$ )	3.037
$F(000)$	1584
scan type	$\omega$ -2 $\theta$
$\theta$ range (deg)	1.62-22.54
index ranges	$h, k, \pm l$
unique reflections	5120 ( $R_{\text{int}} = 0.0499$ )
parameters varied	334
R indices	0.0606 ( $R_w F^2 = 1111$ )
goodness-of-fit on $F^2$	1.077

---

**Table 3.5. Interatomic Distances (Å) in 10b**

---

Ta-P(1)	2.596(4)	Ta-P(2)	2.631(4)
Ta-C(1)	1.977(12)	Ta-C(2)	1.951(12)
Ta-C(3)	2.282(12)	Ta--Si(4)	2.599(4)
P(1)-C(4)	1.797(14)	P(1)-C(5)	1.839(13)
P(1)-C(6)	1.816(13)	P(2)-C(7)	1.81(2)
P(2)-C(8)	1.83(2)	P(2)-C(9)	1.799(14)
Si(1)-C(1)	1.816(13)	Si(1)-C(10)	1.876(14)
Si(1)-C(11)	1.88(2)	Si(1)-C(12)	1.901(14)
Si(2)-C(2)	1.823(13)	Si(2)-C(13)	1.87(2)
Si(2)-C(14)	1.86(2)	Si(2)-C(15)	1.82(2)
Si(3)-C(3)	1.869(12)	Si(3)-C(16)	1.86(2)
Si(3)-C(17)	1.87(2)	Si(3)-C(18)	1.85(2)
Si(4)-C(1)	1.886(13)	Si(4)-C(2)	1.865(13)
Si(4)-C(19)	1.901(13)	Si(4)-C(25)	1.899(13)
C(19)-C(20)	1.39(2)	C(20)-C(21)	1.34(2)
C(21)-C(22)	1.35(2)	C(22)-C(23)	1.36(2)
C(23)-C(24)	1.41(2)	C(24)-C(19)	1.34(2)
C(25)-C(26)	1.40(2)	C(26)-C(27)	1.40(2)
C(27)-C(28)	1.36(2)	C(28)-C(29)	1.39(2)
C(29)-C(30)	1.38(2)	C(25)-C(30)	1.39(2)

---

**Table 3.6. Intramolecular Bond Angles (°) in 10b**

---

C(1)-Ta-C(2)	91.9(5)	C(1)-Ta-C(3)	146.0(5)
C(2)-Ta-C(3)	122.0(5)	C(1)-Ta-P(1)	90.0(4)
C(2)-Ta-P(1)	98.8(4)	C(3)-Ta-P(1)	84.7(3)
C(1)-Ta-P(2)	93.3(4)	C(2)-Ta-P(2)	99.6(4)
C(3)-Ta-P(2)	82.3(3)	P(1)-Ta-P(2)	161.25(12)
C(4)-P(1)-C(6)	102.1(7)	C(4)-P(1)-C(5)	101.9(7)
C(6)-P(1)-C(5)	104.7(6)	C(4)-P(1)-Ta	117.1(5)
C(5)-P(1)-Ta	109.7(5)	C(6)-P(1)-Ta	119.4(5)
C(7)-P(2)-C(8)	102.4(9)	C(7)-P(2)-C(9)	102.9(8)
C(8)-P(2)-C(9)	100.8(7)	C(7)-P(2)-Ta	115.3(6)
C(8)-P(2)-Ta	116.0(5)	C(9)-P(2)-Ta	117.2(5)
C(1)-Si(1)-C(10)	114.0(7)	C(1)-Si(1)-C(11)	113.4(6)
C(1)-Si(1)-C(12)	109.6(7)	C(10)-Si(1)-C(11)	107.1(7)
C(10)-Si(1)-C(12)	105.7(7)	C(11)-Si(1)-C(12)	106.5(7)
C(2)-Si(2)-C(13)	114.7(7)	C(2)-Si(2)-C(14)	112.1(6)
C(2)-Si(2)-C(15)	109.3(7)	C(13)-Si(2)-C(14)	106.4(8)
C(13)-Si(2)-C(15)	106.6(11)	C(14)-Si(2)-C(15)	107.5(11)
C(3)-Si(3)-C(16)	113.0(7)	C(3)-Si(3)-C(17)	112.6(7)
C(3)-Si(3)-C(18)	111.1(7)	C(16)-Si(3)-C(17)	107.9(7)
C(16)-Si(3)-C(18)	106.9(8)	C(17)-Si(3)-C(18)	105.0(8)
C(1)-Si(4)-C(2)	97.7(6)	C(1)-Si(4)-C(19)	115.7(6)

**Table 3.6 (continued)**

---

C(1)-Si(4)-C(25)	113.9(6)	C(2)-Si(4)-C(19)	113.6(6)
C(2)-Si(4)-C(25)	113.0(6)	C(19)-Si(4)-C(25)	103.5(5)
Si(1)-C(1)-Si(4)	133.9(7)	Si(1)-C(1)-Ta	141.4(7)
Si(4)-C(1)-Ta	84.5(5)	Si(2)-C(2)-Si(4)	135.4(7)
Si(2)-C(2)-Ta	138.5(7)	Si(4)-C(2)-Ta	85.8(5)
Si(3)-C(3)-Ta	137.8(7)	C(19)-C(20)-C(21)	120.5(14)
C(20)-C(21)-C(22)	124(2)	C(21)-C(22)-C(23)	118.0(14)
C(22)-C(23)-C(24)	118(2)	C(23)-C(24)-C(19)	123.4(14)
C(19)-C(20)-C(24)	116.1(13)	C(20)-C(19)-Si(4)	120.7(10)
C(24)-C(19)-Si(4)	123.2(11)	C(25)-C(26)-C(27)	120.8(14)
C(26)-C(27)-C(28)	120(2)	C(27)-C(28)-C(29)	120.4(14)
C(28)-C(29)-C(30)	120.6(14)	C(29)-C(30)-C(25)	120(2)
C(30)-C(25)-C(26)	118.7(13)	C(26)-C(25)-Si(4)	118.9(10)
C(30)-C(25)-Si(4)	122.4(11)		

---



**Table 3.7. Crystal Data for 11**

---

formula	$C_{27}H_{55}P_2Si_2Ta$	
formula weight	678.78	
crystal size (mm)	0.30 x 0.22 x 0.05	
temperature (K)	173(2)	
crystal system	Triclinic	
space group	$P\bar{1}$	
lattice parameters	$a = 10.154(3) \text{ \AA}$	$\alpha = 101.92(2)^\circ$
	$b = 10.998(3) \text{ \AA}$	$\beta = 91.86(2)^\circ$
	$c = 16.492(5) \text{ \AA}$	$\gamma = 111.98(2)^\circ$
volume, $\text{\AA}^3$	1658.8(8)	
Z	2	
density (calc) ( $\text{g/cm}^3$ )	1.359	
$\mu$ ( $\text{mm}^{-1}$ )	3.495	
$F(000)$	696	
scan type	$\omega$ -2 $\theta$	
$\theta$ range (deg)	2.05-22.54	
index ranges	$h, \pm k, \pm l$	
unique reflections	4355 ( $R_{\text{int}} = 0.0384$ )	
parameters varied	289	
R indices	0.0450 ( $R_w F^2 = 0.0901$ )	
goodness-of-fit on $F^2$	1.019	

---

**Table 3.8. Interatomic Distances (Å) in 11**

---

Ta-P(1)	2.621(3)	Ta-P(2)	2.605(3)
Ta-C(1)	1.953(8)	Ta-C(2)	1.952(9)
Ta-C(3)	2.271(9)	Ta-Si(1)	2.628(3)
P(1)-C(22)	1.796(9)	P(1)-C(23)	1.833(11)
P(1)-C(24)	1.831(11)	P(2)-C(25)	1.831(10)
P(2)-C(26)	1.823(9)	P(2)-C(27)	1.816(10)
Si(1)-C(1)	1.902(9)	Si(1)-C(2)	1.885(8)
Si(1)-C(12)	1.879(9)	Si(1)-C(13)	1.908(9)
Si(2)-C(3)	1.898(9)	Si(2)-C(19)	1.885(11)
Si(2)-C(20)	1.870(11)	Si(2)-C(21)	1.873(10)
C(1)-C(4)	1.542(12)	C(4)-C(5)	1.504(13)
C(4)-C(6)	1.578(12)	C(4)-C(7)	1.530(13)
C(2)-C(8)	1.534(12)	C(8)-C(9)	1.518(14)
C(8)-C(10)	1.543(14)	C(8)-C(11)	1.504(13)
C(13)-C(14)	1.406(13)	C(14)-C(15)	1.379(13)
C(15)-C(16)	1.371(14)	C(16)-C(17)	1.405(14)
C(17)-C(18)	1.390(13)	C(13)-C(18)	1.401(12)

---

**Table 3.9. Intramolecular Bond Angles (°) in 11**

---

C(1)-Ta-C(2)	91.9(3)	C(1)-Ta-C(3)	146.4(3)
C(2)-Ta-C(3)	121.7(3)	C(1)-Ta-P(1)	94.0(3)
C(1)-Ta-P(2)	93.9(3)	C(2)-Ta-P(1)	100.4(3)
C(2)-Ta-P(2)	96.6(3)	C(3)-Ta-P(1)	81.7(3)
C(3)-Ta-P(2)	82.2(3)	P(1)-Ta-P(2)	160.99(8)
C(22)-P(1)-C(23)	103.8(5)	C(22)-P(1)-C(24)	99.5(5)
C(23)-P(1)-C(24)	101.1(6)	C(22)-P(1)-Ta	119.2(4)
C(23)-P(1)-Ta	114.1(4)	C(24)-P(1)-Ta	116.6(4)
C(25)-P(2)-C(26)	102.7(5)	C(25)-P(2)-C(27)	100.3(5)
C(26)-P(2)-C(27)	100.7(5)	C(25)-P(2)-Ta	113.0(4)
C(26)-P(2)-Ta	117.7(4)	C(27)-P(2)-Ta	119.7(3)
C(1)-Si(1)-C(2)	95.7(4)	C(1)-Si(1)-C(12)	113.2(4)
C(1)-Si(1)-C(13)	117.9(4)	C(2)-Si(1)-C(12)	116.0(4)
C(2)-Si(1)-C(13)	112.3(4)	C(12)-Si(1)-C(13)	102.6(4)
C(3)-Si(2)-C(19)	112.3(5)	C(3)-Si(2)-C(20)	110.3(5)
C(3)-Si(2)-C(21)	113.8(4)	C(19)-Si(2)-C(20)	105.5(5)
C(19)-Si(2)-C(21)	106.7(5)	C(20)-Si(2)-C(21)	107.7(5)
C(4)-C(1)-Si(1)	126.5(6)	C(4)-C(1)-Ta	147.6(6)
Si(1)-C(1)-Ta	85.9(3)	C(8)-C(2)-Si(1)	130.3(7)
C(8)-C(2)-Ta	142.9(6)	Si(1)-C(2)-Ta	86.4(3)
Si(2)-C(3)-Ta	135.7(5)	C(1)-C(4)-C(5)	110.7(8)

**Table 3.9 (continued)**

---

C(1)-C(4)-C(6)	111.3(7)	C(1)-C(4)-C(7)	110.1(7)
C(5)-C(4)-C(6)	108.8(8)	C(5)-C(4)-C(7)	108.6(8)
C(6)-C(4)-C(7)	108.0(8)	C(2)-C(8)-C(9)	112.5(8)
C(2)-C(8)-C(10)	109.0(8)	C(2)-C(8)-C(11)	109.4(8)
C(9)-C(8)-C(10)	108.1(8)	C(9)-C(8)-C(11)	108.5(9)
C(10)-C(8)-C(11)	109.3(9)	C(13)-C(14)-C(15)	121.6(9)
C(14)-C(15)-C(16)	121.6(10)	C(15)-C(16)-C(17)	117.9(10)
C(16)-C(17)-C(18)	121.0(9)	C(17)-C(18)-C(13)	120.9(9)
C(18)-C(13)-C(14)	116.9(8)	C(14)-C(13)-Si(1)	121.7(7)
C(18)-C(13)-Si(1)	121.3(7)		

---

**Table 3.10. Crystal Data for 12**

---

formula	$C_{31}H_{61}P_2Si_5Ta$
formula weight	817.14
crystal size (mm)	0.32 x 0.26 x 0.20
temperature (K)	173(2)
crystal system	Orthorhombic
space group	<i>Pnma</i>
lattice parameters	$a = 10.667(3) \text{ \AA}$ $\alpha = 90^\circ$
	$b = 17.314(4) \text{ \AA}$ $\beta = 90^\circ$
	$c = 25.591(5) \text{ \AA}$ $\gamma = 90^\circ$
volume, $\text{\AA}^3$	4726(2)
Z	4
density (calc) ( $\text{g/cm}^3$ )	1.148
$\mu$ ( $\text{mm}^{-1}$ )	2.536
$F(000)$	1680
scan type	$\omega$ -2 $\theta$
$\theta$ range (deg)	2.07-22.55
index ranges	$h, k, \pm l$
unique reflections	3230 ( $R_{\text{int}} = 0.0744$ )
parameters varied	208
R indices	0.0583 ( $R_w F^2 = 0.1669$ )
goodness-of-fit on $F^2$	1.035

---

**Table 3.11. Interatomic Distances (Å) in 12**

---

Ta-P(1)	2.608(6)	Ta-P(2)	2.624(6)
Ta-C(1)	1.985(15)	Ta-C(1A)	1.985(14)
Ta-C(2)	2.23(3)	Ta-C(2A)	2.23(3)
P(1)-C(10)	1.76(2)	P(1)-C(11)	1.751(18)
P(1)-C(11A)	1.751(18)	P(2)-C(12)	1.79(3)
P(2)-C(13)	1.894(16)	P(2)-C(13A)	1.894(16)
Si(1)-C(1)	1.847(15)	Si(1)-C(4)	1.845(17)
Si(1)-C(5)	1.863(16)	Si(1)-C(6)	1.880(15)
Si(2)-C(2)	1.87(3)	Si(2)-C(7)	1.84(3)
Si(2)-C(8)	1.92(3)	Si(2)-C(9)	1.83(4)
Si(3)-C(1)	1.854(14)	Si(3)-C(3)	1.873(12)
Si(3)-C(14)	1.880(18)	C(14)-C(15)	1.38(3)
C(15)-C(16)	1.34(3)	C(16)-C(17)	1.25(5)
C(17)-C(18)	1.25(5)	C(18)-C(19)	1.55(3)
C(14)-C(19)	1.32(3)		

---

**Table 3.12. Intermolecular Bond Angles (°) in 12**

---

C(1)-Ta-C(1A)	113.0(8)	C(1)-Ta-C(2)	131.7(10)
C(1)-Ta-C(2A)	115.3(11)	C(1A)-Ta-C(2A)	131.7(11)
C(1A)-Ta-C(2)	115.3(11)	C(1)-Ta-P(1)	94.1(4)
C(1A)-Ta-P(1)	94.1(4)	C(2)-Ta-P(1)	82.6(7)
C(2A)-Ta-P(1)	82.6(7)	C(1)-Ta-P(2)	93.0(4)
C(1A)-Ta-P(2)	93.0(4)	C(2)-Ta-P(2)	84.8(7)
C(2A)-Ta-P(2)	84.8(7)	P(1)-Ta-P(2)	167.25(18)
C(10)-P(1)-C(11)	95.4(11)	C(10)-P(1)-C(11A)	95.4(11)
C(11)-P(1)-C(11A)	101.6(17)	C(10)-P(1)-Ta	114.8(9)
C(11)-P(1)-Ta	121.9(8)	C(11A)-P(1)-Ta	121.9(8)
C(12)-P(2)-C(13)	101.9(8)	C(12)-P(2)-C(13A)	101.9(8)
C(13)-P(2)-C(13A)	102.4(11)	C(12)-P(2)-Ta	112.9(8)
C(13)-P(2)-Ta	117.7(6)	C(13A)-P(2)-Ta	117.7(6)
C(1)-Si(1)-C(4)	108.0(8)	C(1)-Si(1)-C(5)	114.3(7)
C(1)-Si(1)-C(6)	113.6(7)	C(4)-Si(1)-C(5)	107.1(8)
C(4)-Si(1)-C(6)	109.0(8)	C(5)-Si(1)-C(6)	104.5(8)
C(1)-Si(3)-C(3)	113.9(8)	C(1)-Si(3)-C(14)	118.2(7)
C(3)-Si(3)-C(14)	101.9(9)	Si(1)-C(1)-Si(3)	112.8(8)
Si(1)-C(1)-Ta	126.0(7)	Si(3)-C(1)-Ta	120.6(8)
Si(3)-C(3)-Si(3A)	113.0(11)	C(14)-C(15)-C(16)	124(3)
C(15)-C(16)-C(17)	116(4)	C(16)-C(17)-C(18)	127(4)

**Table 3.12 (continued)**

---

C(17)-C(18)-C(19)	119(3)	C(18)-C(19)-C(14)	113(3)
C(19)-C(14)-C(15)	119(2)	C(15)-C(14)-Si(3)	121.8(19)
C(19)-C(14)-Si(3)	118(2)	Si(2)-C(2)-Ta	147(2)
Si(2A)-C(2A)-Ta	147(2)	C(2)-Si(2)-C(7)	116.7(13)
C(2)-Si(2)-C(8)	112.1(15)	C(2)-Si(2)-C(9)	106.3(16)
C(7)-Si(2)-C(8)	107.3(15)	C(7)-Si(2)-C(9)	107.3(18)
C(8)-Si(2)-C(9)	106.7(15)		

---



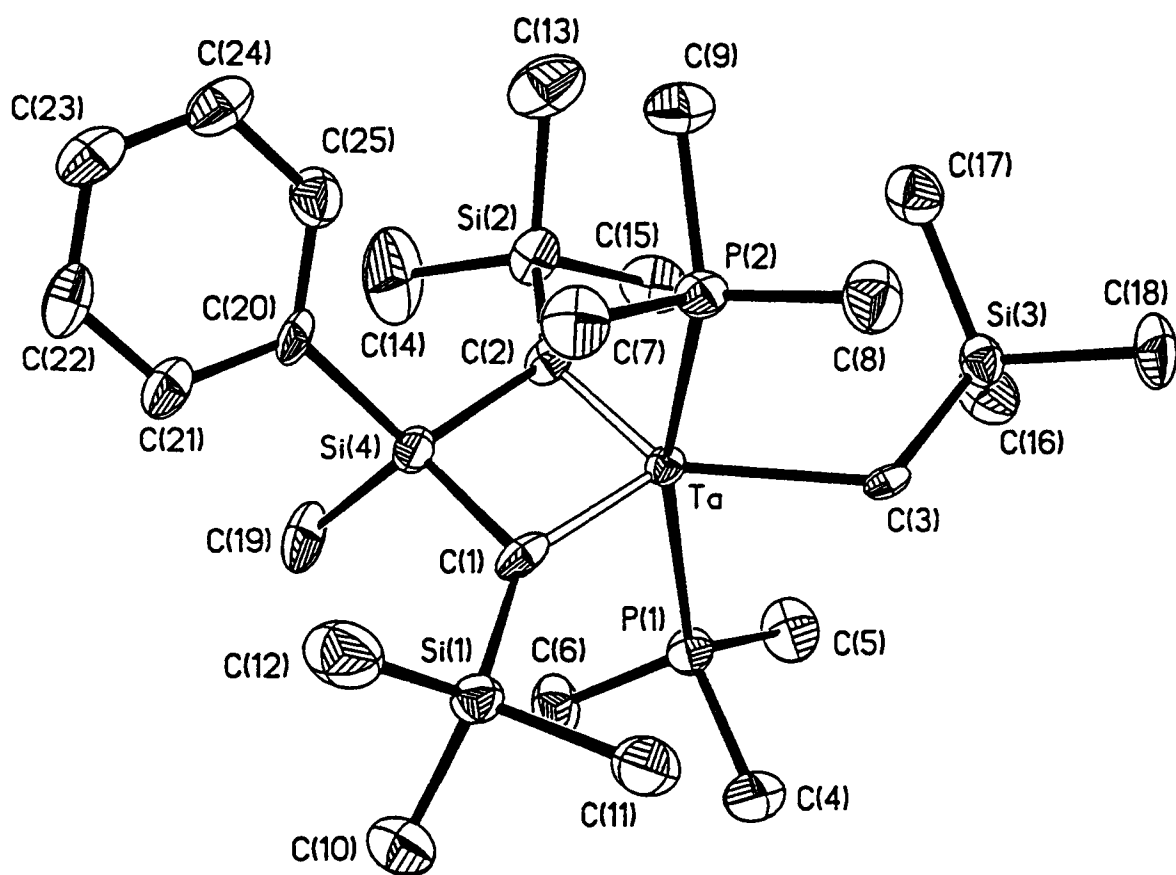


Figure 3.5 ORTEP diagram of 10a, showing 50% ellipsoids.

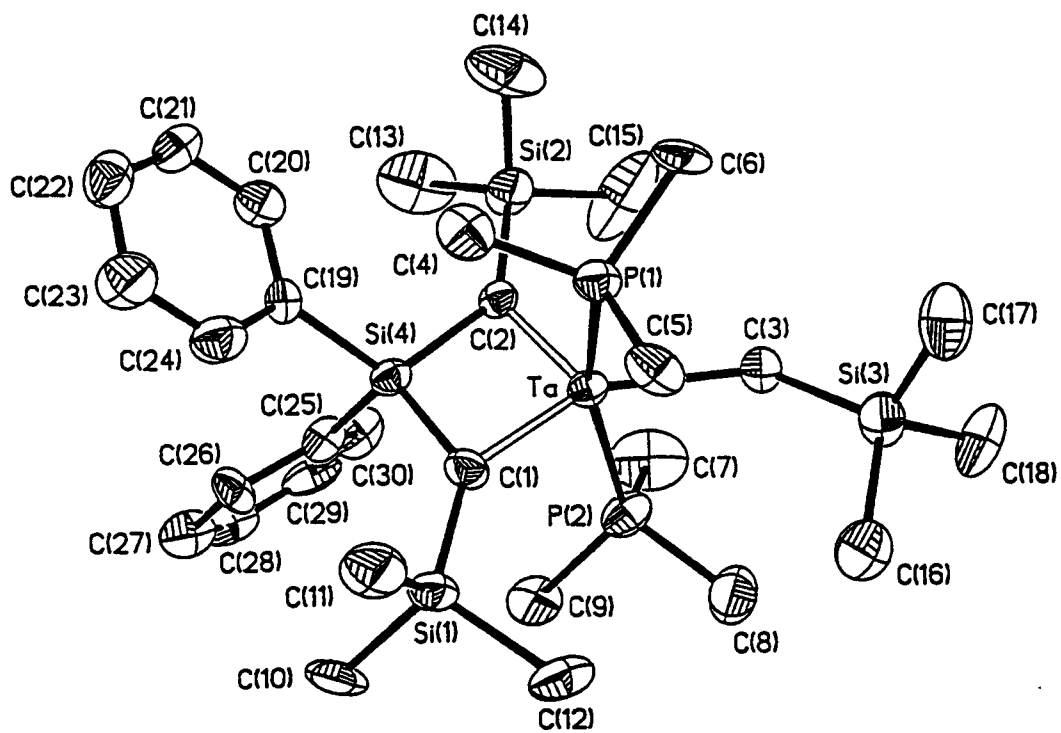


Figure 3.6 ORTEP diagram of 10b, showing 50% ellipsoids

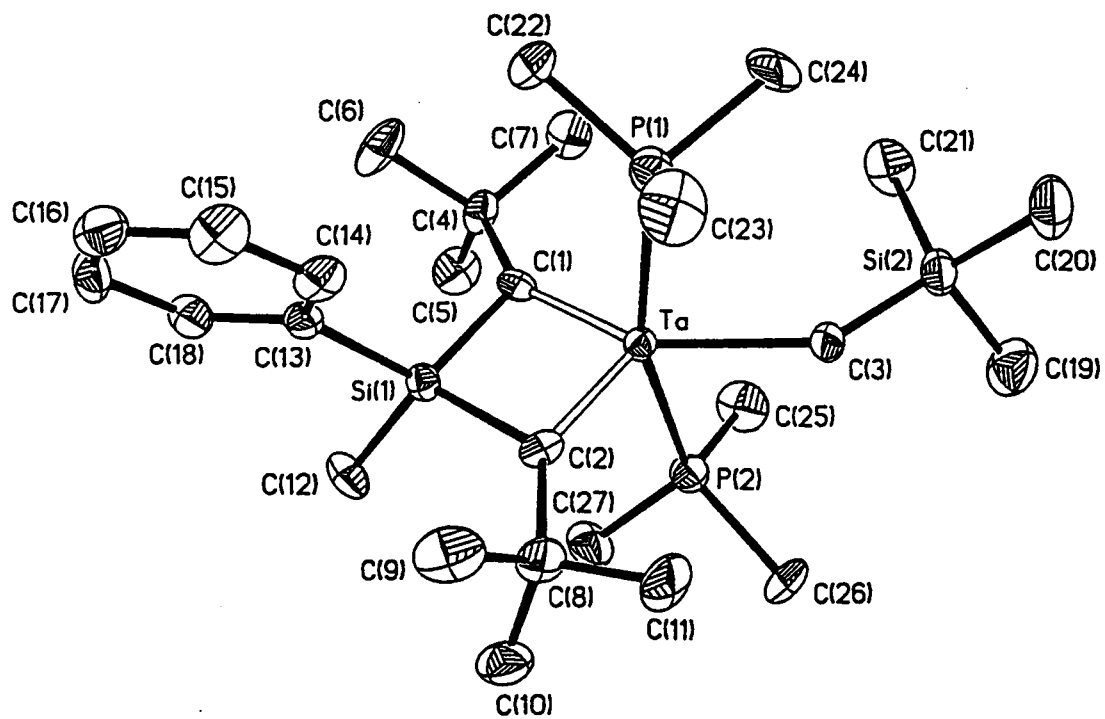


Figure 3.7 ORTEP diagram of 11, showing 50% ellipsoids.

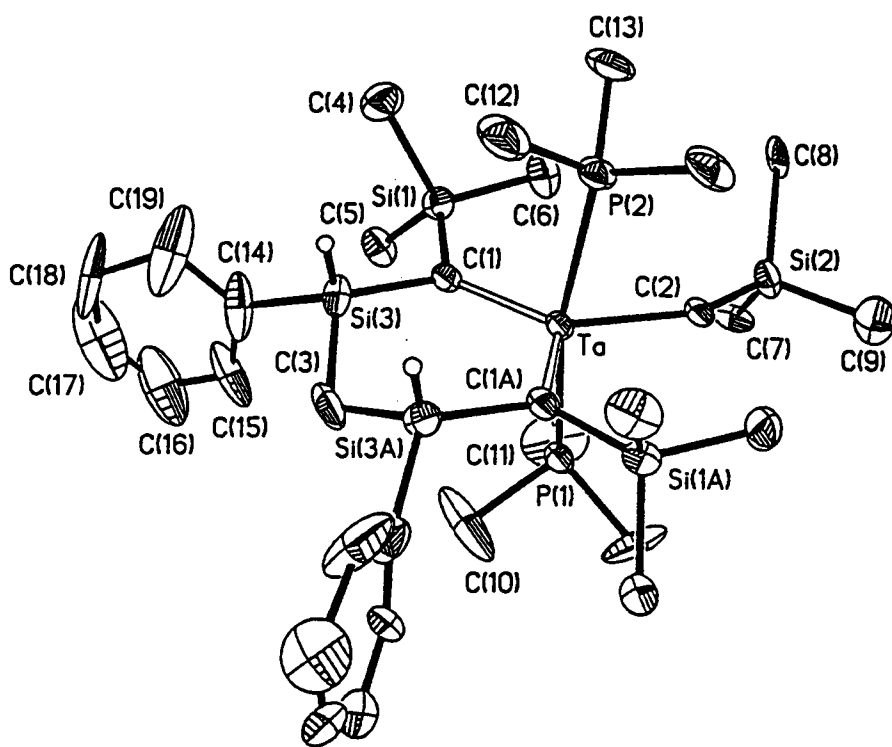


Figure 3.8 ORTEP diagram of 12, showing 30% ellipsoids.

[Ta-Si distance of 2.599(4) Å].

The structure of **11** is similar to **10a**, except that the *exo*-SiMe<sub>3</sub> groups of the metallasilacyclobutadiene ring are replaced by -Bu<sup>t</sup> groups (Figure 3.7). Again, the Ta atom has a distorted trigonal bipyramidal geometry with axial PMe<sub>3</sub> ligands, and the Ta=C bond distances of 1.952(9) and 1.953(8) Å are consistent with the presence of two alkylidene moieties. Despite the instability of **11** in solution, in which it decomposes by loss of a PMe<sub>3</sub> ligand followed by SiMe<sub>4</sub> elimination, there is little in the structure of **11** to indicate increased steric strain around the Ta center. The Ta-P distances of 2.621(3) and 2.628(3) Å are similar to those in **10a** and **10b**, which range from 2.596(4) Å to 2.664(3) Å. The Ta-C-Si angle of the Me<sub>3</sub>SiCH<sub>2</sub>- ligand in **11** is 135.7(5)°, which is wider than that [121.2(6)°] in **10a**, but less than that [137.8(7)°] in **10b**. The Ta-Si distance of 2.621(3) Å is slightly longer than those in **10a-b**. It is therefore unclear from the solid-state structure of **11** why this complex is unstable in solution, while complexes **10a-b** are stable indefinitely in solution. It is possible that the instability of **11** is perhaps the result of a combination of steric and electronic effects caused by the nature of the *exo*-R group on the metallasilacyclobutadiene ring; the presence of a SiMe<sub>3</sub> group *exo*- to the ring in **10a-b** may help to stabilize these complexes towards decomposition. It is well established that a silyl substituent helps to stabilize adjacent metal-carbon bonds.<sup>34</sup> The lack of silyl substituents *exo*- to the metallasilacyclobutadiene ring in **11** may contribute to the lower stability of this complex in solution.

Analysis of the structure of the crystals of **12** revealed them to be that of a *meso*-isomer (Figure 3.8), in which the metalladisilacyclohexadiene ring is in a half-chair conformation, and the Ph rings on the ring Si atoms were found to occupy pseudo-equatorial positions. The molecule was found to exhibit crystallographically imposed mirror symmetry, with the Me<sub>3</sub>SiCH<sub>2</sub>- ligand disordered over the mirror plane. This ligand was therefore refined as two mirror images with site occupancy factors of 0.5. The Ta atom exhibits distorted trigonal bipyramidal geometry, with the PMe<sub>3</sub> ligands occupying axial positions. The Ta=C distances of 1.985(15) and 1.985(14) Å are again consistent with other alkylidene complexes of tantalum. The C=Ta=C bond angle of 113.0(8)° is much wider than those in the metallasilacyclobutadiene complexes **10a-b** and **11** [91.9(3)° to 93.3(5)°]. This large angle causes the *exo*-SiMe<sub>3</sub> groups [Si(1)Me<sub>3</sub>] to be in closer proximity to the Me<sub>3</sub>SiCH<sub>2</sub>- ligand, which in turn leads to a considerable widening of the Ta-C-Si angle [147(2)°] in the Me<sub>3</sub>SiCH<sub>2</sub>- ligand.

### 3.3 Experimental Section

All manipulations were performed under a dry nitrogen atmosphere with the use of either standard Schlenk techniques or a glovebox. All solvents were purified by distillation from potassium/benzophenone ketyl. CH<sub>2</sub>Cl<sub>2</sub> was distilled from CaH<sub>2</sub> before use. Benzene-*d*<sub>6</sub> and toluene-*d*<sub>8</sub> were dried over activated molecular sieves and stored under nitrogen. NMR spectra were

recorded on a Bruker AC-250 or AMX-400 Fourier transform spectrometer, and were referenced to solvents (residual protons in the  $^1\text{H}$  spectra).  $^{29}\text{Si}$  and  $^{31}\text{P}$  chemical shifts were referenced to  $\text{SiMe}_4$  and external 85%  $\text{H}_3\text{PO}_4$ , respectively.  $\text{TaCl}_5$  (Strem) was sublimed before use.  $\text{PMe}_3$  (Aldrich) and 1.0 M anhydrous  $\text{HCl}$  in  $\text{Et}_2\text{O}$  (Aldrich) were used as received.  $\text{PhMeSiH}_2$  (Gelest) and  $\text{Ph}_2\text{SiH}_2$  (Aldrich) were dried over activated molecular sieves and stored under nitrogen.  $\text{Me}_3\text{SiCH}_2\text{MgCl}$ ,<sup>30</sup>  $(^t\text{BuCH}_2)_3\text{Ta}=\text{CHBu}^t$ ,<sup>16</sup>  $(^t\text{BuCH}_2)\text{Ta}(\text{PMe}_3)_2[=\text{CHBu}^t]$ ,<sup>16a</sup> and  $\text{PhSiH}_2\text{Cl}$ <sup>31</sup> were prepared by the literature procedures.  $(\text{Me}_3\text{SiCH}_2)\text{Ta}(\text{PMe}_3)_2[=\text{CHSiMe}_3]_2$  (**4**) was prepared as described in Chapter 2 of this dissertation. Elemental analyses were performed by E + R Microanalytical, Parsippany, NJ.

**Preparation of  $(\text{Me}_3\text{SiCH}_2)_3\text{Ta}(\text{PMe}_3)=\text{CHSiMe}_3$  (**7**).** The following is a modified procedure from the previously reported synthesis.<sup>28</sup> A slurry of 5.0 g (0.014 mol) of  $\text{TaCl}_5$  in 75 mL of hexanes at  $-20\text{ }^\circ\text{C}$  was treated dropwise with 41.0 mL of a  $\text{Me}_3\text{SiCH}_2\text{MgCl}$  solution in  $\text{Et}_2\text{O}$  (1.7 M, 0.070 mol). The mixture turned green, then green-yellow, and finally bright yellow as  $(\text{Me}_3\text{SiCH}_2)_5\text{Ta}$  was produced. The reaction was monitored carefully by  $^1\text{H}$  NMR until complete conversion to  $(\text{Me}_3\text{SiCH}_2)_5\text{Ta}$ <sup>32</sup> was achieved, at which time the solvents were removed *in vacuo*. The yellow residue was taken up in hexanes at  $0\text{ }^\circ\text{C}$  and filtered to remove  $\text{MgCl}_2$ .  $\text{PMe}_3$  (1.7 mL, 0.017 mol) was then added by syringe, and the solution was heated to  $50\text{ }^\circ\text{C}$  for 1 hr, during which time a bright orange color developed. At this time NMR showed the conversion to **7** to

be complete, and the solution was filtered to remove any remaining  $\text{MgCl}_2$ , concentrated, and cooled to  $-20\text{ }^\circ\text{C}$ , producing 7.8 g (92 %) of **7** as bright orange crystals. NMR:  $^1\text{H}$  NMR (benzene- $d_6$ , 250.1 MHz,  $23\text{ }^\circ\text{C}$ )  $\delta$  6.17 (s, 1H, =CHSiMe<sub>3</sub>), 0.89 (d, 9H,  $^2J_{\text{H-P}} = 4.4\text{ Hz}$ , PMe<sub>3</sub>), 0.30 (s, 9H, =CHSiMe<sub>3</sub>), 0.27 (s, 27H, CH<sub>2</sub>SiMe<sub>3</sub>), 0.24 (s, 6H, CH<sub>2</sub>SiMe<sub>3</sub>).  $^{13}\text{C}\{^1\text{H}\}$  NMR (benzene- $d_6$ , 62,9 MHz,  $23\text{ }^\circ\text{C}$ )  $\delta$  251.8 (=CHSiMe<sub>3</sub>), 77.3 (CH<sub>2</sub>SiMe<sub>3</sub>), 15.9 (d,  $^1J_{\text{C-P}} = 8.6\text{ Hz}$ , PMe<sub>3</sub>), 3.6 (=CHSiMe<sub>3</sub>), 3.0 (CH<sub>2</sub>SiMe<sub>3</sub>).

**Preparation of (Me<sub>3</sub>SiCH<sub>2</sub>)Ta(PMe<sub>3</sub>)<sub>2</sub>[=CHBu<sup>t</sup>]<sub>2</sub> (**8**).** A solution of 1.24 g of (tBuCH<sub>2</sub>)<sub>3</sub>Ta=CHBu<sup>t</sup> (2.67 mmol) in 20 mL of toluene at  $-60\text{ }^\circ\text{C}$  was treated dropwise with 12.6 mL of HCl in Et<sub>2</sub>O (0.21 M, 2.6 mmol). The HCl/Et<sub>2</sub>O was prepared by diluting 2.6 mL of 1.0 M HCl in Et<sub>2</sub>O with 10 mL of Et<sub>2</sub>O. The resulting solution of (tBuCH<sub>2</sub>)<sub>4</sub>TaCl<sup>16b</sup> was then treated with 0.60 mL of PMe<sub>3</sub> (5.8 mmol, excess) and warmed to room temperature with stirring. After 4 hr NMR spectra of the resulting orange solution showed complete conversion to ClTa(PMe<sub>3</sub>)<sub>2</sub>[=CHBu<sup>t</sup>]<sub>2</sub>.<sup>16a</sup> 2.8 mL of a Me<sub>3</sub>SiCH<sub>2</sub>MgCl solution in Et<sub>2</sub>O (1.12 M, 3.1 mmol) was then added to the solution. After 1 hr, the volatiles were removed by vacuum, and the yellow-brown residue extracted with 30 mL of pentane. The pentane solution was then filtered, concentrated, and cooled to  $-20\text{ }^\circ\text{C}$ , yielding 3 crops of orange crystals totaling 0.743 g [49.9 % yield based on (tBuCH<sub>2</sub>)<sub>3</sub>Ta=CHBu<sup>t</sup>]. NMR:  $^1\text{H}$  NMR (benzene- $d_6$ , 250.1 MHz,  $23\text{ }^\circ\text{C}$ )  $\delta$  7.27 (s, 1H, =CHBu<sup>t</sup>), 1.44 (s, 1H, =CHBu<sup>t</sup>), 1.26 (t, 18H,  $^2J_{\text{H-P}} = 2.7\text{ Hz}$ , PMe<sub>3</sub>), 1.25 (s, 18H, =CHCMe<sub>3</sub>), 0.27 (s, 9H, CH<sub>2</sub>SiMe<sub>3</sub>), -0.27 (t, 2H,  $^3J_{\text{H-P}} = 20.1\text{ Hz}$ ,



$\text{CH}_2\text{SiMe}_3$ ).  $^{13}\text{C}\{^1\text{H}\}$  NMR (benzene- $d_6$ , 62.9 MHz, 23 °C)  $\delta$  273.1, 242.2 (=CHBu<sup>t</sup>), 47.4, 44.1 (=CHCMe<sub>3</sub>), 37.3 (CH<sub>2</sub>SiMe<sub>3</sub>), 35.3, 34.3 (=CHCMe<sub>3</sub>), 19.3 (t,  $^1J_{\text{C-P}} = 11.6$  Hz, PMe<sub>3</sub>), 5.2 (CH<sub>2</sub>SiMe<sub>3</sub>). Anal. Calcd for C<sub>20</sub>H<sub>49</sub>SiP<sub>2</sub>Ta: C, 42.85; H, 8.81. Found: C, 42.84; H, 8.82.

**Preparation of (Me<sub>3</sub>SiCH<sub>2</sub>)<sub>3</sub>Ta[=C(SiMe<sub>3</sub>)SiPhRH] (R = Me, 9a; Ph, 9b).** A solution of 0.90 g (1.5 mmol) of **7** in 30 mL of hexanes was treated dropwise with a solution of 0.20 g (1.6 mmol) of PhMeSiH<sub>2</sub> in 5 mL of hexanes. The reaction mixture was then stirred for 18 hr at room temperature, during which time the color changed from orange to red-orange. Removal of solvent yielded ca. 0.9 g of a red-orange oil of **9a** which also contained a small (< 5% by <sup>1</sup>H NMR) amount of (Me<sub>3</sub>SiCH<sub>2</sub>)<sub>4</sub>Ta<sub>2</sub>(μ-CSiMe<sub>3</sub>)<sub>2</sub>. Attempts to crystallize the compound were unsuccessful, and the instability of **9** in solution precluded attempts to obtain analytically pure samples for microanalysis. A similar result was obtained for **9b**. Data for **9a**: <sup>1</sup>H NMR (benzene- $d_6$ , 250.1 MHz, 23 °C)  $\delta$  7.20-7.90 (m, 5H, SiPhMeH), 4.90 (q, 1H,  $^3J_{\text{H-H}} = 3.6$  Hz, SiPhMeH), 1.20 (d, 3H,  $^2J_{\text{H-H}} = 12.1$  Hz, CH<sub>a</sub>H<sub>b</sub>SiMe<sub>3</sub>), 0.92 (d, 3H, CH<sub>a</sub>H<sub>b</sub>SiMe<sub>3</sub>), 0.80 (d, 3H, SiPhMeH), 0.30 (s, 9H, =CSiMe<sub>3</sub>), 0.19 (s, 27H, CH<sub>2</sub>SiMe<sub>3</sub>).  $^{13}\text{C}\{^1\text{H}\}$  NMR (benzene- $d_6$ , 62.9 MHz, 23 °C)  $\delta$  240.6 (=CSiMe<sub>3</sub>), 137.6, 135.3, 129.5, 128.0 (SiPhMeH), 89.6 (CH<sub>2</sub>SiMe<sub>3</sub>), 5.0 (=CSiMe<sub>3</sub>), 2.7 (CH<sub>2</sub>SiMe<sub>3</sub>), -1.9 (SiPhMeH).  $^{29}\text{Si}\{^1\text{H}\}$  NMR (benzene- $d_6$ , 79.5 MHz, 27 °C)  $\delta$  0.08 (CH<sub>2</sub>SiMe<sub>3</sub>), -13.2 (=CSiMe<sub>3</sub>), -49.9 (=CSiPhMeH). Data for **9b**: <sup>1</sup>H NMR (benzene- $d_6$ , 250.1 MHz, 23 °C)  $\delta$  7.20-7.90 (m, 10H, SiPh<sub>2</sub>H), 5.07 (s, 1H, SiPh<sub>2</sub>H), 1.19 (s, 6H,

CH<sub>2</sub>SiMe<sub>3</sub>), 0.31 (s, 9H, =CSiMe<sub>3</sub>), 0.19 (s, 27H, CH<sub>2</sub>SiMe<sub>3</sub>). <sup>13</sup>C{<sup>1</sup>H} NMR (benzene-*d*<sub>6</sub>, 62.9 MHz, 23 °C) δ 238.2 (=CSiMe<sub>3</sub>), 137.5, 136.5, 129.7, 128.1 (SiPh<sub>2</sub>H), 90.7 (CH<sub>2</sub>SiMe<sub>3</sub>), 5.19 (=CSiMe<sub>3</sub>), 2.72 (CH<sub>2</sub>SiMe<sub>3</sub>). <sup>29</sup>Si{<sup>1</sup>H} NMR (benzene-*d*<sub>6</sub>, 79.5 MHz, 27 °C) δ 0.37 (CH<sub>2</sub>SiMe<sub>3</sub>), -13.1 (=CSiMe<sub>3</sub>), -48.3 (=CSiPh<sub>2</sub>H).

#### Preparation of Metallasilacyclobutadiene Complexes. Synthesis of

**10a.** A solution of 0.204 g (0.344 mmol) of (Me<sub>3</sub>SiCH<sub>2</sub>)Ta(PMe<sub>3</sub>)<sub>2</sub>[=CHSiMe<sub>3</sub>]<sub>2</sub> (**4**) in 10 mL of hexanes was treated with 0.044 g (0.35 mmol) of PhMeSiH<sub>2</sub> in 5 mL of hexanes. The solution was stirred at room temperature for 3 h, during which time the color changed from bright orange to yellow. The solution was then concentrated and cooled to -20 °C, producing 0.190 g (78%) of **10a** as yellow crystals. NMR: <sup>1</sup>H NMR (benzene-*d*<sub>6</sub>, 250.1 MHz, 23 °C) δ 7.17-7.86 (m, 5H, SiMePh), 1.12 (d, 9H, <sup>2</sup>J<sub>H-P</sub> = 6.6 Hz, PMe<sub>3</sub>), 1.00 (s, 3H, SiMePh), 0.88 (d, 9H, <sup>2</sup>J<sub>H-P</sub> = 6.7 Hz, PMe<sub>3</sub>), 0.35 (s, 18H, =CSiMe<sub>3</sub>), 0.25 (s, 9H, CH<sub>2</sub>SiMe<sub>3</sub>), -0.46 (t, 2H, <sup>3</sup>J<sub>H-P</sub> = 16.0 Hz, CH<sub>2</sub>SiMe<sub>3</sub>). <sup>13</sup>C{<sup>1</sup>H} NMR (benzene-*d*<sub>6</sub>, 62.9 MHz, 23 °C) δ 255.1 (=CSiMe<sub>3</sub>), 145.8, 136.3, 127.8, 127.2 (SiMePh), 50.4 (CH<sub>2</sub>SiMe<sub>3</sub>), 17.9 (d, <sup>1</sup>J<sub>C-P</sub> = 12.5 Hz, PMe<sub>3</sub>), 17.6 (d, <sup>1</sup>J<sub>C-P</sub> = 12.9 Hz, PMe<sub>3</sub>), 5.9 (=CSiMe<sub>3</sub>), 5.8 (SiMePh), 5.8 (CH<sub>2</sub>SiMe<sub>3</sub>). <sup>29</sup>Si{<sup>1</sup>H} NMR (benzene-*d*<sub>6</sub>, 79.5 MHz, 27 °C) δ 0.40 (CH<sub>2</sub>SiMe<sub>3</sub>), -15.4 (=CSiMe<sub>3</sub>), -76.8 (SiMePh). <sup>31</sup>P{<sup>1</sup>H} NMR (benzene-*d*<sub>6</sub>, 162.0 MHz, 27 °C) δ -4.51 (d, <sup>2</sup>J<sub>P-P</sub> = 125 Hz), -7.03 (d). The <sup>13</sup>C resonance assignments were confirmed by the use of <sup>13</sup>C-<sup>1</sup>H HETCOR NMR. Anal. Calcd for C<sub>25</sub>H<sub>55</sub>P<sub>2</sub>Si<sub>4</sub>Ta: C, 42.24; H, 7.80. Found: C, 42.11; H,

7.69.

**Synthesis of 10b.** A solution of 0.199 g (0.336 mmol) of **4** in 10 mL of hexanes was treated dropwise with 0.070 g (0.38 mmol) of  $\text{Ph}_2\text{SiH}_2$  in 5 mL of hexanes. The reaction solution was stirred for 4 h, during which time the color changed from bright orange to yellow. The solution was then concentrated and cooled to  $-20\text{ }^\circ\text{C}$ , producing 0.114 g of **10b** as yellow needles (44.0% yield).

NMR:  $^1\text{H}$  NMR (benzene- $d_6$ , 250.1 MHz,  $23\text{ }^\circ\text{C}$ )  $\delta$  7.09-7.89 (m, 10H,  $\text{SiPh}_2$ ), 0.94 (t, 18H,  $^2J_{\text{H-P}} = 3.14\text{ Hz}$ ,  $\text{PMe}_3$ ), 0.41 (s, 18H,  $=\text{CSiMe}_3$ ), 0.26 (s, 9H,  $\text{CH}_2\text{SiMe}_3$ ), -0.41 (t, 2H,  $^3J_{\text{H-P}} = 15.8\text{ Hz}$ ,  $\text{CH}_2\text{SiMe}_3$ ).  $^{13}\text{C}\{^1\text{H}\}$  NMR (benzene- $d_6$ , 62.9 MHz,  $23\text{ }^\circ\text{C}$ )  $\delta$  255.4 ( $=\text{CSiMe}_3$ ), 143.3, 137.4, 128.0, 127.1 ( $\text{SiPh}_2$ ), 52.5 ( $\text{CH}_2\text{SiMe}_3$ ), 17.5 (t,  $^1J_{\text{C-P}} = 11.3\text{ Hz}$ ,  $\text{PMe}_3$ ), 6.55 ( $=\text{CSiMe}_3$ ), 5.83 ( $\text{CH}_2\text{SiMe}_3$ ).  $^{29}\text{Si}\{^1\text{H}\}$  NMR (benzene- $d_6$ , 79.49 MHz,  $27\text{ }^\circ\text{C}$ )  $\delta$  0.70 ( $\text{CH}_2\text{SiMe}_3$ ), -16.6 ( $=\text{CSiMe}_3$ ), -75.5 ( $\text{SiPh}_2$ ).  $^{31}\text{P}\{^1\text{H}\}$  NMR (benzene- $d_6$ , 162.0 MHz,  $27\text{ }^\circ\text{C}$ )  $\delta$  -6.72. Anal. Calcd for  $\text{C}_{30}\text{H}_{57}\text{P}_2\text{Si}_4\text{Ta}$ : C, 46.61; H, 7.43. Found: C, 46.45; H, 7.49.

**Synthesis of 11.** A solution of 0.548 g of  $(\text{Me}_3\text{SiCH}_2)\text{Ta}(\text{PMe}_3)_2[=\text{CHBu}^t]_2$  (**8**) (0.978 mmol) in 10 mL of pentane was treated with 0.236 mL of  $\text{PhMeSiH}_2$  (1.93 mmol) in 2 mL of pentane. The solution was stirred for 2 h, during which time the color changed from yellow-orange to orange. Concentration and cooling of the solution to  $-20\text{ }^\circ\text{C}$  yielded 0.249 g of **11** as yellow crystals (37.5%). NMR:  $^1\text{H}$  NMR (benzene- $d_6$ , 250.1 MHz,  $23\text{ }^\circ\text{C}$ )  $\delta$  7.10-8.00 (m, 5H,  $\text{SiPhMe}$ ), 1.40 (s, 18H,  $=\text{CCMe}_3$ ), 1.18 (d, 9H,

$^2J_{\text{H-P}} = 6.2$  Hz,  $\text{PMe}_3$ ), 1.12 (s, 3H,  $\text{SiPhMe}$ ), 1.09 (br d, 9H,  $^2J_{\text{H-P}} = 6.3$  Hz,  $\text{PMe}_3$ ), 0.28 (s, 9H,  $\text{CH}_2\text{SiMe}_3$ ), -0.46 (br t, 2H,  $^3J_{\text{H-P}} = 15.2$  Hz,  $\text{CH}_2\text{SiMe}_3$ ).  $^{13}\text{C}\{^1\text{H}\}$  NMR (benzene- $d_6$ , 62.9 MHz, 23 °C)  $\delta$  271.9 (=C $\text{Bu}^\dagger$ ), 145.4, 138.0, 127.1, 126.5 ( $\text{SiPhMe}$ ), 51.0 ( $\text{CH}_2\text{SiMe}_3$ ), 47.9 (=C $\text{CMe}_3$ ), 37.3 (=C $\text{CMe}_3$ ), 18.5 (overlapping d,  $\text{PMe}_3$ ), 5.95 ( $\text{CH}_2\text{SiMe}_3$ ), 3.82 ( $\text{SiPhMe}$ ). Anal. Calcd for  $\text{C}_{27}\text{H}_{55}\text{Si}_2\text{P}_2\text{Ta}$ : C, 47.78; H, 8.17. Found: C, 47.76; H, 8.18.

**Reaction of ( $\text{tBuCH}_2$ )Ta( $\text{PMe}_3$ )[=CH $\text{Bu}^\dagger$ ] $_2$  (3) with  $\text{PhMeSiH}_2$ .** Complex 3 (0.029 g, 0.053 mmol) was dissolved in benzene- $d_6$  in an NMR tube.  $\text{PhMeSiH}_2$  (0.025 g, 0.20 mmol) was added to the NMR tube. NMR spectra of the solution showed the products to be  $\text{H}_2$ , neopentane ( $\text{CMe}_4$ ),  $\text{PMe}_3$ , and other unidentified species. Another attempt in hexanes with 0.191 g of 3 and 0.050 g of  $\text{PhMeSiH}_2$  gave, after removal of solvent, a red oil whose NMR spectra were similar to those observed above.

**Synthesis of Bis(phenylsilyl)methane ( $\text{PhSiH}_2$ ) $_2\text{CH}_2$ .**<sup>29</sup> A flame-dried flask was charged with 0.76 g (0.031 mol) of Mg turnings, followed by 0.70 g of Zn dust, 0.90 mL (1.2 g, 0.014 mol) of  $\text{CH}_2\text{Cl}_2$ , and 4.0 g (0.028 mol) of  $\text{PhSiH}_2\text{Cl}$ . A condenser was added to the flask, and the mixture was stirred and heated to 40 °C. 50 mL of THF was then added dropwise, and the mixture stirred at 40 °C for 36 h. The supernatant was filtered into 50 mL of 10% aq. HCl, and the  $\text{MgCl}_2/\text{Zn}$  washed with 50 mL of hexanes. The organic phase was dried over  $\text{MgSO}_4$ , and the solvents evaporated. Vacuum distillation at 105-110 °C/0.05 torr yielded 1.39 g (43 %) of ( $\text{PhSiH}_2$ ) $_2\text{CH}_2$ . NMR:  $^1\text{H}$  NMR

(benzene- $d_6$ , 250.1 MHz, 23 °C)  $\delta$  7.11-7.45 (m, 10H, *Ph*), 4.57 (t, 4H,  $^3J_{\text{H-H}} = 4.4$  Hz,  $\text{SiH}_2$ ), 0.13 (pentet, 2H,  $\text{CH}_2$ ).  $^{13}\text{C}\{^1\text{H}\}$  NMR (benzene- $d_6$ , 62.9 MHz, 23 °C)  $\delta$  135.3, 133.0, 129.9, 128.3 (*Ph*), -11.1 ( $\text{CH}_2$ ). HRMS: Calcd for  $\text{C}_{13}\text{H}_{16}\text{Si}_2$ : 228.079. Found: 228.080.

### Synthesis of the Metalladisilacyclohexadiene Complex 12. A

solution of 0.860 g (1.45 mmol) of **4** in 15 mL of pentane was treated dropwise with a solution of 0.378 g (1.65 mmol) of  $(\text{PhSiH}_2)_2\text{CH}_2$  in 2 mL of pentane. The solution was stirred for 16 h, during which time the color changed from bright orange to yellow-orange. The solution was concentrated and cooled to -20 °C, yielding 0.119 g of *meso*-**12** as yellow crystals (10.0%). *Meso*-**12** was found to isomerize in toluene- $d_8$  at 23 °C to *rac*-**12**. Data for *meso*-**12**: NMR:  $^1\text{H}$  NMR (toluene- $d_8$ , 400.1 MHz, 27 °C)  $\delta$  7.13-7.75 (m, 10H,  $\text{SiHPh}$ ), 5.82 (m, 2H,  $\text{SiHPh}$ ), 1.41 (dd, 1H,  $^2J_{\text{H-H}} = 12.6$  Hz,  $^3J_{\text{H-H}} = 8.42$  Hz,  $\text{Si-CH}_a\text{H}_b\text{-Si}$ ), 1.38 (2 overlapping d, 18H,  $\text{PMe}_3$ ), 0.88 (dd, 1H,  $^3J_{\text{H-H}} = 2.18$  Hz,  $\text{Si-CH}_a\text{H}_b\text{-Si}$ ), 0.22 (s, 9H,  $\text{CH}_2\text{SiMe}_3$ ), 0.039 (s, 18H,  $=\text{CSiMe}_3$ ), -0.58 (br t, 2H,  $^3J_{\text{H-P}} = 15.6$  Hz,  $\text{CH}_2\text{SiMe}_3$ ).  $^{13}\text{C}\{^1\text{H}\}$  NMR (toluene- $d_8$ , 100.6 MHz, 27 °C)  $\delta$  262.7 ( $=\text{CSiMe}_3$ ), 145.4, 135.3, 128.5, 127.7 (*Ph*), 67.1 ( $\text{CH}_2\text{SiMe}_3$ ), 18.6 (d,  $^1J_{\text{C-P}} = 21.1$  Hz,  $\text{PMe}_3$ ), 16.7 (br d,  $^1J_{\text{C-P}} = 21.1$  Hz,  $\text{PMe}_3$ ), 13.7 ( $\text{Si-CH}_2\text{-Si}$ ), 6.22 ( $=\text{CSiMe}_3$ ), 5.24 ( $\text{CH}_2\text{SiMe}_3$ ).  $^{29}\text{Si}\{^1\text{H}\}$  NMR (toluene- $d_8$ , 79.5 MHz, 27 °C)  $\delta$  10.5 ( $\text{CH}_2\text{SiMe}_3$ ), -11.9 ( $\text{Si-CH}_2\text{-Si}$ ), -19.3 ( $=\text{CSiMe}_3$ ).  $^{31}\text{P}\{^1\text{H}\}$  NMR (toluene- $d_8$ , 162.0 MHz, 27 °C)  $\delta$  3.07 (d,  $^2J_{\text{P-P}} = 155.8$  Hz), -0.21 (d). Anal. Calcd for  $\text{C}_{31}\text{H}_{61}\text{Si}_5\text{P}_2\text{Ta}$ : C, 45.57; H, 7.52. Found: C, 45.53; H, 7.53. Data for *rac*-**12**:

NMR:  $^1\text{H}$  NMR (toluene- $d_8$ , 400.1 MHz, 27 °C)  $\delta$  7.10-7.90 (m, 10H, SiHPh), 4.59 (dd, 2H,  $^3J_{\text{H-H}} = 5.2, 4.4$  Hz, SiHPh), 1.17 (d, 9H,  $^2J_{\text{H-P}} = 6.40$  Hz, PMe $_3$ ), 0.96 (dd, 2H, Si-CH $_2$ -Si), 0.85 (d, 9H,  $^2J_{\text{H-P}} = 6.80$  Hz, PMe $_3$ ), 0.38 (s, 18H, =CSiMe $_3$ ), 0.24 (s, 9H, CH $_2$ SiMe $_3$ ), -0.47 (t, 2H,  $^3J_{\text{H-P}} = 16.0$  Hz, CH $_2$ SiMe $_3$ ).  $^{13}\text{C}\{^1\text{H}\}$  NMR (toluene- $d_8$ , 100.6 MHz, 27 °C)  $\delta$  257.5 (=CSiMe $_3$ ), 144.1, 136.6, 135.2, 128.2 (Ph), 51.4 (CH $_2$ SiMe $_3$ ), 17.8 (d,  $^1J_{\text{C-P}} = 19.1$  Hz, PMe $_3$ ), 17.4 (d,  $^1J_{\text{C-P}} = 20.1$  Hz, PMe $_3$ ), 6.2 (=CSiMe $_3$ ), 5.2 (CH $_2$ SiMe $_3$ ), 2.4 (Si-CH $_2$ Si).  $^{29}\text{Si}\{^1\text{H}\}$  NMR (toluene- $d_8$ , 79.5 MHz, 27 °C)  $\delta$  5.8 (CH $_2$ SiMe $_3$ ), -11.9 (=CSiMe $_3$ ), -14.1 (Si-CH $_2$ -Si).  $^{31}\text{P}\{^1\text{H}\}$  NMR (toluene- $d_8$ , 162.0 MHz, 27 °C)  $\delta$  -0.12 (d,  $^2J_{\text{P-P}} = 126$  Hz), -1.61 (d).

**X-ray Crystal Structure Determinations of 10a, 10b, 11 and 12.** All crystal structures were determined on a Siemens R3m/V diffractometer fitted with a Nicolet LT-2 low temperature device. Suitable crystals were coated with Paratone oil (Exxon) and mounted under a stream of nitrogen at -100 °C. The unit cell parameters and orientation matrix were determined from a least-squares fit of at least 25 reflections obtained from a rotation photograph and an automatic peak search routine. The refined lattice parameters and other pertinent crystallographic information are given in Tables 3.1, 3.4, 3.7, and 3.10.

Intensity data were measured with graphite-monochromated Mo K $\alpha$  radiation ( $\lambda = 0.71073$  Å). Background counts were measured at the beginning and end of each scan with the crystal and counter kept stationary. The intensities of three standard reflections were measured after every 97

reflections. The intensity data were corrected for Lorentz and polarization effects and for absorption using an empirical absorption correction based upon  $\psi$  scans.

The structures were solved by direct methods using the Siemens SHELXTL 93 (versions 5.0 and 5.10) software packages. All non-hydrogen atoms were refined anisotropically. Hydrogen atoms were placed in calculated positions and introduced into the refinement as fixed contributors with isotropic  $U$  values of  $0.08 \text{ \AA}^2$ .

## CHAPTER 4

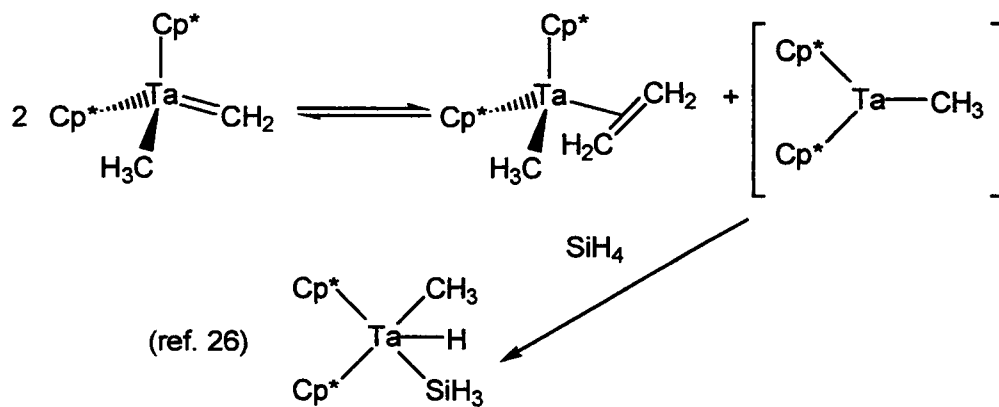
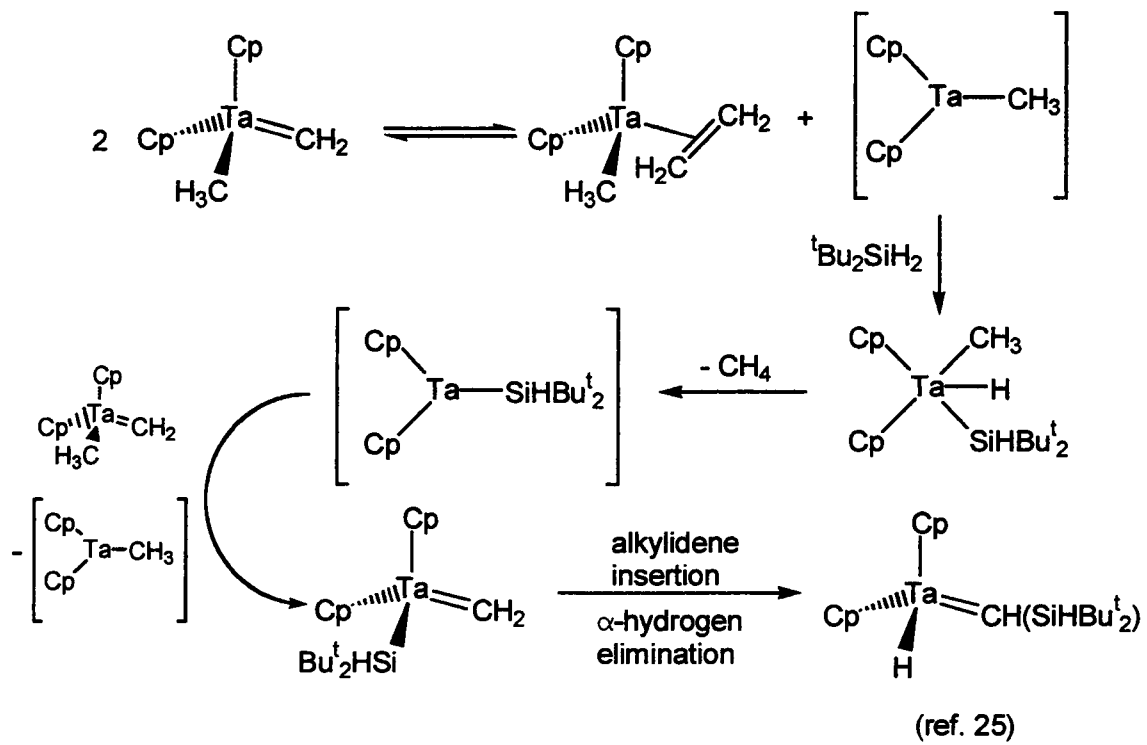
### Kinetic and Mechanistic Studies of Reactions of Tantalum Alkylidene Complexes with Silanes

#### 4.1 Introduction

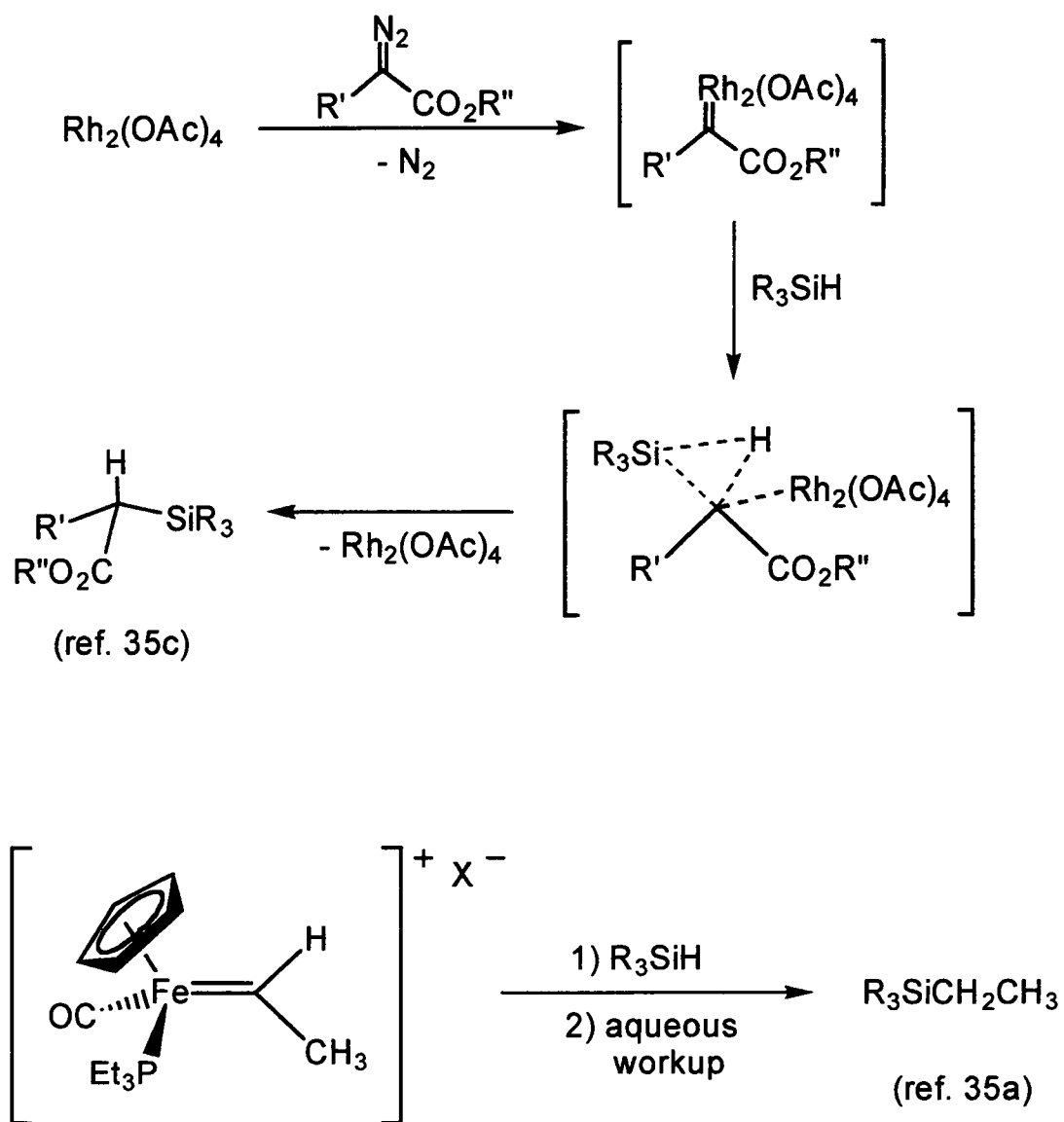
In Chapter 3 of this dissertation, the synthesis and characterization of novel metallasilacyclobutadiene, metalladisilacyclohexadiene, and disilyl-substituted alkylidene complexes **9-12** were reported. These complexes were observed to form through the preferential reactions of phenyl-containing silanes with the alkylidene ligands of the precursors **3**, **4**, and **8**.

Very few studies of the reactions of transition metal alkylidene or carbene complexes with silanes have been reported. The reactions of the tantalum alkylidene complexes  $\text{Cp}_2\text{Ta}(=\text{CH}_2)\text{CH}_3$  and  $\text{Cp}^*_2\text{Ta}(=\text{CH}_2)\text{H}$  with  ${}^t\text{Bu}_2\text{SiH}_2$  and  $\text{SiH}_4$ , respectively, were reported to give  $\text{Cp}_2\text{Ta}(\text{H})=\text{CHSiH}{}^t\text{Bu}_2$  and  $\text{Cp}^*_2\text{Ta}(\text{H})(\text{CH}_3)\text{SiH}_3$ .<sup>25,26</sup> These reactions were found to proceed via oxidative additions of the silanes to the metal center rather than a direct reaction with the alkylidene ligand (Scheme 4.1).<sup>25,26</sup> In contrast, the reactions of Fischer carbene complexes with silanes led to insertion reactions of the carbene moiety into the Si-H bond to yield alkyl silanes (Scheme 4.2).<sup>35</sup>





Scheme 4.1<sup>25,26</sup>



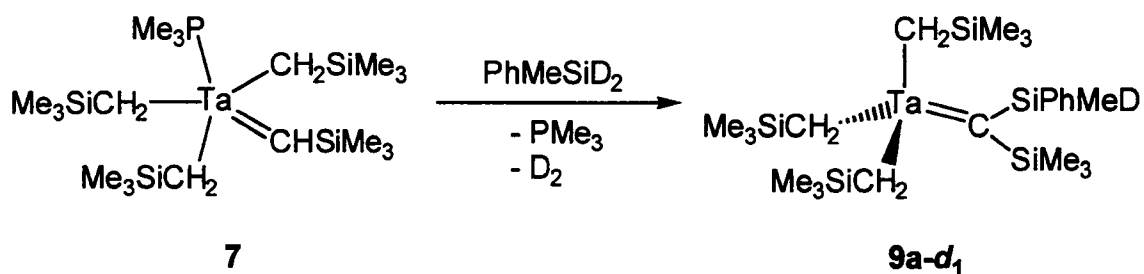
Scheme 4.2

Mechanistic studies revealed that these reactions involved direct insertion of the carbene unit into the Si-H bond,<sup>35a</sup> and that the cleavage of the Si-H bond and the formation of the new C-Si and C-H bonds were concerted.<sup>35c</sup> To our knowledge, no such direct reactions of silanes with the M=CHR moiety of a Schrock alkylidene complex have been observed. In addition, the conversion of **7** to **9a** is distinctively different from those in Schemes 4.1 and 4.2. We therefore decided to undertake kinetic and mechanistic studies of the conversion of **7-9a** to confirm that the reactions discussed in Chapter 3 of this dissertation were the result of direct reactions of silanes with alkylidene ligands, and also to understand the origins of the selectivity of these reactions.

## 4.2 Results and Discussion

### 4.2.1 Deuterium Labeling Studies of the Conversion of **7** to **9a**

To further study the reaction of **7** with PhMeSiH<sub>2</sub> to give the disilyl-substituted alkylidene complex **9a**, the reaction of **7** with the deuterated silane PhMeSiD<sub>2</sub> was investigated. Monitoring the reaction of **7** with PhMeSiD<sub>2</sub> by NMR showed the product to be (Me<sub>3</sub>SiCH<sub>2</sub>)<sub>3</sub>Ta[=C(SiMe<sub>3</sub>)SiPhMeD] (**9a-d**<sub>1</sub>) (Scheme 4.3). In addition, when 2.1 equiv of PhMeSiD<sub>2</sub> was used for the reaction, the formation of PhMeSiHD and PhMeSiH<sub>2</sub> was also observed; at larger excesses of silane (> 10 equiv), only PhMeSiHD was found in the reaction solution by NMR. The reaction of **7** with PhMeSiD<sub>2</sub> was also observed



Scheme 4.3

to be slower than that of **7** with PhMeSiH<sub>2</sub>; the latter was nearly complete after a few hours at room temperature, while the former reaction took 1 day to go to completion. This observation was confirmed by kinetic studies of this reaction, which are discussed in Section 4.2.2. The incorporation of hydrogen into the excess deuterated silane was unexpected, and the reaction was thus monitored by <sup>2</sup>H NMR to investigate whether the hydrogen incorporation into PhMeSiD<sub>2</sub> was due to exchange of deuterium in PhMeSiD<sub>2</sub> with protons in the alkyl ligands of **7**. The <sup>2</sup>H NMR spectrum of the reaction solution of **7** with 10.4 equiv of PhMeSiD<sub>2</sub> is shown in Figure 4.1. No incorporation of deuterium into the alkyl ligands of the product **9a-d<sub>1</sub>** was observed, and the only deuterium signals observed were those from PhMeSiD<sub>2</sub>, PhMeSiHD (overlapping signals), and (Me<sub>3</sub>SiCH<sub>2</sub>)<sub>3</sub>Ta[=C(SiMe<sub>3</sub>)SiPhMeD]. This result rules out the possibility that hydrogen incorporation into PhMeSiD<sub>2</sub> is the result of exchange of deuterium in PhMeSiD<sub>2</sub> with protons in the alkyl ligands of **7**. In a separate experiment, <sup>1</sup>H NMR spectra of a PhMeSiD<sub>2</sub> solution in toluene-*d*<sub>8</sub> showed no exchange of the residual hydrogen in toluene-*d*<sub>8</sub> with PhMeSiD<sub>2</sub> after 3 h at

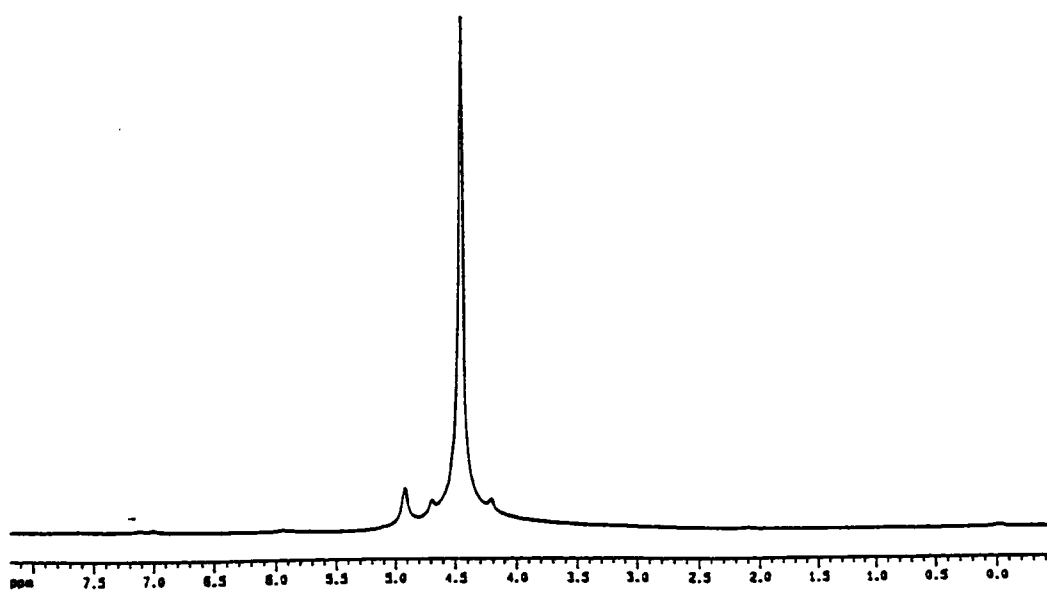


Figure 4.1  $^2\text{H}$  NMR spectrum of the reaction mixture of 7  
with 10.4 equivalents of  $\text{PhMeSiD}_2$

File:DJ80A Ident:7 Acq:19-JUN-1997 15:25:00 +0:57 Cal:D380A  
ZAB-SEQ4F EI> Magnet BpI:933778 TIC:31115728  
File Text: Gas from rkn, Se-5, afsae-4

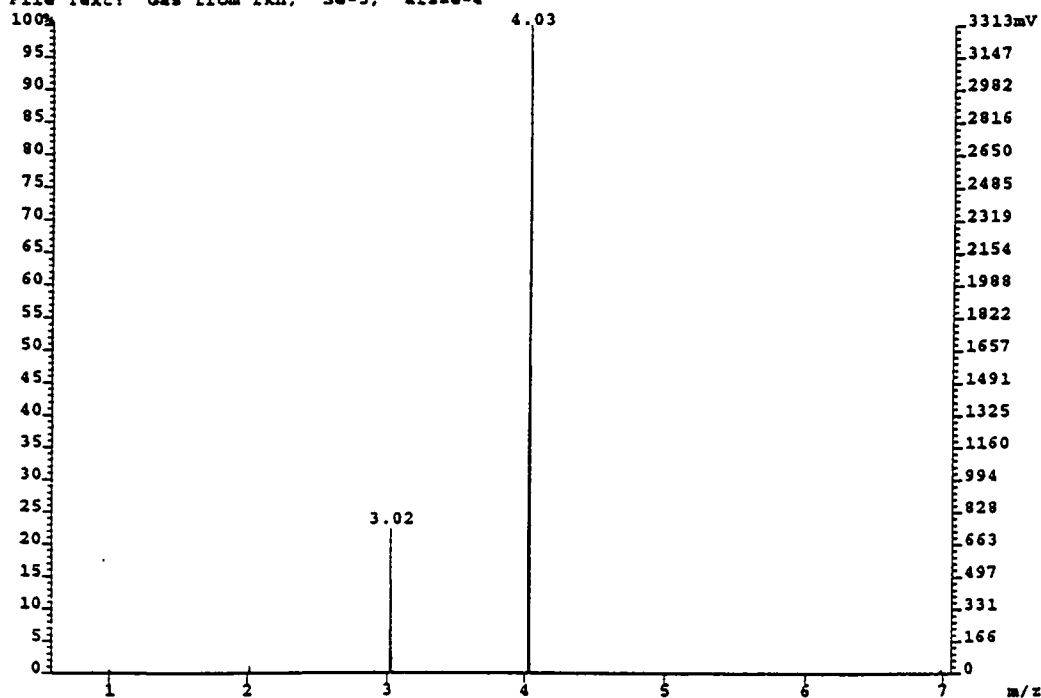


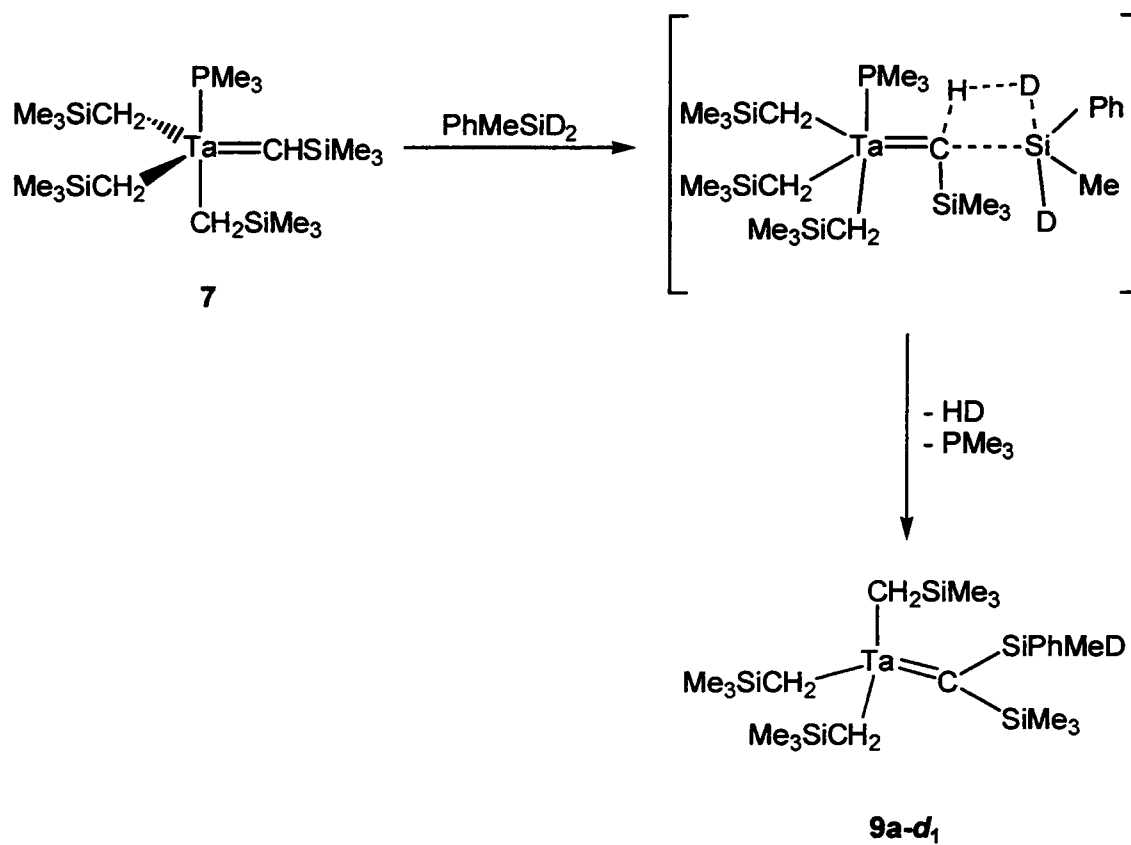
Figure 4.2 Mass spectrum of the gaseous products from the reaction of 7 with 4.7 equivalents of PhMeSiD<sub>2</sub>

50 °C.

The gaseous products from the reaction of **7** with 4.7 equiv of PhMeSiD<sub>2</sub> were analyzed by mass spectrometry (Figure 4.2). The mass spectrum showed the products to be D<sub>2</sub>, HD, and H<sub>2</sub> in an 83 :16 :1.0 ratio (by total ion current). This result indicated that the mechanism of this reaction involved more than merely a  $\sigma$ -bond metathesis reaction between the alkylidene ligand and the silane; such a mechanism would have given only HD as the product (Scheme 4.4).

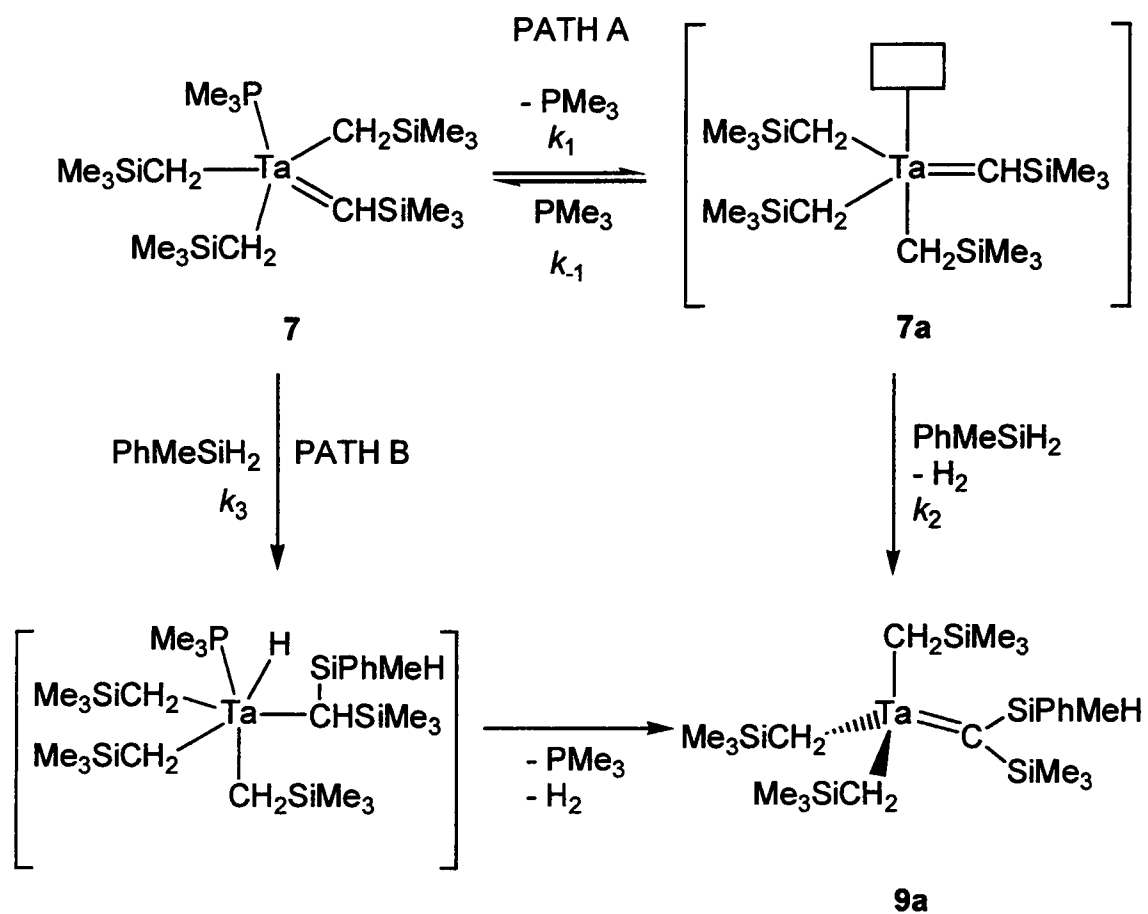
#### 4.2.2 Kinetic Studies of the Conversion of **7** to **9a**

In order to further investigate the reaction of phenyl-containing silanes with alkylidene complexes, kinetic studies of the reactions of **7** with PhMeSiH<sub>2</sub> and PhMeSiD<sub>2</sub> at 10 °C were performed. During the NMR studies of this reaction, no disilanes such as PhMeHSiSiHPhMe or polysilanes were observed. In addition, when the reaction of **7** with PhMeSiH<sub>2</sub> was conducted in the presence of Ph<sub>3</sub>SiH (which had been shown in Chapter 3 of this dissertation to be unreactive towards **7**), no crossover disilanes PhMeHSiSiPh<sub>3</sub> were observed. Thus it is unlikely that a mechanism involving silyl radicals is involved in this reaction, as such a mechanism is expected to involve disilane formation through combination of silyl radicals as one of the chain termination steps. We therefore focused our attention on two possible reaction pathways which are shown in Scheme 4.5. The first pathway (Path A) involves the loss



Scheme 4.4





Scheme 4.5

of a  $\text{PMe}_3$  ligand to open a coordination site on the tantalum center, followed by addition of the silane to the  $\text{Ta}=\text{C}$  bond, leading to products. The second pathway (Path B) would involve an addition of the silane to the  $\text{Ta}=\text{C}$  alkylidene bond, followed by loss of phosphine and conversion to products. When monitored by NMR, no intermediates were observed in the conversion of **7** to **9a**.

If the dissociative mechanism in Path A (Scheme 4.5) were operative in this reaction, then the following relationships would exist:

$$(1) \quad \frac{d[\mathbf{7}]}{dt} = k_{-1}[\mathbf{7a}][\text{PMe}_3] - k_1[\mathbf{7}]$$

$$(2) \quad \frac{d[\mathbf{7a}]}{dt} = k_1[\mathbf{7}] - k_{-1}[\mathbf{7a}][\text{PMe}_3] - k_2[\mathbf{7a}][\text{PhMeSiH}_2].$$

Using a steady-state approximation ( $\frac{d[\mathbf{7a}]}{dt} = 0$ ), rearrangement of Equation (2) gives

$$(3) \quad [\mathbf{7a}] = \frac{k_1[\mathbf{7}]}{k_{-1}[\text{PMe}_3] + k_2[\text{PhMeSiH}_2]}$$

Substituting into Equation (1) gives

$$(4) \quad \frac{d[\mathbf{7}]}{dt} = \frac{k_1 k_{-1} [\text{PMe}_3] [\mathbf{7}]}{(k_{-1} [\text{PMe}_3] + k_2 [\text{PhMeSiH}_2])} - k_1 [\mathbf{7}]$$

or

$$(5) \quad v = -d[7]/dt = \frac{k_1 k_2 [\text{PhMeSiH}_2][7]}{k_{-1}[\text{PMe}_3] + k_2[\text{PhMeSiH}_2]}$$

or  $v = k_{\text{obs}}[7]$  where

$$(6) \quad k_{\text{obs}} = \frac{k_1 k_2 [\text{PhMeSiH}_2]}{k_{-1}[\text{PMe}_3] + k_2[\text{PhMeSiH}_2]}$$

which may also be expressed in a linear form

$$(7) \quad \frac{1}{k_{\text{obs}}} = \frac{k_{-1}[\text{PMe}_3]}{k_1 k_2 [\text{PhMeSiH}_2]} + \frac{1}{k_1}$$

Thus under conditions of excess PhMeSiH<sub>2</sub>, one would expect to observe pseudo-first order kinetics in [7]. When [PhMeSiH<sub>2</sub>] >> [PMe<sub>3</sub>], the silane terms in the rate expression [Equation (6)] would become dominant and the observed rate would simplify to  $k_{\text{obs}} \approx k_1$ . In other words, one would observe saturation kinetics at large PhMeSiH<sub>2</sub> excesses. Also, a plot of  $1/k_{\text{obs}}$  vs [PMe<sub>3</sub>]/[PhMeSiH<sub>2</sub>] would be linear, yielding values for  $k_1$  and  $k_{-1}/k_2$ .

If the reaction proceeded by the associative mechanism shown in Path B of Scheme 4.5, and if the first step was rate controlling, a much simpler rate

expression would be obtained:

$$(8) \quad d[7]/dt = k_3[7][\text{PhMeSiH}_2]$$

For reactions conducted with an excess of  $\text{PhMeSiH}_2$ , pseudo-first order kinetics are expected;  $k_{\text{obs}} = k_3[\text{PhMeSiH}_2]$

Kinetic studies were performed with  $[\text{PhMeSiH}_2]_0/[7]_0$  ranging from 5.34 to 34.8 and  $[\text{PhMeSiD}_2]_0/[7]_0$  ranging from 5.00 to 35.1. Under these conditions the disappearance of 7 with time was found to obey first-order kinetics, as is shown in the kinetic plots in Figures 4.3-4.5. Values for the observed rate constants are given in Table 4.1. A plot of the observed rate constants vs.  $[\text{PhMeSiH}_2]_{\text{av}}/[\text{PMe}_3]_{\text{av}}$  is shown in Figure 4.6. In Figure 4.6 one observes that at higher  $[\text{PhMeSiH}_2]_{\text{av}}/[\text{PMe}_3]_{\text{av}}$  ratios, the observed rate begins to level out, which is consistent with the onset of saturation kinetics. Such an observation is consistent with the mechanistic pathway Path A shown in Scheme 4.5, in which there is a dissociative mechanism involving loss of  $\text{PMe}_3$  from 7 prior to the reaction of 7 with  $\text{PhMeSiH}_2$ . In addition, plots of  $1/k_{\text{obs}}$  vs.  $[\text{PMe}_3]/[\text{PhMeSiH}_2]$  and  $[\text{PMe}_3]/[\text{PhMeSiD}_2]$  were found to be linear (Figure 4.7), as would also be expected from the dissociate mechanism rate law (Equation 7). From these plots, a value of  $k_1 = 5.45(10) \times 10^{-2} \text{ min}^{-1}$  was obtained. In addition, from the slopes of the plots shown in Figure 4.6, a kinetic isotope

**Table 4.1. Observed Rate Constants for the Conversion 7 to 9a**

$[7]_0, M \times 10^2$	$[\text{PhMeSiH}_2]_0, M$	$[\text{PhMeSiH}_2]_{\text{av}}/[\text{PMe}_3]_{\text{av}}$	$k_{\text{obs}}, \text{min}^{-1} \times 10^3$
11.5	0.614	9.68	4.58
9.79	0.524	9.68	5.92
6.67	0.507	14.0	6.64
9.31	0.698	14.0	7.71
7.55	0.661	16.5	8.25
9.17	0.801	16.5	8.92
8.87	0.950	20.4	10.1
11.3	1.21	20.4	10.5
8.98	1.21	26.0	12.9
9.47	1.28	26.0	12.3
11.2	2.02	35.2	15.6
5.60	1.02	35.2	16.7
5.89	1.21	38.6	16.8
5.95	1.18	38.6	17.6
10.5	2.31	43.0	16.9
5.32	1.17	43.0	17.6
5.76	1.46	49.6	18.3
7.86	2.00	49.6	17.8
8.61	2.34	53.4	19.6
8.81	2.40	53.4	19.7
5.60	1.85	65.0	20.8
6.44	2.12	65.0	21.5
3.48	1.21	68.6	21.6
5.40	1.87	68.6	24.4

**Table 4.2. Observed Rate Constants for the Conversion 7 to 9a-d,**

$[7]_0, M \times 10^2$	$[\text{PhMeSiD}_2]_0, M$	$[\text{PhMeSiD}_2]_{\text{av}}/[\text{PMe}_3]_{\text{av}}$	$k_{\text{obs}}, \text{min}^{-1} \times 10^3$
10.5	0.524	9.00	2.83
15.7	0.782	9.00	2.69
10.1	1.52	29.0	8.25
13.1	1.96	29.0	8.31
13.2	3.30	49.0	12.5
8.96	2.24	49.0	12.1
11.2	3.92	69.2	15.2
6.95	2.45	69.2	15.3

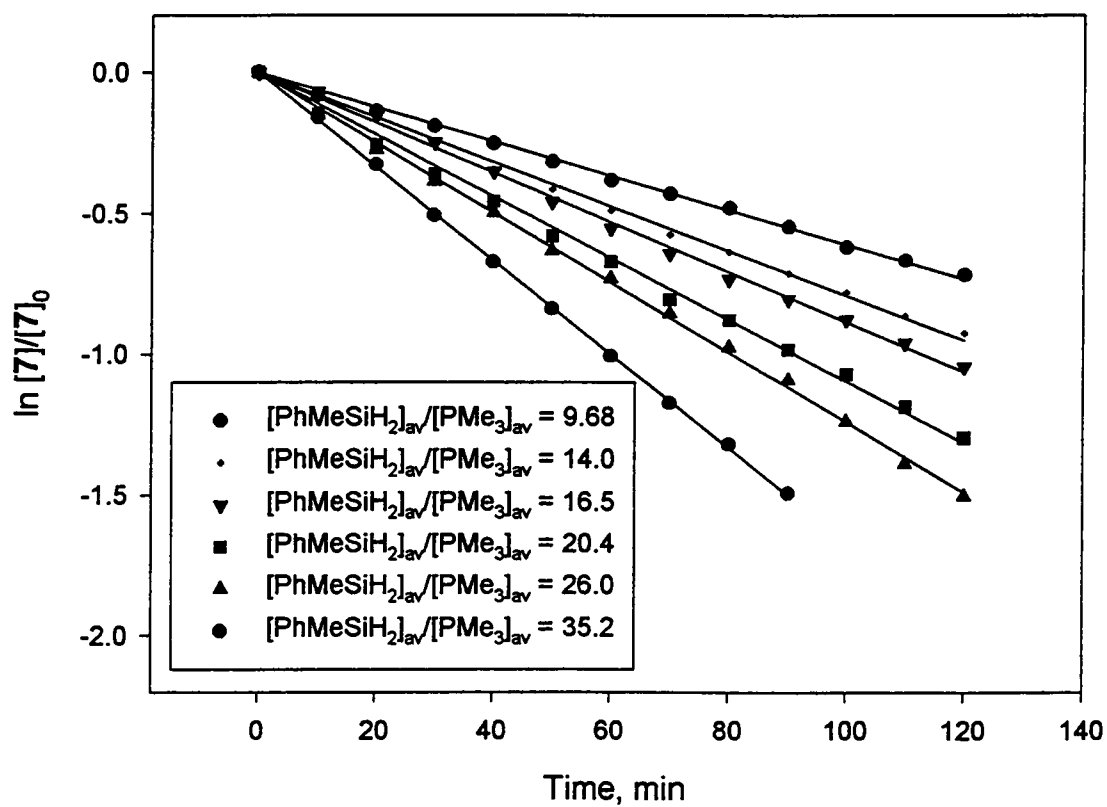


Figure 4.3 Kinetic plots of the reaction of 7 with PhMeSiH<sub>2</sub>

( $[\text{PhMeSiH}_2]_{\text{av}}/[\text{PMe}_3]_{\text{av}} = 9.68 - 35.2$ )

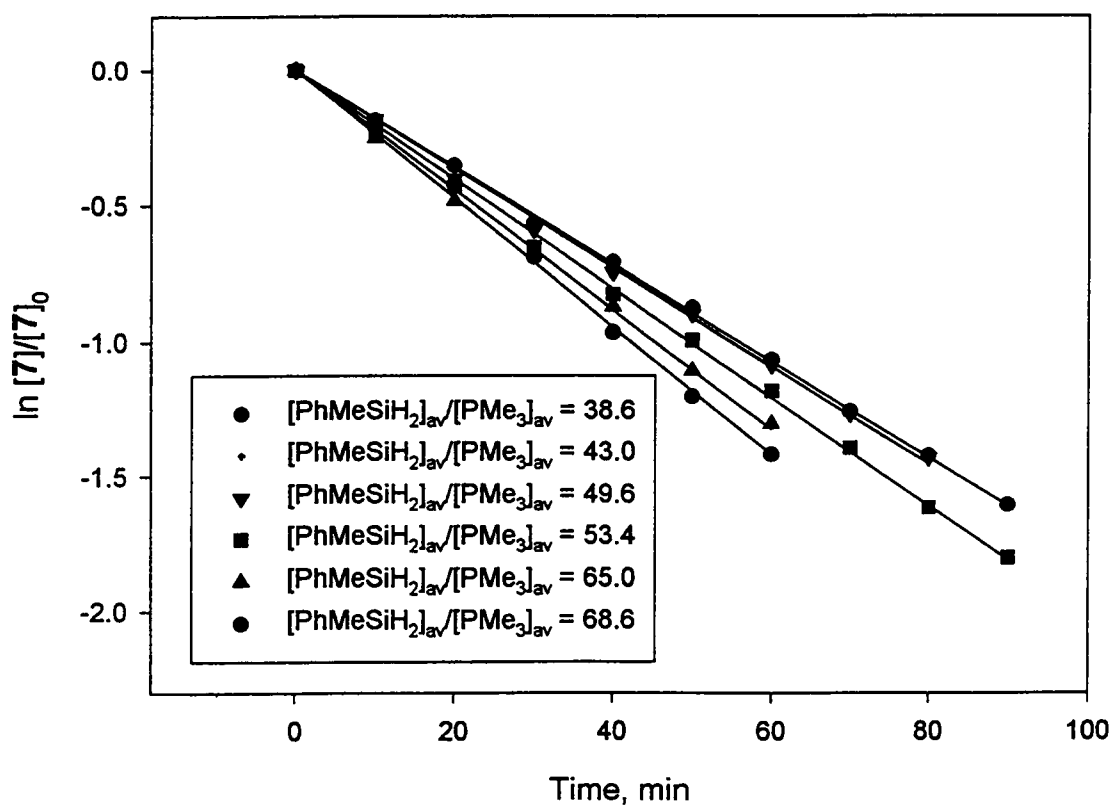


Figure 4.4 Kinetic plots of the reaction of 7 with PhMeSiH<sub>2</sub>

( $[\text{PhMeSiH}_2]_{\text{av}}/[\text{PMe}_3]_{\text{av}} = 38.6 - 68.6$ )



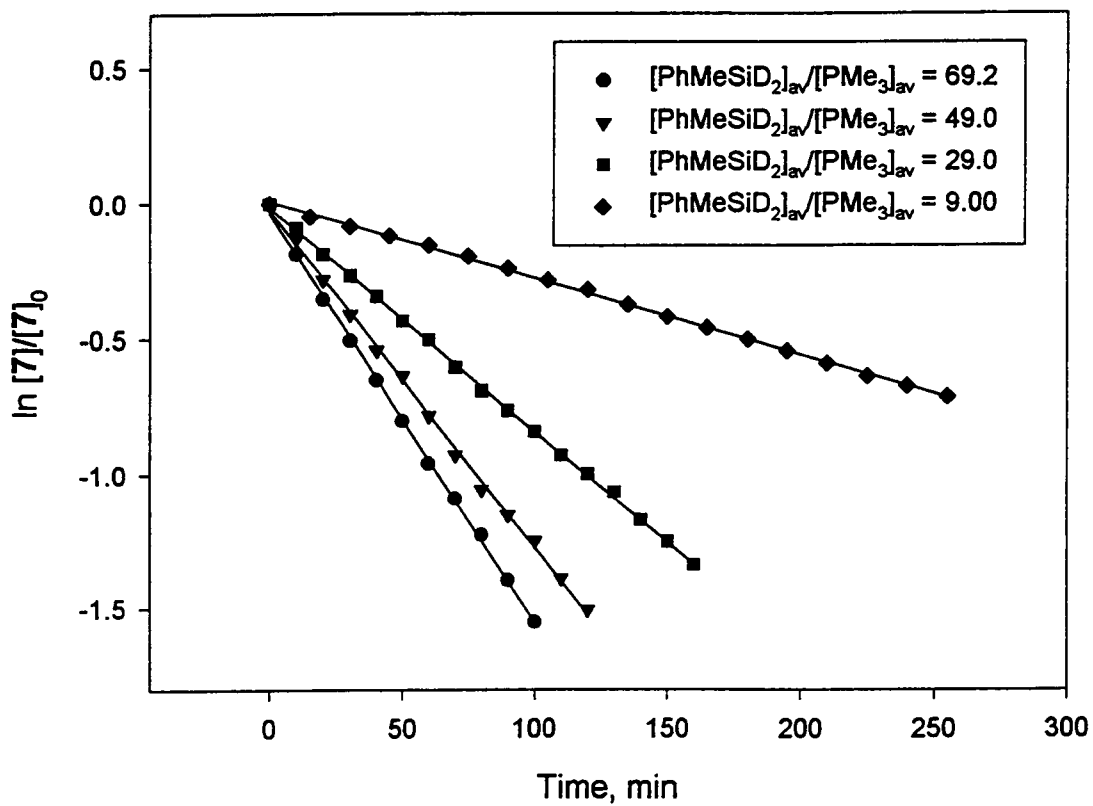


Figure 4.5 Kinetic plots of the reaction of 7 with PhMeSiD<sub>2</sub>

( $[\text{PhMeSiD}_2]_{\text{av}}/[\text{PMe}_3]_{\text{av}} = 9.00 - 69.2$ )

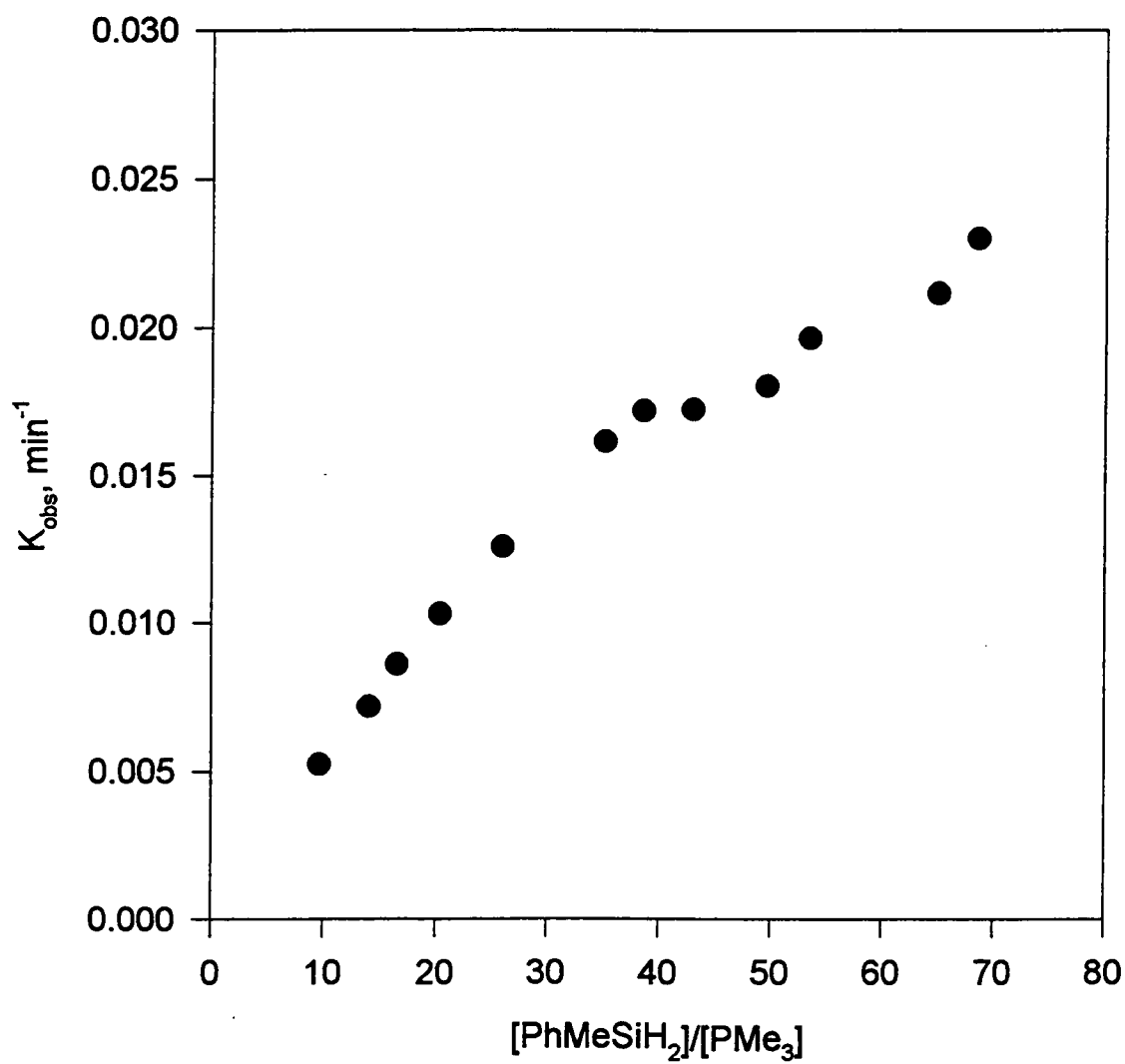


Figure 4.6 Plot of  $k_{\text{obs}}$  vs.  $[\text{PhMeSiH}_2]_{\text{av}}/[\text{PMe}_3]_{\text{av}}$

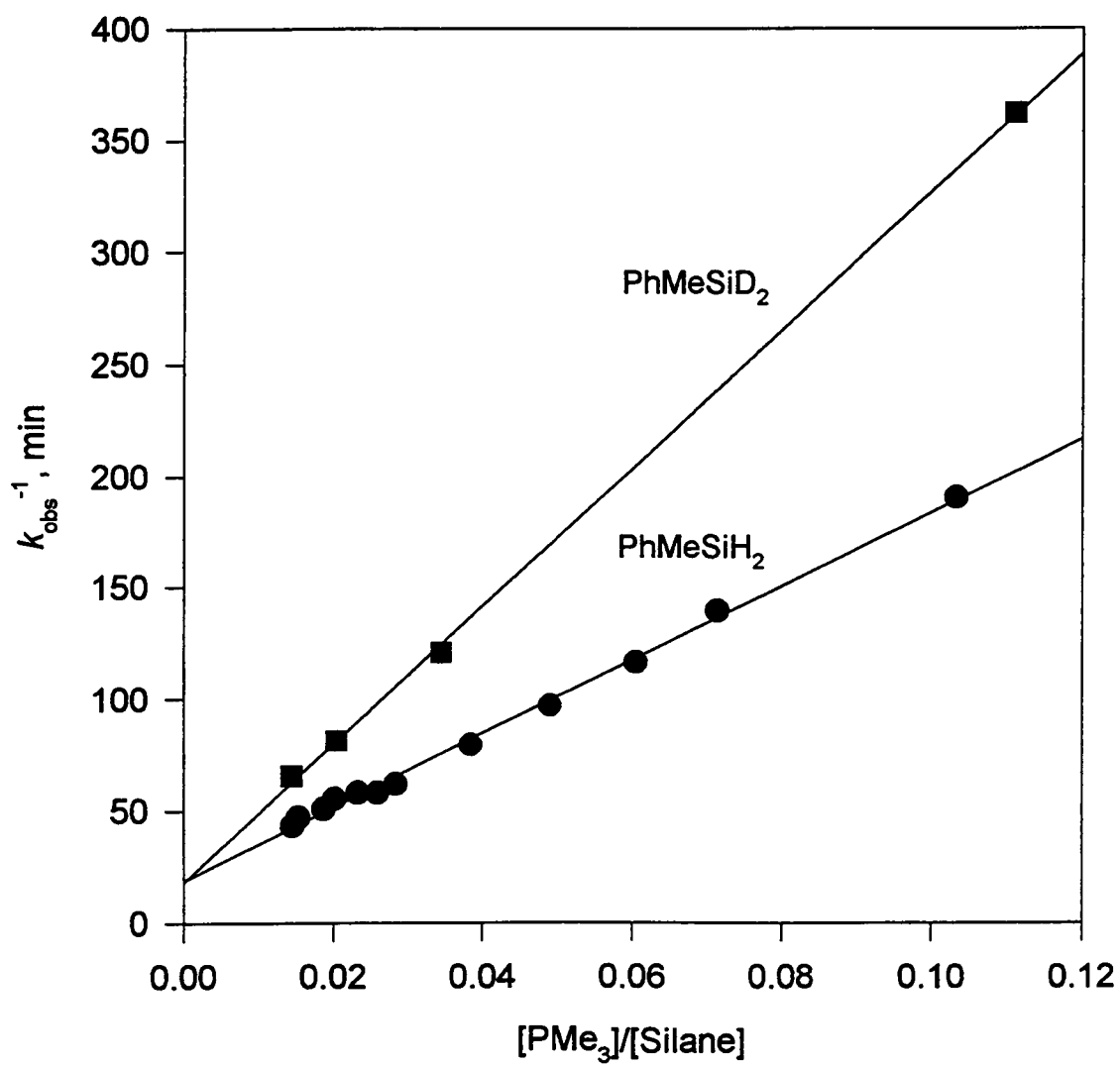


Figure 4.7 Plot of  $k_{\text{obs}}^{-1}$  vs.  $[\text{PMe}_3]_{\text{av}}/[\text{Silane}]_{\text{av}}$

effect value  $k_{2H}/k_{2D}$  was calculated to be 1.87. The magnitude of this kinetic isotope effect is consistent with the formation of or the breaking of a silicon-deuterium bond in the rate controlling step, and is similar to that (1.5) observed in a kinetic study of the reactions of a Fischer carbene complex with silanes (Scheme 4.2).<sup>35c</sup>

#### 4.2.3 Mechanism of the Conversion of 7 to 9a

The proposed pathways for the conversion of 7 to 9a are shown in Scheme 4.5. From the kinetic studies of this reaction, it was found that the observed rate constant  $k_{obs}$  was initially approximately proportional to the concentration of excess of PhMeSiH<sub>2</sub> used in the reaction. At larger excesses of silane, saturation kinetics started to appear, consistent with the dissociative mechanism in Path A of Scheme 4.5. In addition, a kinetic isotope effect was observed when the reaction was conducted using the deuterated silane PhMeSiD<sub>2</sub>, indicating that a Si-H bond formation or bond cleavage occurs in the rate controlling step of the reaction. Finally, deuterium labeling studies showed that D<sub>2</sub> was the major gaseous product in the reaction of 7 with excess PhMeSiD<sub>2</sub>, and hydrogen incorporation into unreacted excess PhMeSiD<sub>2</sub> to yield PhMeSiHD was also observed. These observations are consistent with the mechanism shown in Scheme 4.6, in which PMe<sub>3</sub> dissociates from 7 to give an intermediate complex 7a with an open coordination site for the approach of silane. The silane then reacts with the alkylidene ligand to yield a hydride

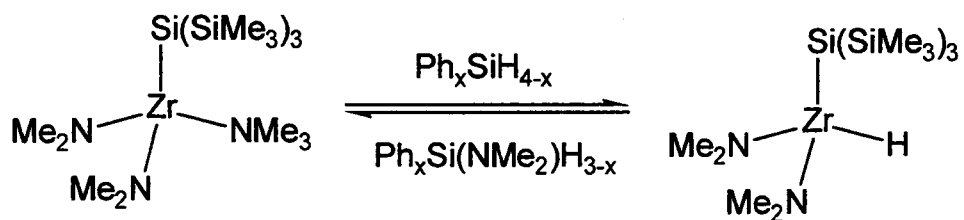
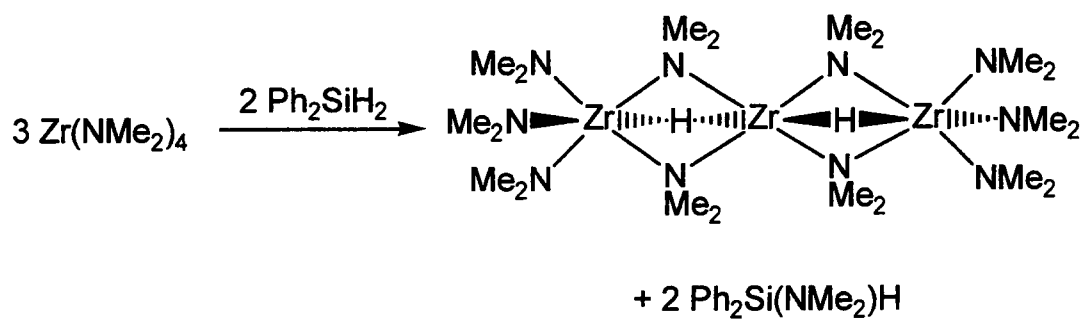


(deuteride) intermediate **15**, possibly through nucleophilic attack on the silane by the  $\pi$ -electron density of the alkylidene bond. The alkylidene ligands of Schrock alkylidene complexes have been shown to be nucleophilic in nature, and reactions of alkylidene complexes with olefins and ketones are also believed to involve some degree of nucleophilic attack on the olefin and ketone by the alkylidene ligand.<sup>24</sup> Similar reactions of alkyl or amido complexes with silanes to give metal hydride complexes and alkylsilanes or amidosilanes have recently been reported.<sup>36,37</sup> The hydride intermediate **15** then reacts with a second silane molecule through a dehydrogenative coupling reaction to yield  $H_2$  ( $D_2$ ) and a silyl intermediate **16**. Such reactions of hydride complexes with silanes have been proposed in the dehydrogenative polymerization of silanes.<sup>2h, 14</sup> The silyl ligand in **16** then undergoes  $\alpha$ -hydrogen abstraction to give  $PhMeSiH_2$  or  $PhMeSiHD$  and **9**. The mechanism shown in Scheme 4.6 is thus consistent with the observed dissociative mechanism from the kinetic studies and also accounts for the preferential formation of  $D_2$  and the proton incorporation into the unreacted  $PhMeSiD_2$  to give  $PhMeSiHD$  in the deuterium labeling studies.

It is interesting to note that the reaction of phenyl-containing silanes with **7** may proceed through a step involving some degree of nucleophilic attack on the silicon center of the incoming silane molecule by the  $\pi$ -electron density of the alkylidene ligand, leading to the formation of a product **9** in which a new carbon-silicon bond is formed. Similar chemistry was observed in the reaction

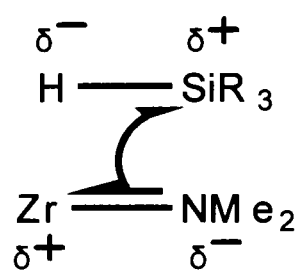
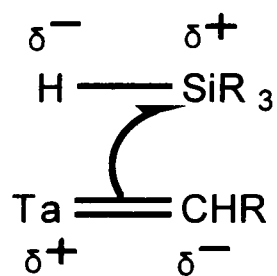
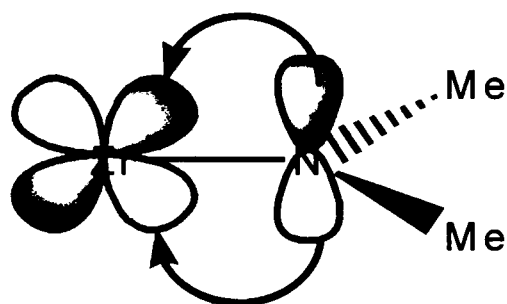
of zirconium amide complexes  $Zr(NMe_2)_4$  and  $Zr(NMe_2)_3[SiR_3]$  ( $R_3 = SiMe_3$ ) with phenyl-containing silanes  $Ph_xSiH_{4-x}$  ( $x = 1, 2$ ) to yield amidosilanes and unstable zirconium hydride complexes (Scheme 4.7).<sup>37</sup> These amide complexes possess some degree of  $\pi$ -character ( $d-p$   $\pi$  bonds) in the N-Zr bonds through interaction of the lone pair on the nitrogen atom of the amide ligand with the unfilled  $d$ -orbitals on the zirconium atom (Scheme 4.8). The  $d-p$   $\pi$ -bonds may also be involved in the nucleophilic attack on the silicon center of an incoming silane molecule in the reactions of silanes with the zirconium amide complexes, leading to the formation of a silicon-nitrogen bond and a metal hydride (Scheme 4.8).<sup>37</sup> It should be also pointed out that such reactivity is also in agreement with the formal bond polarities of the reactants in both the alkylidene/silane and amide/silane systems: the metal-carbon and metal-nitrogen bonds are both polarized with a partial negative charge on the carbon and nitrogen atoms, respectively, while the Si-H bond of the silane is polarized with a partial negative charge on the hydrogen atom (the Pauling electronegativities of silicon and hydrogen being 1.8 and 2.1, respectively). Such nucleophilic attack of the  $\pi$ -electron density of the alkylidene ligand in **7** on the incoming silane may explain the observed preferential reaction of only the alkylidene ligands, and not the alkyl ligands, of **4**, **7**, and **8** with silanes.

In the reaction of **7** with excess  $PhRSiH_2$  ( $R = Ph, Me$ ) to give **9**, the partial formation of 1,1'-metallasilacyclobutadiene **10** was also observed (Section 3.2.1). This observation was somewhat surprising. A proposed

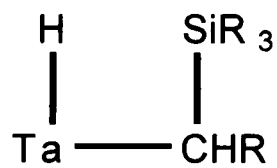


Scheme 4.7





- R<sub>3</sub>SiNMe<sub>2</sub>



Scheme 4.8



mechanism for this conversion is given in Scheme 4.9. This conversion may involve the loss of an alkyl ligand, possibly induced by the coordination of a  $\text{PMe}_3$  molecule to give a (bis)alkylidene intermediate, followed by an intramolecular reaction of the  $\text{SiPhR}'\text{H}$  group with the newly formed alkylidene ligand and coordination of a second  $\text{PMe}_3$  molecule to produce **10**.

### 4.3 Experimental Section

All manipulations were performed under a dry nitrogen atmosphere with the use of either a drybox or standard Schlenk techniques. Solvents were purified by distillation from potassium/benzophenone ketyl before use. Benzene- $d_6$  and toluene- $d_8$  were dried over activated molecular sieves and stored under nitrogen. NMR spectra, unless noted, were recorded at 23 °C on a Bruker AC-250 or AMX-400 Fourier transform spectrometer.  $^1\text{H}$  and  $^{13}\text{C}$  chemical shifts were referenced to solvents (residual protons in the  $^1\text{H}$  spectra).  $^2\text{H}$  chemical shifts were referenced to external toluene- $d_8$ . Mass spectra were recorded on a VG ZAB-EQ hybrid high performance mass spectrometer at an ionization voltage of 70 eV.  $\text{PhMeSiH}_2$  (Gelest) was dried over activated molecular sieves and stored under nitrogen.  $\text{PhMeSiD}_2$  was prepared by the literature procedure<sup>38</sup> and was dried over molecular sieves and stored under nitrogen.  $(\text{Me}_3\text{SiCH}_2)_3\text{Ta}(\text{PMe}_3)=\text{CHSiMe}_3$  (**7**) was prepared as described in Chapter 3 of this dissertation.

**Reaction of 7 with  $\text{PhMeSiD}_2$ .** 0.0303 g (0.0501 mmol) of **7** was

dissolved in 0.4 mL of toluene- $d_8$  and placed in an NMR tube. 20.0  $\mu\text{L}$  (0.143 mmol) of  $\text{PhMeSiD}_2$  was then added to the tube. The tube was then placed on an NMR spectrometer which had been preheated to 50  $^\circ\text{C}$ , and the reaction was monitored by NMR. After 20 min all of **7** had been consumed, and the products were identified as **9a-d**<sub>4</sub> and  $\text{PMe}_3$ .  $\text{PhMeSiHD}$ ,  $\text{PhMeSiH}_2$ , and a trace amount of **9a** were also identified. Data for **9a-d**<sub>4</sub>:  $^1\text{H}$  NMR (toluene- $d_8$ , 400.1 MHz, 50  $^\circ\text{C}$ )  $\delta$  7.20-7.81 (m, 5H,  $\text{SiPhMeD}$ ), 1.10 (d, 3H,  $^2J_{\text{H-H}} = 12.1$  Hz,  $\text{CH}_a\text{H}_b\text{SiMe}_3$ ), 0.91 (d, 3H,  $\text{CH}_a\text{H}_b\text{SiMe}_3$ ), 0.75 (s, 3H,  $\text{SiPhMeD}$ ), 0.26 (s, 9H,  $=\text{CSiMe}_3$ ), 0.18 (s, 27H,  $\text{CH}_2\text{SiMe}_3$ ).  $^{13}\text{C}\{^1\text{H}\}$  NMR (toluene- $d_8$ , 100.6 MHz, 50  $^\circ\text{C}$ )  $\delta$  241.1 ( $=\text{CSiMe}_3$ ), 137.8, 135.3, 129.7, 128.0 ( $\text{SiPhMeD}$ ), 89.7 ( $\text{CH}_2\text{SiMe}_3$ ), 5.0 ( $=\text{CSiMe}_3$ ), 2.8 ( $\text{CH}_2\text{SiMe}_3$ ), -1.8 ( $\text{SiPhMeD}$ ).  $^2\text{H}$  NMR (toluene, 61.42 MHz, 27  $^\circ\text{C}$ )  $\delta$  4.92 (br s,  $\text{SiPhMeD}$ ).

**Analysis of the Gaseous Products from the Reaction of 7 with  $\text{PhMeSiD}_2$  by Mass Spectrometry.** A J. Young valved NMR tube was charged with a solution of 0.045 g (0.074 mmol) of **7** in 0.4 mL of toluene and 50  $\mu\text{L}$  (0.34 mmol) of  $\text{PhMeSiD}_2$ . The solution was immediately frozen in liquid nitrogen, and the tube was evacuated to remove nitrogen. The teflon valve on the tube was then sealed, and the solution allowed to thaw and shaken for 30 min, at which time gas evolution from the solution had ceased. The solution was frozen again in liquid nitrogen, and the tube connected to the mass spectrometer. The gaseous products were then pumped into the mass spectrometer.

**Kinetic Studies of the Conversion of 7-9a and 7-9a-*d*<sub>1</sub>.** In a glovebox an NMR tube was charged with 7 (12.8-45.0 mg) and 4,4'-dimethylbiphenyl (2.8-9.5 mg, an internal standard), which were then dissolved in 400  $\mu$ L of toluene-*d*<sub>8</sub>. PhMeSiH<sub>2</sub> or PhMeSiD<sub>2</sub> was then added to the NMR tube via calibrated micropipet so as to make [PhMeSiH<sub>2</sub>]/[7] between 5.34 and 34.8 and [PhMeSiD<sub>2</sub>]/[7] between 5.00 and 35.1. The contents of the NMR tube were then mixed, and the tube was cooled to -78 °C. The sample was then placed on an NMR spectrometer which had been precooled to 10 °C, and NMR spectra were recorded. The concentration of 7 was determined by integration with respect to the internal standard 4,4'-dimethylbiphenyl.

## CHAPTER 5

# Synthesis of Bis[tris(trimethylsilyl)silyl]methane and Bis[tris(trimethylsilyl)silyl]ethane and Attempted Synthesis of Dianionic Bis(silyl) Compounds

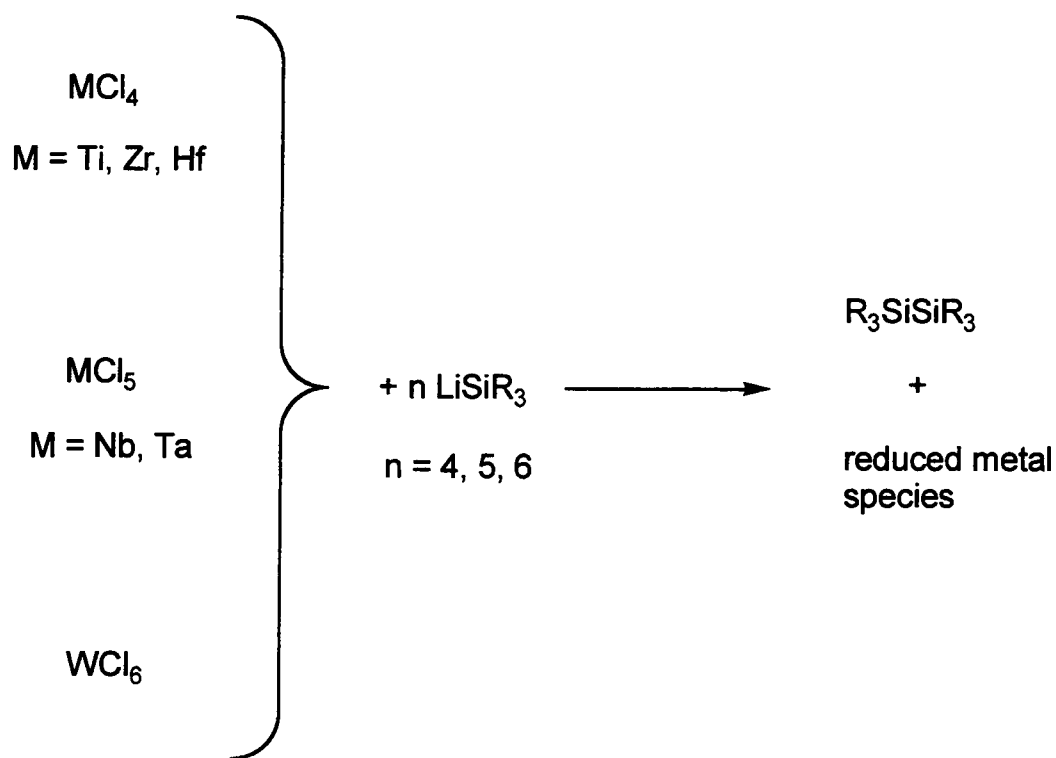
### 5.1 Introduction

In Chapters 3 and 4 of this dissertation, studies of the reactions of tantalum alkylidene complexes with silanes were reported. These studies were inspired by our interest in the use of early-transition-metal alkyl, alkylidene, and alkylidyne complexes as possible precursors to metal silicide materials, and the fundamental chemistry involved in such processes. In addition to the reaction of volatile early-transition-metal complexes with silanes in a chemical vapor deposition (CVD) process as a possible method for the production of metal silicide materials, the possibility of using metal poly- or persilyl complexes as single source precursors presents another possible route to metal silicide materials. The use of metal silyl complexes as silicide precursors would have some advantages over the use of metal halide or metal alkyl complexes in a CVD process, including the elimination of the need for the use of pyrophoric reagents such as  $\text{SiH}_4$  or  $\text{Si}_2\text{H}_6$ , and the additional benefit of possibly being able to modify the silyl ligands so as to control the stoichiometry of the resulting

silicide material.

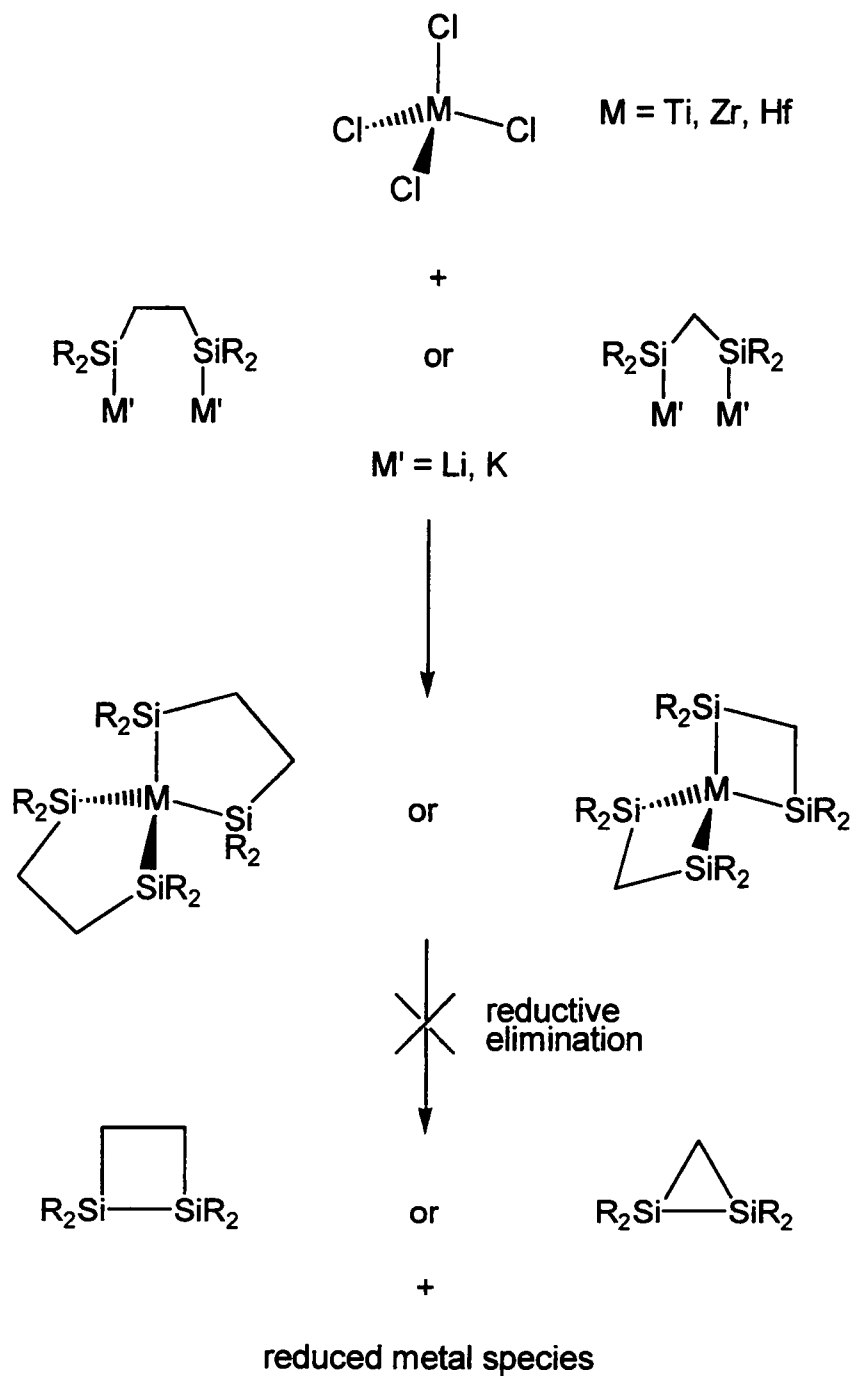
The synthesis and isolation, however, of  $d^0$  early-transition-metal polysilyl and persilyl complexes remain a considerable synthetic challenge. Although the peralkyl metal complexes  $(RCH_2)_nM$  ( $n = 4$ ,  $M = \text{Ti triad}$ ;  $n = 5$ ,  $M = \text{Ta}$ ;  $n = 6$ ,  $M = \text{W}$ ) have been known for some time,<sup>32,43</sup> no stable  $d^0$  persilyl analogs have been isolated.<sup>12,13</sup> An earlier report of  $\text{Ti}(\text{SiPh}_3)_4$  was later shown to actually be  $\text{Ti}(\text{OSiPh}_3)_4$ .<sup>12</sup> Attempts to synthesize persilyl complexes by the reaction of  $\text{MCl}_n$  with  $n$  equivalents of  $\text{LiSiR}_3$  have only led to formation of disilanes  $\text{R}_3\text{SiSiR}_3$  and reduced metal species, presumably as a result of reductive elimination of the disilane from the metal center (Scheme 5.1). Reductive elimination was also observed in the attempt to prepare a  $d^0$  disilyl complex  $(\text{Me}_3\text{SiO})_2\text{Zr}(\text{SiR}_3)_2$  [ $\text{SiR}_3 = \text{Si}(\text{SiMe}_3)_3$ ,  $\text{SiPh}_2\text{Bu}^t$ ] through the reaction of  $(\text{Me}_3\text{SiO})_2\text{ZrCl}_2$  with two equivalents of  $\text{LiSiR}_3$ .<sup>11f</sup> Recently, however, we reported the synthesis and characterization of the first Cp-free bis(silyl)  $d^0$  complexes of zirconium and tantalum,  $\text{Li}(\text{THF})_4(\text{Me}_2\text{N})_3\text{Zr}(\text{SiPh}_2\text{Bu}^t)_2$  and  $(\text{Me}_2\text{N})_3\text{Ta}[\text{Si}(\text{SiMe}_3)_3]_2$  as part of studies of Cp-free bis(silyl) and polysilyl complexes.<sup>6c</sup>

In order to reduce the likelihood of reductive elimination from a metal center, and thus increase the possibility of obtaining a polysilyl or persilyl metal complex, we decided to investigate the use of chelating dianionic bis(silyl) ligands  $\text{MSi}(\text{R})_2[\text{CH}_2]_n(\text{R})_2\text{SiM}$  ( $n = 1, 2$ ;  $M = \text{Li, K}$ ) [Scheme 5.2]. It was anticipated that the entropic advantage of these chelating ligands, in



Scheme 5.1

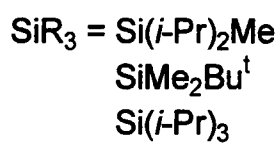
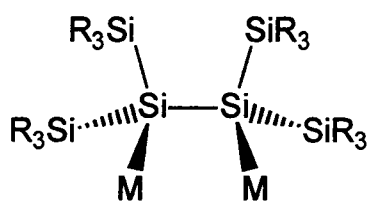




Scheme 5.2

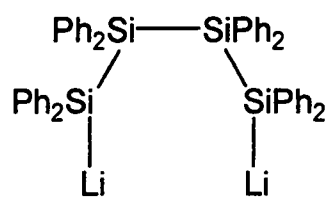
addition to the strained disilacyclopropane or -butane which would result from reductive elimination from the metal center, would serve to enhance the stability of any resulting metal complex and possibly lead to the isolation of a stable persilyl complex (Scheme 5.2).

In comparison to alkyl lithium, sodium, and potassium compounds, anionic silyl analogs are relatively few in number.<sup>44</sup> Only a handful of dianionic bis(silyl) ligands have been previously reported (Scheme 5.3), all of which contain an all-silicon backbone. We wished to utilize ligands containing a hydrocarbon backbone to minimize the possibility of oxidative cleavage in the ligand backbone during reaction with transition metal complexes. We therefore identified the bis(silyl)methane and -ethane compounds bis[tris(trimethylsilyl)silyl]methane (**18**) and bis[tris(trimethylsilyl)silyl]ethane (**19**) as possible ligand precursors (Scheme 5.4). We anticipated that reaction of **18** and **19** with MeLi in THF would lead to the formation of dianionic bis(silyl)methane and -ethane compounds  $[\text{LiSi}(\text{SiMe}_3)_2]\text{CH}_2$  (**21**) and  $\text{LiSi}(\text{SiMe}_3)_2\text{CH}_2\text{CH}_2(\text{SiMe}_3)_2\text{SiLi}$  (**22**); such a reaction was used for the production of  $\text{Li}(\text{THF})_3\text{SiR}(\text{SiMe}_3)_2$  from  $\text{SiR}(\text{SiMe}_3)_3$  (Scheme 5.6).<sup>45</sup> Although attempts to synthesize **21** and **22** have been unsuccessful to date, we were successful in synthesizing and characterizing the previously unreported bis(silyl)methane and -ethane derivatives **18** and **19**.

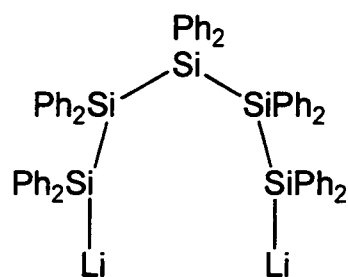


M = Li, K

(ref. 46)

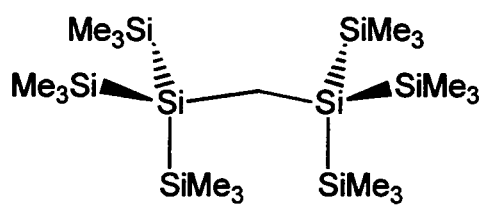


(ref. 47)

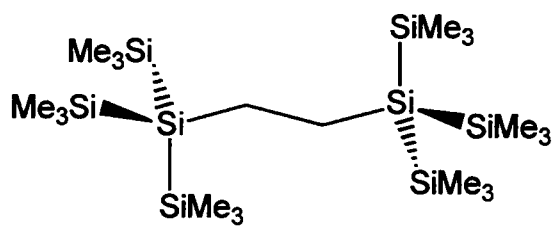


(ref. 48)

Scheme 5.3 Known dianionic silyl ligands



18



19

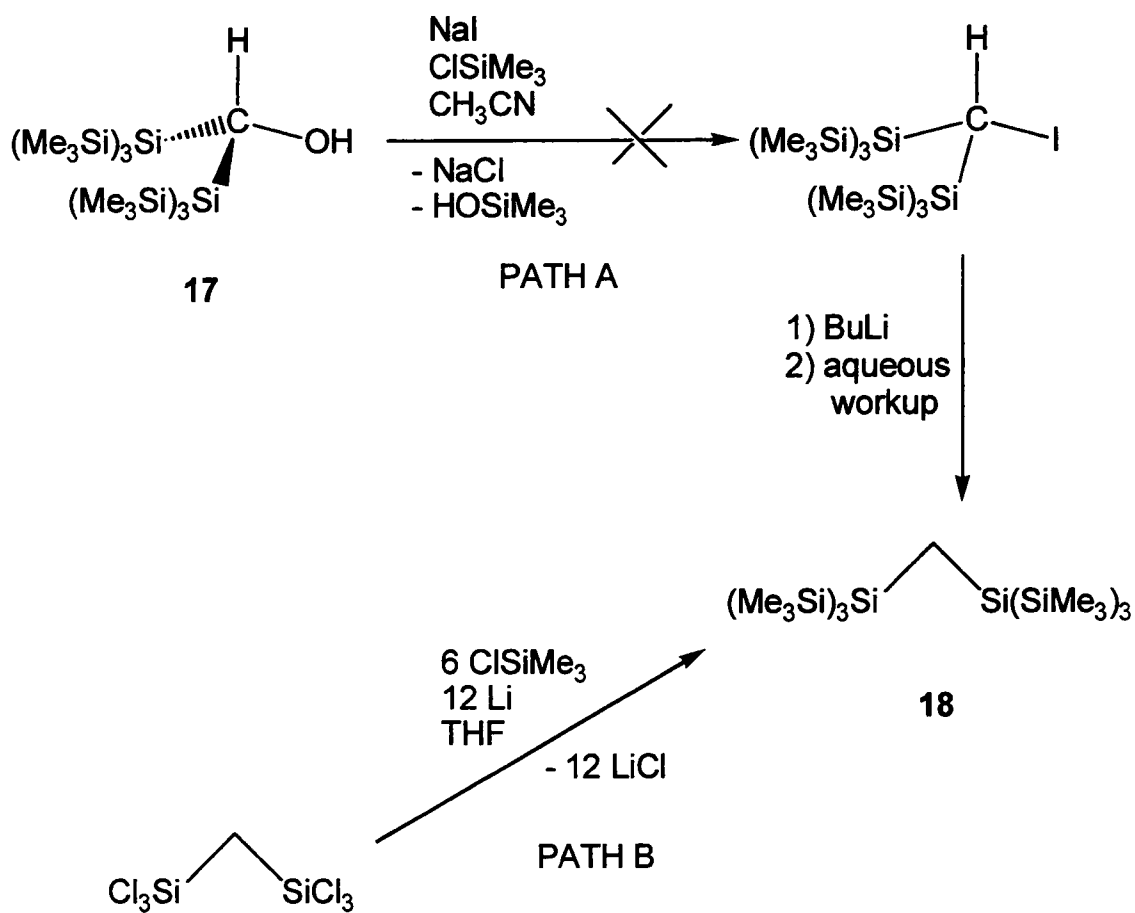
Scheme 5.4

## 5.2 Results and Discussion

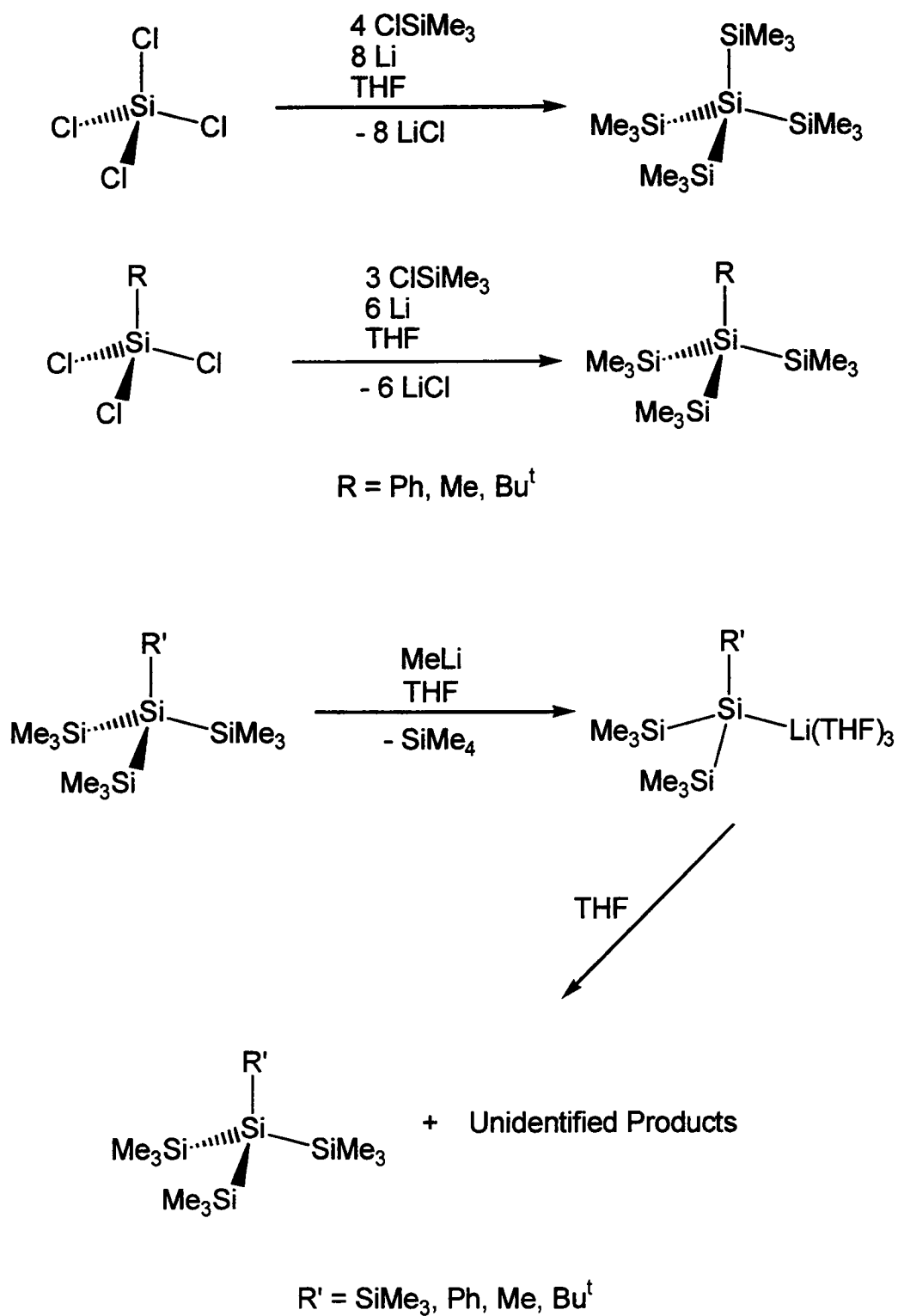
### 5.2.1 Synthesis of Bis[tris(trimethylsilyl)silyl]methane $[(\text{Me}_3\text{Si})_3\text{Si}]_2\text{CH}_2$ (**18**) and 1,2-Bis[tris(trimethylsilyl)silyl]ethane $(\text{Me}_3\text{Si})_3\text{SiCH}_2\text{CH}_2\text{Si}(\text{SiMe}_3)_3$ (**19**)

In the synthesis of the ligand precursor **18**, two synthetic pathways were considered (Scheme 5.5). In the first pathway (Path A), halogenation of the bis(silyl) methanol derivative  $[(\text{Me}_3\text{Si})_3\text{Si}]_2\text{CHOH}$  (**17**),<sup>40</sup> followed by metalation and hydrolysis of the resulting alkyl lithium complex was expected to yield the bis(silyl)methane derivative **18**. However, attempts to prepare the bis(silyl)methyl iodide  $[(\text{Me}_3\text{Si})_3\text{Si}]_2\text{CHI}$  (**20**) using the protocol reported by Olah and co-workers<sup>41</sup> was unsuccessful. A mixture of products was obtained, presumably due to oxidative cleavage of the Si-Si bonds in the  $-\text{Si}(\text{SiMe}_3)_3$  groups by trace amounts of iodine generated in the reaction mixture. We then pursued the second pathway (Path B) shown in Scheme 5.5, which involved silylation of bis(trichlorosilyl)methane  $[(\text{Cl}_3\text{Si})_2\text{CH}_2]$  by  $\text{ClSiMe}_3/\text{Li}$  in THF. The silylation of  $(\text{Cl}_3\text{Si})_2\text{CH}_2$  proceeded smoothly to **18** in 71% yield after crystallization from acetone. The reaction to produce **18** is similar to that reported in the literature<sup>45</sup> for the preparation of  $\text{SiR}(\text{SiMe}_3)_3$  from  $\text{SiCl}_4$  or  $\text{RSiCl}_3$ , Li and  $\text{ClSiMe}_3$  (Scheme 5.6).

Spectroscopic properties of **18** are consistent with the structure assignment. The  $^1\text{H}$  and  $^{13}\text{C}\{^1\text{H}\}$  NMR spectra consist of 2 signals corresponding to the  $-\text{Si}(\text{SiMe}_3)_3$  and  $-\text{CH}_2-$  moieties. The  $^{29}\text{Si}\{^1\text{H}\}$  spectrum



Scheme 5.5



Scheme 5.6

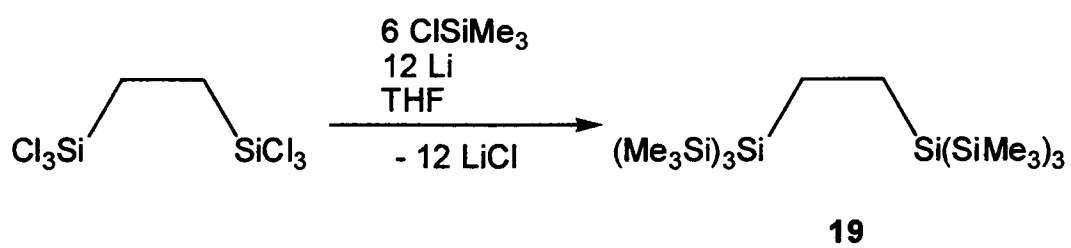
also consists of 2 signals, with the quaternary silicon resonance found at  $\delta$  -78.0 ppm and the  $\text{SiMe}_3$  signal at -11.9 ppm. The  $^{29}\text{Si}$  NMR chemical shifts found in **18** are in good agreement with those reported for  $\text{EtSi}(\text{SiMe}_3)_3$  (-78.8 and -12.4 ppm),<sup>42</sup> but the quaternary silicon resonance in **18** is significantly downfield shifted from those in  $\text{HSi}(\text{SiMe}_3)_3$  (-115.4 ppm) and  $\text{Si}(\text{SiMe}_3)_4$  (-135.6 ppm).<sup>42</sup> Attempts to obtain crystals of **18** suitable for analysis by X-ray crystallography were unsuccessful.

The synthesis of the bis(silyl)ethane derivative **19** was achieved by silylation of bis(trichlorosilyl)ethane with  $\text{ClSiMe}_3/\text{Li}$  in THF, which was isolated in 75.3% yield after recrystallization from acetone/hexanes (Scheme 5.7). The spectroscopic properties of **19** are similar to those of **18**. The  $^{29}\text{Si}\{^1\text{H}\}$  NMR spectrum of **19** consists of 2 resonances at  $\delta$  -12.7 and -76.6 ppm, which are similar to those observed above for **18** and  $\text{EtSi}(\text{SiMe}_3)_3$ . Attempts to obtain X-ray quality crystals of **19** for structural study were unsuccessful.

### 5.2.2 Attempted Metalation of **18** and **19**

Having obtained the ligand precursors **18** and **19**, attempts were made to produce the dianionic disilyl compounds  $[\text{LiSi}(\text{SiMe}_3)_2]\text{CH}_2$  (**21**) and  $\text{LiSi}(\text{SiMe}_3)_2\text{CH}_2\text{CH}_2(\text{SiMe}_3)_2\text{SiLi}$  (**22**) by the treatment of **18** and **19** with two equivalents of  $\text{MeLi}$  in THF (Scheme 5.8). This attempted approach parallels that used in the preparation of  $\text{Li}(\text{THF})_3\text{Si}(\text{SiMe}_3)_3$ .<sup>45</sup> When the reaction of **18**



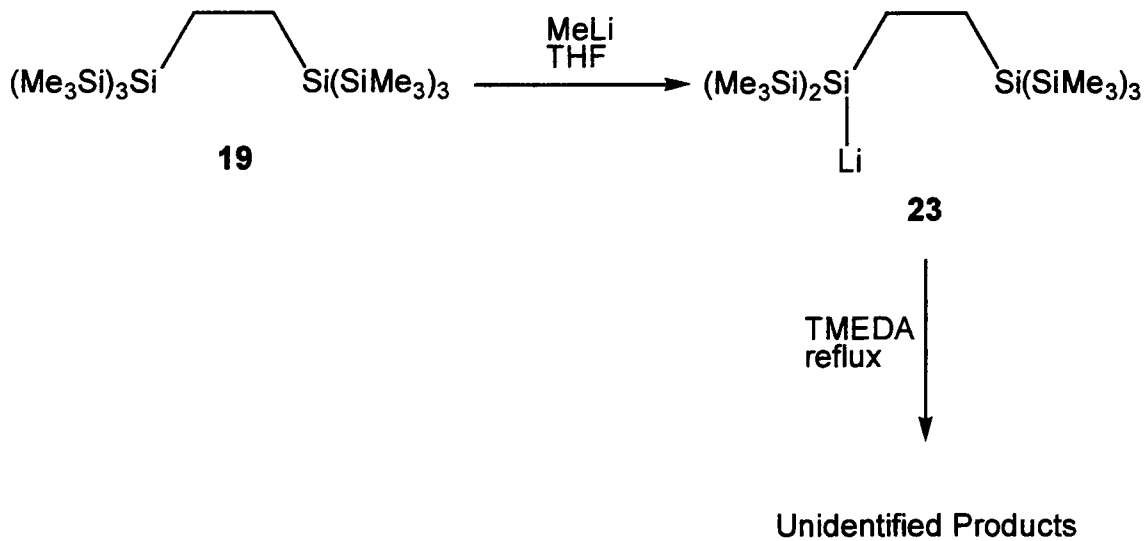


Scheme 5.7

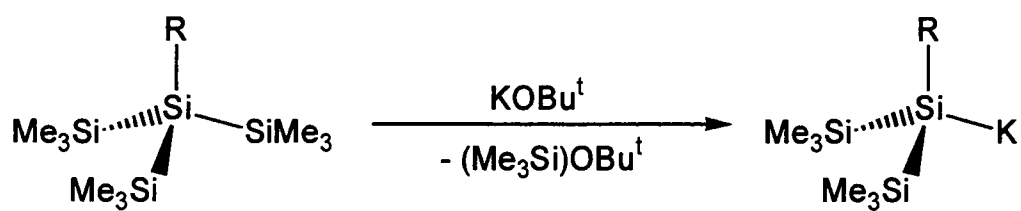
with MeLi was monitored by NMR, several products were observed to initially form in the reaction mixture. Addition of excess MeLi resulted in the disappearance of most of these signals from the NMR spectra of the reaction mixture and the appearance of a single  $-\text{SiMe}_3$  resonance. However, removal of solvent, extraction of the residue with hexanes, and cooling the hexanes solution yielded a mixture of unidentified products (Scheme 5.8).

The reaction of **19** with excess MeLi in THF was found to cleanly produce an initial product whose NMR spectra were consistent with the monolithiated complex  $\text{LiSi}(\text{SiMe}_3)_2\text{CH}_2\text{CH}_2\text{Si}(\text{SiMe}_3)_3$  (**23**) (Scheme 5.8). Attempts to lithiate the other  $-\text{Si}(\text{SiMe}_3)_3$  group by the addition of *N,N,N',N'*-tetramethylethylenediamine (TMEDA) to the solution (to enhance the reactivity of the MeLi) and refluxing the solution resulted in the decomposition of **23** to a mixture of unidentified compounds. Product decomposition in ether solvents was also observed in the reaction of MeLi with  $\text{SiR}(\text{SiMe}_3)_3$  to form  $\text{Li}(\text{THF})_3\text{SiR}(\text{SiMe}_3)_2$  (Scheme 5.6).<sup>45</sup>

Since MeLi seemed to be unable to achieve metalation of both  $-\text{Si}(\text{SiMe}_3)_3$  groups in **19**, we turned to tert-butoxy potassium as a metalation reagent, as it had been recently shown to be a very efficient reagent in the synthesis of silyl potassium complexes from  $\text{RSi}(\text{SiMe}_3)_3$  precursors (Scheme 5.9).<sup>42</sup> The reaction of two equivalents of  $\text{KO}^t\text{Bu}$  with **19** in DME was followed by GC/MS of hydrolyzed aliquots. After 2 h no **19** was observed by GC/MS to be left in the reaction mixture, and the only identifiable products were

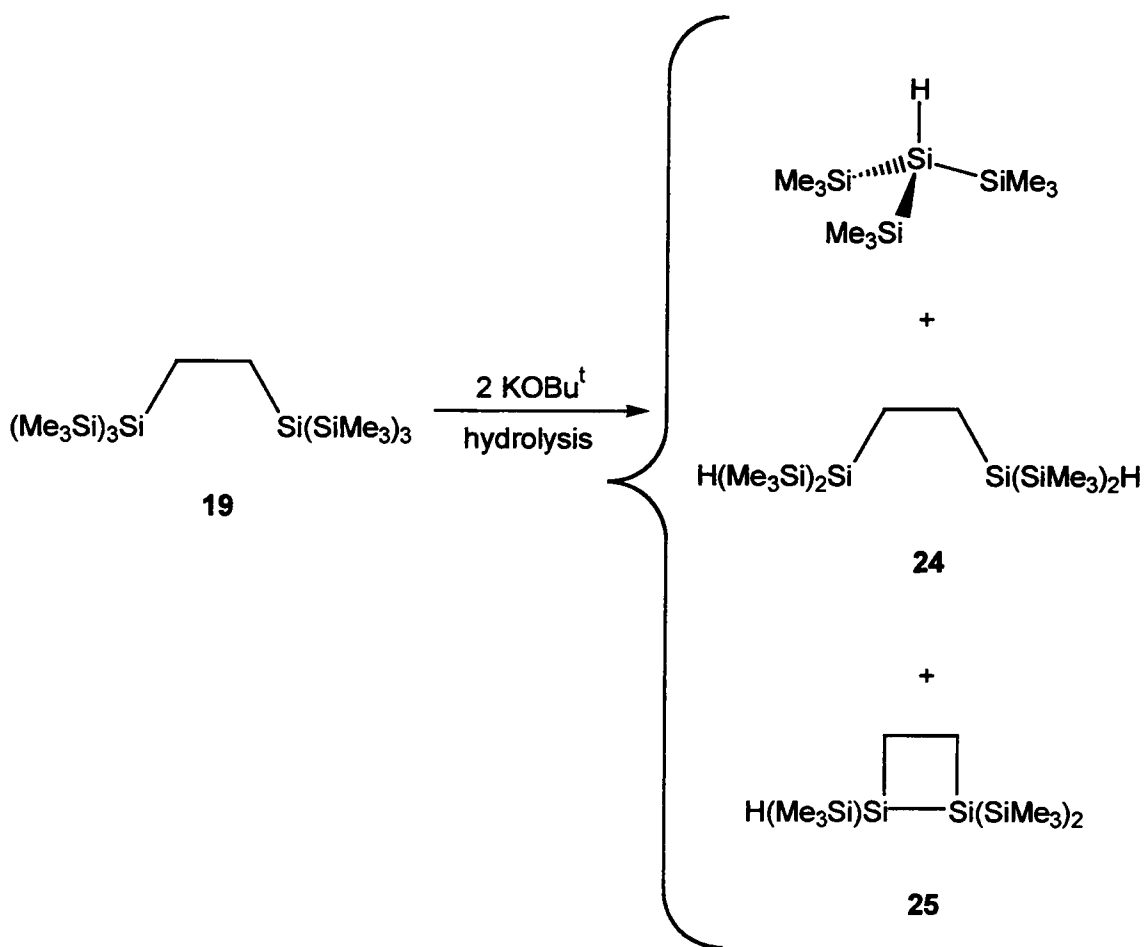


Scheme 5.8



R = SiMe<sub>3</sub>  
 Si(SiMe<sub>3</sub>)<sub>3</sub>  
 SiMe<sub>2</sub>[Si(SiMe<sub>3</sub>)<sub>3</sub>]  
 CH<sub>2</sub>CH<sub>3</sub>  
 H

Scheme 5.9<sup>42</sup>



Scheme 5.10

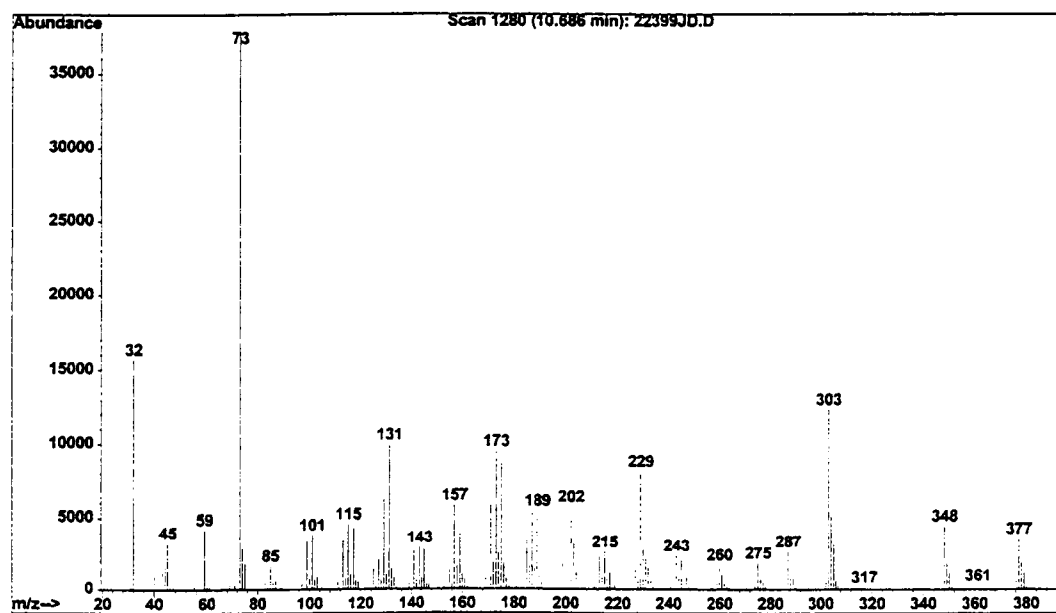
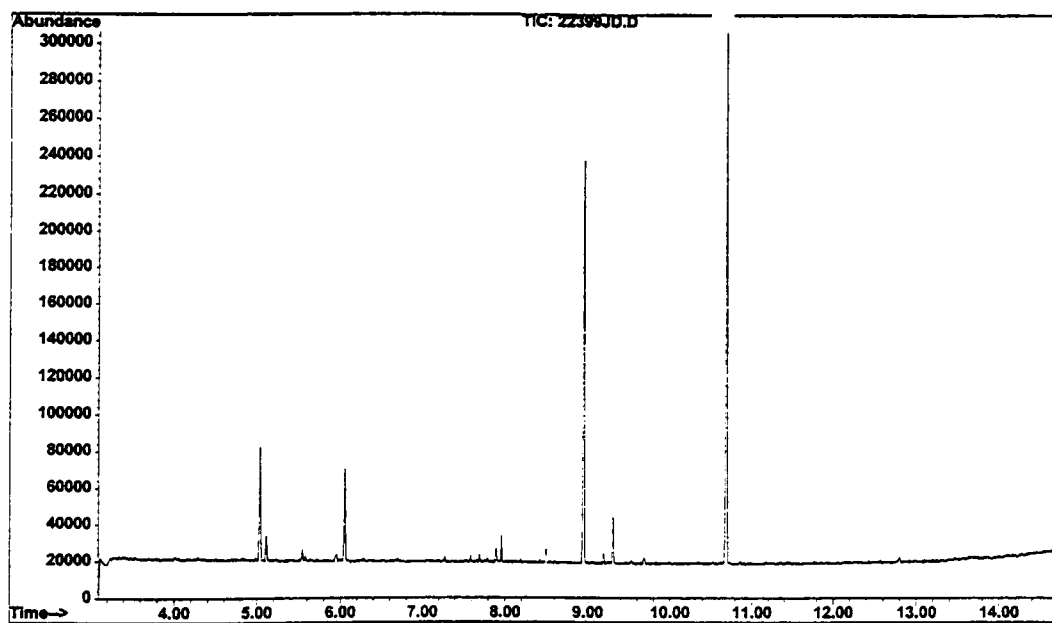


Figure 5.1 GC/MS peak for 24 from the reaction of 19 with  $\text{KOBU}^t$

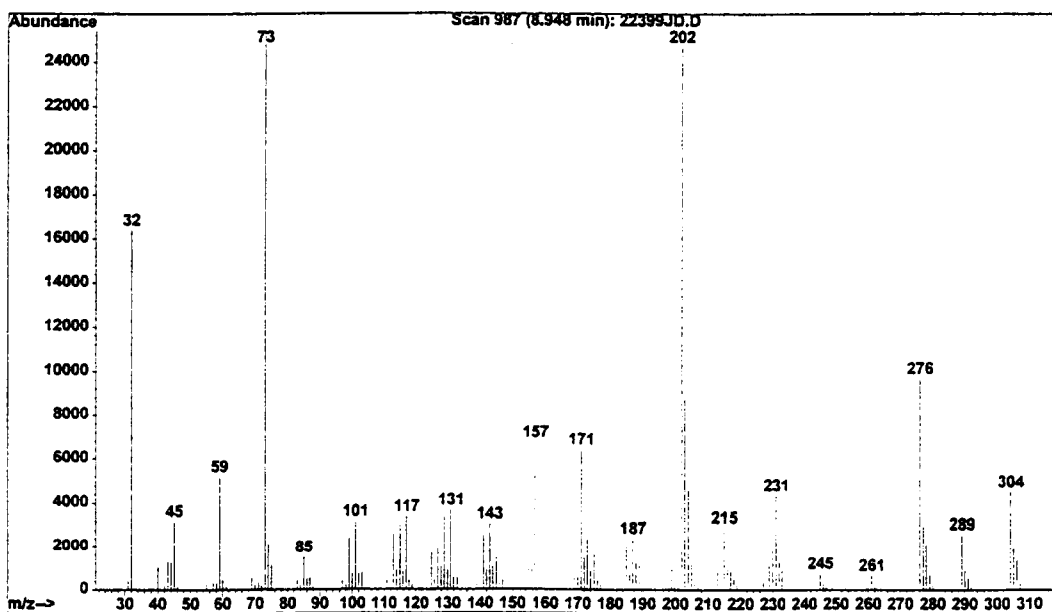
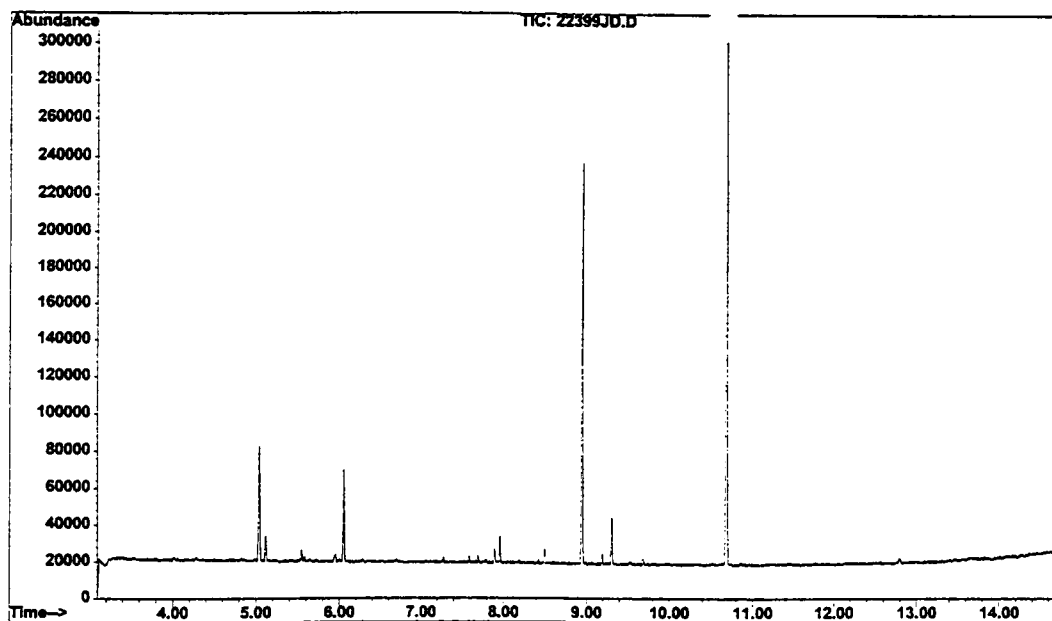


Figure 5.2 GC/MS peak for 25 from the reaction of 19 with  $\text{KOBU}^t$

HSi(SiMe<sub>3</sub>)<sub>3</sub>, HSi(SiMe<sub>3</sub>)<sub>2</sub>CH<sub>2</sub>CH<sub>2</sub>(SiMe<sub>3</sub>)<sub>2</sub>SiH (**24**), and 1,1,2-tris(trimethylsilyl)-1,2-disilacyclobutane (**25**) [Scheme 5.10]. GC/MS traces of **24** and **25** from the reaction mixture of **19** and KOBu<sup>t</sup> are shown in Figures 5.1 and 5.2. The presence of **24** and **25** in the hydrolyzed aliquot from the reaction mixture of **19** and KOBu<sup>t</sup> was indicative of the formation of KSi(SiMe<sub>3</sub>)<sub>2</sub>CH<sub>2</sub>CH<sub>2</sub>(SiMe<sub>3</sub>)<sub>2</sub>SiK (**25**) in the reaction mixture. However, attempts to isolate **25** by crystallization from toluene have to date been unsuccessful.

Although the isolation of dianionic bis(silyl)alkane compounds have to date been unsuccessful, the reactions of **18** and **19** with MeLi and KOBu<sup>t</sup> indicate that some metalation of these compounds are occurring, although the resulting products may be somewhat unstable. Possible future directions may include conducting these reactions at lower temperatures, or, in the case of the reaction of **19** with KOBu<sup>t</sup>, using the reaction mixture *in situ* for further reactions with transition metal halide complexes with purification of the resulting products by crystallization at this later stage. Such approaches to poly- and persilyl complexes may yet prove fruitful and result in the discovery of new and interesting chemistry.

### 5.3 Experimental Section

All manipulations were performed under a dry nitrogen or argon atmosphere with the use of either a drybox or standard Schlenk techniques. Solvents, unless otherwise noted, were purified by distillation from



potassium/benzophenone ketyl before use. Benzene- $d_6$  was dried over activated molecular sieves and stored under nitrogen. Acetonitrile was purified by distillation from  $\text{CaH}_2$ . Acetone was used as received.  $\text{ClSiMe}_3$  (Strem) was distilled before use.  $\text{NaI}$  (Fisher) was dried under vacuum before use. NMR spectra were recorded on a Bruker AC-250 or AMX-400 Fourier transform spectrometer.  $^1\text{H}$  and  $^{13}\text{C}$  chemical shifts were referenced to solvents (residual protons in the  $^1\text{H}$  spectra).  $^{29}\text{Si}$  chemical shifts were referenced to  $\text{SiMe}_4$ . GC/MS spectra were recorded on a Hewlett-Packard 6890 gas chromatograph with a 5793 mass selective detector (MSD) operating at an ionization voltage of 70 eV. The column used was a Hewlett-Packard DB5MS capillary column (30 m x 250  $\mu\text{m}$ ) with a 0.25  $\mu\text{m}$  5% phenyl methyl siloxane film coating. Methyl lithium (1.5 M in  $\text{Et}_2\text{O}$ , stabilized with  $\text{LiBr}$ , Aldrich), bis(trichlorosilyl)methane (Gelest), bis(trichlorosilyl)ethane (Gelest), and Li wire (high Na content, Aldrich) were used as received.  $\text{KOBU}^{\text{t}}$ <sup>39</sup> and  $[(\text{Me}_3\text{Si})_3\text{Si}]_2\text{CHOH}$  (17)<sup>40</sup> were prepared by the literature procedures. Elemental analyses were performed by E + R Microanalytical, Parsippany, NJ.

**Synthesis of  $[(\text{Me}_3\text{Si})_3\text{Si}]_2\text{CH}_2$  (18).** A flame-dried Schlenk flask under argon was charged with 1.10 g of cut Li wire (159 mmol), which was suspended in 50 mL of THF.  $\text{ClSiMe}_3$  (8.9 mL, 7.6 g, 70 mmol) was added via syringe, and the Li/ $\text{ClSiMe}_3$  mixture was cooled to 0 °C. The Li/ $\text{ClSiMe}_3$  mixture was then treated dropwise with vigorous stirring with a solution of 3.0 g (11 mmol) of  $(\text{Cl}_3\text{Si})_2\text{CH}_2$  in 10 mL of THF. The resulting cloudy brown reaction

mixture was then stirred for an additional 16 h at room temperature. The solution was filtered into 100 mL of 10% aqueous HCl, and the organic phase separated and dried over MgSO<sub>4</sub>. Evaporation of solvent, followed by recrystallization from acetone yielded 3.82 g of **18** (71%). NMR: <sup>1</sup>H NMR (benzene-*d*<sub>6</sub>, 250.1 MHz, 23 °C) δ 0.28 [s, 54 H, Si(SiMe<sub>3</sub>)<sub>3</sub>], 0.19 [s, 2 H, CH<sub>2</sub>]. <sup>13</sup>C{<sup>1</sup>H} NMR (benzene-*d*<sub>6</sub>, 62.9 MHz, 23 °C) δ 1.75 [Si(SiMe<sub>3</sub>)<sub>3</sub>, <sup>1</sup>J<sub>C-H</sub> = 119.6 Hz], -20.8 [CH<sub>2</sub>, <sup>1</sup>J<sub>C-H</sub> = 111.9 Hz]. <sup>29</sup>Si{<sup>1</sup>H} NMR (benzene-*d*<sub>6</sub>, 79.5 MHz, 27 °C) δ -11.9 [Si(SiMe<sub>3</sub>)<sub>3</sub>], -78.0 [Si(SiMe<sub>3</sub>)<sub>3</sub>]. Anal. Calcd for C<sub>19</sub>H<sub>56</sub>Si<sub>8</sub>: C, 44.81; H, 11.08. Found: C, 44.61; H, 11.10.

**Synthesis of [(Me<sub>3</sub>Si)<sub>3</sub>Si]CH<sub>2</sub>CH<sub>2</sub>[Si(SiMe<sub>3</sub>)<sub>3</sub>] (19).** A flame-dried Schlenk flask under argon was charged with 1.48 g (213 mmol) of cut Li wire and suspended in 40 mL of THF. ClSiMe<sub>3</sub> (14.0 mL, 12.0 g, 110 mmol) was then added, and the Li/ClSiMe<sub>3</sub> mixture cooled to 0 °C. The Li/ClSiMe<sub>3</sub> mixture was then treated dropwise with vigorous stirring with a solution of 4.99 g (16.8 mmol) of Cl<sub>3</sub>SiCH<sub>2</sub>CH<sub>2</sub>SiCl<sub>3</sub> in 10 mL of THF. The resulting cloudy dark brown reaction mixture was stirred for an additional 30 h at room temperature, and then was filtered into 100 mL of 10% aqueous HCl. The organic fraction was dried over MgSO<sub>4</sub>, and the solvent was evaporated. Recrystallization of the residue from acetone/hexanes yielded 3 crops of crystals totaling 6.62 g of **19** (75.3%). NMR: <sup>1</sup>H NMR (benzene-*d*<sub>6</sub>, 250.1 MHz, 23 °C) δ 1.13 [s, 4 H, Si-CH<sub>2</sub>CH<sub>2</sub>-Si], 0.27 [s, 54 H, Si(SiMe<sub>3</sub>)<sub>3</sub>]. <sup>13</sup>C{<sup>1</sup>H} NMR (benzene-*d*<sub>6</sub>, 62.9 MHz, 23 °C) δ 7.95 [Si-CH<sub>2</sub>CH<sub>2</sub>-Si, <sup>1</sup>J<sub>C-H</sub> = 125.4 Hz], 1.46 [Si(SiMe<sub>3</sub>)<sub>3</sub>, <sup>1</sup>J<sub>C-H</sub> = 119.7

Hz].  $^{29}\text{Si}\{^1\text{H}\}$  NMR (benzene- $d_6$ , 79.5 MHz, 27 °C)  $\delta$  -12.7 [Si(SMe $_3$ ) $_3$ ], -76.6 [Si(SiMe $_3$ ) $_3$ ]. Anal. Calcd for C $_{20}$ H $_{58}$ Si $_8$ : C, 45.90; H, 11.17. Found: C, 46.11; H, 11.22.

**Attempted Iodination of 17.**<sup>41</sup> 1.73 g (3.29 mmol) of **17** and 0.491 g (3.28 mmol) of NaI were dissolved in 50 mL of acetonitrile. The resulting solution was treated with vigorous stirring with 0.42 mL (0.36 g, 3.3 mmol) of ClSiMe $_3$ . The reaction was followed by TLC (silica gel, hexanes). After 2 h all starting material had been consumed, and 50 mL of Et $_2$ O was added to the reaction mixture, followed by 50 mL of distilled water. The organic phase was separated and washed with 30 mL of 10% aqueous Na $_2$ S $_2$ O $_3$  followed by 30 mL of brine, and then dried over CaSO $_4$ . Evaporation of solvent, followed by recrystallization from acetone, yielded 0.851 g of material which was found by NMR to be a mixture of unidentified products.

**Attempted Lithiation of 18.** A flame-dried Schlenk flask was charged with 0.980 g (1.92 mmol) of **18**, which was dissolved in 35 mL of THF. 3.0 mL of a MeLi solution (1.5 M in Et $_2$ O, 4.62 mmol) was then added, resulting in the immediate development of a yellow-orange color in the reaction solution. The reaction was monitored by NMR, and after 42 h the  $^1\text{H}$  NMR spectrum of an aliquot from the reaction mixture showed predominantly one -SiMe $_3$  resonance. The solvents were removed *in vacuo*, and the resulting oily yellow-orange residue was dissolved in 30 mL of hot hexanes and filtered to remove LiBr. Cooling of the hexanes solution yielded a yellow powder which was found by

NMR to be a mixture of unidentified products.

**Attempted Lithiation of 19.** A flame-dried Schlenk flask was charged with 2.00 g (3.82 mmol) of **19**, which was dissolved in 40 mL of THF. 7.6 mL of a MeLi solution (1.5 M in Et<sub>2</sub>O, 11.5 mmol) was then added, resulting in the development of an orange color in the reaction solution. The reaction was monitored by NMR, and after 22 h three signals in a 18:27:2 ratio (by integration) were observed in the <sup>1</sup>H NMR spectrum of an aliquot from the reaction mixture, indicating the formation of the monolithiated complex (Me<sub>3</sub>Si)<sub>3</sub>SiCH<sub>2</sub>CH<sub>2</sub>Si(SiMe<sub>3</sub>)<sub>2</sub>Li. The reaction mixture remained unchanged after 30 h, at which time 2.0 mL (13.3 mmol) of TMEDA was added to the reaction mixture, and the solution was refluxed for an additional 24 h. Removal of solvents yielded an oily orange-brown residue which was found by NMR to be a mixture of unidentified products.

**Attempted Potassiation of 19.**<sup>42</sup> A flame-dried Schlenk flask was charged with 2.08 g (3.97 mmol) of **19** and 0.939 g (8.37 mmol) of KOBu<sup>t</sup>. The mixture was then dissolved in 30 mL of DME, resulting in the development of an orange solution. After 2 h an analysis of a hydrolyzed aliquot from the reaction mixture by GC/MS showed HSi(SiMe<sub>3</sub>)<sub>3</sub>, HSi(SiMe<sub>3</sub>)<sub>2</sub>CH<sub>2</sub>CH<sub>2</sub>Si(SiMe<sub>3</sub>)<sub>2</sub>H, and 1,1,2-tris(trimethylsilyl)-1,2-disilacyclobutane to be present. The solvent was removed *in vacuo*, and the oily brown residue was redissolved in 20 mL of toluene. Concentration and cooling of the toluene solution yielded an oily colorless solid which NMR

showed to be a mixture of unidentified products.

## REFERENCES

## References

1. Piper, T. S.; Lemal, D.; Wilkinson, G. *Naturwissenschaften* **1956**, *43*, 129.
2. (a) Tilley, T. D. in *The Silicon-Heteroatom Bond*; Patai, S., Rappoport, Z., Eds.; Wiley: New York, 1991, Chapters 9 and 10. (b) Tilley, T. D. *Comments Inorg. Chem.* **1990**, *10*, 37. (c) Harrod, J. F.; Mu, Y.; Samuel, E. *Polyhedron* **1991**, *11*, 1239. (d) Corey, J. Y. in *Advances in Silicon Chemistry*; Larson, G., Ed.; JAI Press, Inc.: Greenwich, CT, 1991; Vol. 1, p 327. (e) Tilley, T. D. *Acc. Chem. Res.* **1993**, *26*, 22. (f) Sharma, H. K.; Pannell, K. H. *Chem. Rev.* **1995**, *95*, 1351. (g) Xue, Z. *Comments Inorg. Chem.* **1996**, *18*, 223. (h) Gauvin, F.; Harrod, J. F.; Woo, H. G. *Adv. Organomet. Chem.* **1998**, *42*, 363. (i) Corey, J. Y.; Braddock-Wilking, J. *Chem. Rev.* **1999**, *99*, 175.
3. See, for example (a) Speier, J. L.; Webster, J. A.; Barnes, G. H. *J. Am. Chem. Soc.* **1957**, *79*, 974. (b) Corey, J. Y.; Zhu, X. H. *Organometallics* **1992**, *11*, 672. (c) Kesti, M. R.; Waymouth, R. M. *Organometallics* **1992**, *11*, 1095.
4. For examples see (a) Allinson, J. S.; Aylett, B. J.; Colquhoun, H. M. *J. Organomet. Chem.* **1976**, *112*, C7. (b) Isaacs, E. E.; Graham, W. A. G. *Can. J. Chem.* **1975**, *53*, 467. (c) Darensbourg, D. J.; Bauch, C. G.; Riebenspies, J. H.; Rheingold, A. L. *Inorg. Chem.* **1988**, *27*, 4203. (d)

- Jetz, W. Graham, W. A. G. *Inorg. Chem.* **1971**, *10*, 4. (e) Schubert, U.; Müller, J.; Alt, H. G. *Organometallics* **1987**, *6*, 469. (f) Bennett, M. J.; Simpson, K. A. *J. Am. Chem. Soc.* **1971**, *93*, 7156. (g) Schubert, U.; Kirchgässner, U.; Grönen, J.; Piana, H. *Polyhedron* **1989**, *8*, 1589. (h) Handwerker, H.; Paul, M.; Blümel, J.; Zybill, C. *Angew. Chem. Int. Ed. Engl.* **1993**, *32*, 1313. (i) Heyn, R. H.; Tilley, T. D. *Inorg. Chem.* **1990**, *29*, 4051. (j) Luo, X.-L.; Kubas, G. J.; Bryan, J. C.; Burns, C. J.; Unkefer, C. J. *J. Am. Chem. Soc.* **1994**, *116*, 10312.
5. Heyn, R. H.; Tilley, T. D. *Inorg. Chem.* **1989**, *28*, 1768.
6. (a) Wu, Z.; Diminnie, J. B.; Xue, Z. *Inorg. Chem.* **1998**, *37*, 6366. (b) Wu, Z.; Diminnie, J. B.; Xue, Z. *J. Am. Chem. Soc.* **1999**, *121*, in press. (c) Wu, Z.; Diminnie, J. B.; Xue, Z. *Organometallics* **1999**, *18*, 1002.
7. Barron, A. R.; Wilkinson, G.; Motevalli, M.; Hursthouse, M. B. *J. Chem. Soc., Dalton Trans.* **1987**, 837.
8. (a) Silicide Thin Films - Fabrication, Properties, and Applications. *Mat. Res. Soc. Symp. Proc.* **1996**, *Vol. 402*. (b) Silicides, Germanides and Their Interfaces. *Mat. Res. Soc. Symp. Proc.* **1994**, *Vol. 320*. (c) *Silicides for VLSI Applications*. Murarka, S. P., Academic Press: New York, 1983. (d) Murarka, S. P. *NATO ASI Series, Series E* **1989**, *164*, 275. (e) Chemical Vapor Deposition of Tungsten and Tungsten Silicides for VLSI/ULSI Applications. Schmitz, J. E. J., Noyes, Park Ridge, NJ,



1992. (f) High Temperature Silicides and Refractory Alloys. *Mat. Res. Soc. Symp. Proc.* **1994**, Vol. 322. (g) Silverman, J.; Mooney, J. M.; Shepherd, F. D. *Sci. Am.* **March 1992**, 78. (h) Bernard, C.; Madar, R.; Pauleau, Y. *Solid State Technol.* **February 1989**, 79. (i) Smith, P. M.; Custer, J. S. *Appl. Phys. Lett.* **1997**, 70, 3116. (j) Smith, P. M.; Custer, J. S.; Jones, R. V.; Maverick, A. W.; Roberts, D. A.; Norman, J. A. T.; Hochberg, A. K.; Bai, G.; Reid, J. S.; Nicolet, M.-A. *Mat. Res. Soc. Symp. Proc.* **1996**, V11, 249. (k) Reid, J. S.; Sun, X.; Kolawa, E.; Nicolet, M.-A. *IEEE Electron Device Lett.* **1994**, 15, 298. (l) Mendicino, M. A.; Southwell, R. P.; Seebauer, E. G. *Thin Solid Films* **1994**, 253, 473.
9. (a) Aylett, B. J. *Mat. Res. Soc. Symp. Proc.* **1989**, 131, 383. (b) Stauf, G. T.; Dowben, P. A.; Boag, N. M.; Morales de la Garza, L.; Dowben, S. L. *Thin Solid Films* **1988**, 156, 327.
10. Suzuki, H. *Jpn. Tokkyo Koho JP 07,254,575* (1995). *Chem Abstr.* **1996**, 124, Abstr. No. 73934w.
11. (a) Xue, Z.; Li, L.; Hoyt, L. K.; Diminnie, J. B.; Pollitte, J. L. *J. Am. Chem. Soc.* **1994**, 116, 2169. (b) Li, L.; Diminnie, J. B.; Liu, X.; Pollitte, J. L.; Xue, Z. *Organometallics* **1996**, 15, 5231. (c) McAlexander, L. H.; Hung, M.; Li, L.; Diminnie, J. B.; Xue, Z.; Yap, G. P. A.; Rheingold, A. L. *Organometallics* **1996**, 15, 5231. (d) Diminnie, J. B.; Hall, H. D.; Xue, Z. *J. Chem. Soc., Chem. Commun.* **1996**, 2383. (e) Diminnie, J. B.; Xue,

- Z. *J. Am. Chem. Soc.* **1997**, *119*, 12657. (f) Wu, Z.; Diminnie, J. B.; Xue, Z. *Organometallics* **1998**, *17*, 2917. (g) Wu, Z.; McAlexander, L. H.; Diminnie, J. B.; Xue, Z. *Organometallics* **1998**, *17*, 4583. (h) Chen T.; Wu, Z.; Sorasaenee, K. R.; Diminnie, J. B.; Pan, H.; Guzei, I. A.; Rheingold, A. L.; Xue, Z. *J. Am. Chem. Soc.* **1998**, *120*, 13519.
12. (a) Hengge, E.; Zimmermann, H. *Angew. Chem. Int. Ed. Engl.* **1968**, *7*, 142. (b) Kingston, B. M.; Lappert, M. F. *J. Chem. Soc., Dalton Trans.* **1972**, 69.
13. Razuvaev, G. A.; Latyaeva, V. N.; Vyshinskaya, L. I.; Malysheva, A. V.; Vasileva, G. A. *Dokl. Akad. Nauk. SSSR* **1977**, *237*, 605.
14. (a) Woo, H.-G.; Heyn, R. H.; Tilley, T. D. *J. Am. Chem. Soc.* **1992**, *114*, 5698. (b) Woo, H.-G.; Walzer, J. F.; Tilley, T. D. *J. Am. Chem. Soc.* **1992**, *114*, 7047. (c) Imori, T.; Tilley, T. D.; *Polyhedron* **1994**, *13*, 2231. (d) Aitken, C. T.; Harrod, J. F.; Samuel, E. *J. Am. Chem. Soc.* **1986**, *108*, 4059. (e) Xin, S. X.; Harrod, J. F. *J. Organomet. Chem.* **1995**, *499*, 181. (f) Dioumaev, V. K.; Harrod, J. F. *J. Organomet. Chem.* **1996**, *521*, 133. (g) Procopio, L. J.; Carroll, P. J.; Berry, D. H. *Polyhedron* **1995**, *14*, 45. (h) Procopio, L. J.; Carroll, P. J.; Berry, D. H. *J. Am. Chem. Soc.* **1994**, *116*, 177. (i) Corey, J. Y.; Zhu, X. H.; Bedard, T. C.; Lange, L. D. *Organometallics* **1991**, *10*, 924. (j) Corey, J. Y.; Zhu, X. H. *Organometallics* **1992**, *11*, 672. (k) Corey, J. Y.; Huhmann, J. L.; Zhu, X.

- H. *Organometallics* **1993**, *12*, 1121. (l) Corey, J. Y.; Rooney, S. M. *J. Organomet. Chem.* **1996**, *521*, 75. (m) Shaltout, R. M.; Corey, J. Y. *Organometallics* **1996**, *15*, 2866. (n) Huhmann, J. L.; Corey, J. Y.; Rath, N. P. *J. Organomet. Chem.* **1997**, *533*, 61. (o) Hengge, E.; Gspaltl, P.; Pinter, E. *J. Organomet. Chem.* **1996**, *521*, 145. (p) Kesti, M. R.; Waymouth, R. M. *Organometallics* **1992**, *11*, 1095. (q) Banovetz, J. P.; Suzuki, H.; Waymouth, R. M. *Organometallics* **1993**, *12*, 4700. (r) Spaltenstein, E.; Palma, P.; Kreutzer, K. A.; Willoughby, C. A.; Davis, W. M.; Buchwald, S. L. *J. Am. Chem. Soc.* **1994**, *116*, 10308. (s) Verdaguer, X.; Lange, U. E. W.; Reding, M. T.; Buchwald, S. L. *J. Am. Chem. Soc.* **1996**, *118*, 6784. (t) Kreutzer, K. A.; Fisher, R. A.; Davis, W. M.; Spaltenstein, E.; Buchwald, S. L. *Organometallics* **1991**, *10*, 4031. (u) Takahashi, T.; Hasegawa, M.; Suzuki, N.; Saburi, M.; Rousset, C. J.; Fanwick, P. E.; Negishi, E. *J. Am. Chem. Soc.* **1991**, *113*, 8564.
15. (a) Huq, F.; Mowat, W.; Skapski, A. C.; Wilkinson, G. *J. Chem. Soc., Chem. Commun.* **1971**, 1477. (b) Mowat, W.; Wilkinson, G. *J. Chem. Soc., Dalton Trans.* **1973**, 1120.
16. (a) Fellmann, J. D.; Schrock, R. R.; Rupprecht, G. A. *J. Am. Chem. Soc.* **1981**, *103*, 5752. (b) Fellmann, J. D.; Rupprecht, G. A.; Wood, C. D.; Schrock, R. R. *J. Am. Chem. Soc.* **1978**, *100*, 5964.

17. LaPointe, A. M.; Schrock, R. R.; Davis, W. M. *J. Am. Chem. Soc.* **1995**, *117*, 4802.
18. (a) Li, L.; Xue, Z.; Yap, G. P. A.; Rheingold, A. L. *Organometallics* **1995**, *14*, 4992. (b) Liu, X.; Li, L.; Diminnie, J. B.; Yap, G. P. A.; Rheingold, A. L.; Xue, Z. *Organometallics* **1998**, *17*, 4597.
19. Churchill, M. R.; Youngs, W. J. *Inorg. Chem.* **1979**, *18*, 1930.
20. Chamberlain, L.; Rothwell, I. P.; Huffman, J. C. *J. Am. Chem. Soc.* **1982**, *104*, 7338.
21. (a) Churchill, M. R.; Wasserman, H. J. *Inorg. Chem.* **1981**, *20*, 2899. (b) Turner, H. W.; Fellmann, J. D.; Rocklage, S. M.; Schrock, R. R.; Churchill, M. R.; Wasserman, H. J. *J. Am. Chem. Soc.* **1980**, *102*, 7809.
22. Schrock, R. R.; Fellmann, J. D. *J. Am. Chem. Soc.* **1978**, *100*, 3359.
23. Campion, B. K.; Heyn, R. H.; Tilley, T. D. *Organometallics* **1993**, *12*, 2584. When synthesized in our group, this compound was isolated as both the (THF)<sub>2</sub> and (THF)<sub>3</sub> adducts, depending on crystallization conditions.
24. (a) *Olefin Metathesis*. Ivin, K. J., Academic Press: London, 1983. (b) Schrock, R. R. *Acc. Chem. Res.* **1990**, *23*, 158. (c) Breslow, D. S. *Prog Polym. Sci.* **1993**, *18*, 1141. (d) Sundararajan, G. *J. Sci. Ind. Res.* **1994**, *53*, 418.
25. Berry, D. H.; Koloski, T. S.; Carroll, P. J. *Organometallics* **1990**, *9*, 2952.
26. Parkin, G.; Bunel, E.; Burger, B. J.; Trimmer, M. S.; van Asselt, A.;

- Bercaw, J. E. *J. Mol. Catal.* **1987**, *41*, 21.
27. McAlexander, L. H. Ph.D. Thesis, University of Tennessee, 1997.
28. Rupprecht, G. A. Ph.D. Thesis, Massachusetts Institute of Technology, 1979.
29. Bacqué, E.; Birot, M.; Pillot, J.-P.; Lapouyade, P.; Gerval, P.; Biran, C.; Dunoguès, J. *J. Organomet. Chem.* **1996**, *521*, 99.
30. (a) Whitmore, F. C.; Sommer, L. H. *J. Am. Chem. Soc.* **1946**, *68*, 481.  
(b) Moorhouse, S.; Wilkinson, G. *J. Organomet. Chem.* **1973**, *52*, C5.  
(c) Moorhouse, S.; Wilkinson, G. *J. Chem. Soc., Dalton Trans.* **1974**, 2187.
31. Kunai, A.; Kawakami, T.; Toyoda, E.; Ishikawa, M. *Organometallics* **1992**, *11*, 2708.
32. Li, L.; Hung, M.; Xue, Z. *J. Am. Chem. Soc.* **1995**, *117*, 12746.
33. (a) Corriu, R. J. P.; Henner, M. *J. Organomet. Chem.* **1974**, *74*, 1. (b) Corriu, R. J. P.; Lanneau, G. F. *J. Organomet. Chem.* **1974**, *64*, 63. For reviews of nucleophilic attack at silicon centers, see (c) Corriu, R. J. P.; Guerin, C.; Moreau, J. J. E. in *The Chemistry of Organic Silicon Compounds*. Patai, S.; Rappoport, Z., Eds. Wiley: New York, 1991, Chapter 4. (d) Bassindale, A. R.; Taylor, P. G. in *The Chemistry of Organic Silicon Compounds*. Patai, S.; Rappoport, Z., Eds. Wiley: New York, 1991, Chapter 13.
34. Fleming, I. in *Comprehensive Organic Chemistry*, Jones, D. N., Ed.;

- Pergamon: New York, 1979; Vol. 3, Chapter 13, p. 541.
35. (a) Scherrer, E.; Brookhart, M. *J. Organomet. Chem.* **1995**, *497*, 61. (b) Mak, C. C.; Tse, M. K.; Chan, K. S. *J. Org. Chem.* **1994**, *59*, 3585. (c) Landais, Y.; Parra-Rapado, L.; Planchenault, D.; Weber, V. *Tetrahedron Lett.* **1997**, *38*, 229. (d) Fischer, E. O.; Dötz, K. H. *J. Organomet. Chem.* **1972**, *36*, C4.
36. Voskoboynikov, A. Z.; Parshina, I. N.; Shestakova, A. K.; Butin, K. P.; Beletskaya, I. P.; Kuz'mina, L. G.; Howard, J. A. K. *Organometallics* **1997**, *16*, 4041.
37. Liu, X.; Wu, Z.; Peng, Z.; Wu, Y.-D.; Xue, Z. submitted to *J. Am. Chem. Soc.*
38. Watanabe, H.; Ohsawa, N.; Sudo, T.; Hirakata, K.; Nagai, Y. *J. Organomet. Chem.* **1977**, *128*, 27.
39. Bains, M. S. *Res. Bull. Punjab Univ.* **1964**, *15*, 303. Graves, B. B.; Vincent, B. F. *Chem Ind. (London)* **1962**, 2137.
40. Gross, T.; Kempe, R.; Oehme, H. *J. Organomet. Chem.* **1997**, *534*, 229.
41. Olah, G. A.; Narang, S. C.; Balaram Gupta, B. G.; Malhotra, R. *J. Org. Chem.* **1979**, *44*, 1247.
42. Marschner, C. *Eur. J. Inorg. Chem.* **1998**, 221.
43. (a) Davidson, P. J.; Lappert, M. F.; Pearce, R. *Chem. Rev.* **1976**, *76*, 219. (b) Schrock, R. R.; Parshall, G. W. *Chem. Rev.* **1976**, *76*, 243. (c) Wu, Y.-D.; Chan, K. W. K.; Xue, Z. *J. Am. Chem. Soc.* **1995**, *117*, 9259.

- (d) Wu, Y.-D.; Peng, Z.-H.; Xue, Z. *J. Am. Chem. Soc.* **1996**, *118*, 9772.
44. (a) Tamao, K.; Kawachi, A. *Adv. Organomet. Chem.* **1995**, *38*, 1. (b) Lickiss, P. D.; Smith, C. M. *Coord. Chem. Rev.* **1995**, *145*, 75.
45. (a) Gutekunst, G.; Brook, A. G. *J. Organomet. Chem.* **1982**, *225*, 1. (b) Baines, K. M.; Brook, A. G.; Ford, R. R.; Lickiss, P. D.; Saxena, A. K.; Chatterton, A. J.; Sawyer, J. F.; Behnam, B. A. *Organometallics* **1989**, *8*, 693.
46. Kira, M.; Maruyama, T.; Kabuto, C.; Ebata, K.; Sakurai, H. *Angew. Chem., Int. Ed. Engl.* **1994**, *33*, 1489.
47. (a) Jarvie, A. W.; Winkler, H. J. S.; Peterson, D. J.; Gilman, H. *J. Am. Chem. Soc.* **1961**, *83*, 1921. (b) Gilman, H.; Tomasi, R. A. *Chem. Ind. (London)* **1963**, 954.
48. Becker, G.; Hartmann, H. M.; Hengge, E.; Schrank, F. *Z. Anorg. Allg. Chem.* **1989**, *572*, 63.

## VITA

Jonathan Bruce Diminnie was born in 1972 in Olean, NY, and grew up in nearby Allegany, NY. He graduated from Allegany Central School in June 1990. The following August he enrolled at Clemson University in Clemson, SC, where he studied chemistry. He participated in an undergraduate research project on the study of palladium-catalyzed Heck coupling reactions of alkenes in near supercritical water, under the direction of Professor Edith J. Parsons. He graduated with a B.S. degree in Chemistry in May 1994 and immediately began his graduate work at the University of Tennessee under the direction of Professor Ziling (Ben) Xue. He investigated the syntheses of thermally unstable tantalum silyl complexes and the reactions of tantalum alkylidene complexes with silanes. He synthesized the first known 1,1'-metalla-3-silacyclobutadiene and 1,1'-metalla-3,5-disilacyclohexadiene complexes as well as novel bis(silyl) substituted alkylidene complexes.

His next position will be as a research chemist with Olin Corporation in Charleston, TN.